Title
Discs Large Homolog 1: Molecular Scaffolds Guiding T Cell Activation and Effector Function

Author
Silva, Oscar

Publication Date
2013

Peer reviewed|Thesis/dissertation

UNIVERSITY OF CALIFORNIA

Los Angeles

Discs Large Homolog 1:

Molecular Scaffolds Guiding T Cell Activation and Effector Function

A dissertation submitted in partial satisfaction of the requirements
for the degree Doctor of Philosophy
in Microbiology, Immunology and Molecular Genetics

by

Oscar Silva

2013

ABSTRACT OF THE DISSERTATION

Discs Large Homolog 1:

Molecular Scaffolds Guiding T Cell Activation and Effector Function

by

Oscar Silva

Doctor of Philosophy in Microbiology, Immunology, and Molecular Genetics

University of California, Los Angeles, 2013

Professor M. Carrie Miceli, Chair

Discs large homolog 1 (Dlgh1) is a scaffold protein that couples T cell receptor (TCR) engagement to signal transduction and cytoskeletal reorganization. Specifically, Dlgh1 directs Lck and ZAP70 kinase activity toward the selective activation of mitogen-activated protein kinase p38 and transcription factor NFAT. In addition, Dlgh1 controls actin polymerization, TCR and lipid raft clustering, and MTOC positioning during TCR engagement. The ability to selectively activate, integrate and tune these pathways may allow Dlgh1 to promote discrete cellular responses including: T cell differentiation, proliferation, cytokine production, cell-mediated cytotoxicity and memory generation. Therefore, understanding how Dlgh1 channels proximal TCR signals to specific downstream pathways to trigger distinct cellular responses in T cells requires 1) an understanding of how Dlgh1 is regulated by post-transcriptional and post-translational modifications, and 2) the development of a suitable Dlgh1 knockout ($Dlgh1^{KO}$) mouse model to assess Dlgh1 function *in vivo*.

Alternative splicing and phosphorylation of Dlgh1 are post-transcriptional and post-translational modifications that regulate Dlgh1 localization, expression and function. We found that alternative splicing of Dlgh1 in CD8+ effector T cells resulted in the expression of two distinct Dlgh1 protein variants: Dlgh1 AB and Dlgh1 B. Further, these two Dlgh1 variants served as molecular conduits to drive distinct cytotoxic T lymphocyte (CTL) responses. While both Dlgh1 AB and Dlgh1 B promoted p38-independent lytic factor degranulation, which required actin polymerization and the cytoskeletal regulator WASp, only Dlgh1 AB coupled Lck to p38-dependent production of proinflammatory cytokines. In addition, this CTL effector function was found to require Lck-mediated Dlgh1 AB tyrosine phosphorylation at tyrosine 222, suggesting that Dlgh1 AB tyrosine phosphorylation may provide a unique mechanism to specifically regulate p38-dependent functions in T cells. Lastly, we found that acute inducible knockout of Dlgh1 in mature peripheral T cells prevented optimal T cell activation and effector function in CD8+ T cells, while knockout of Dlgh1 in the germline or developing T cells had little or no effect on T cell function. Together, these data suggests that the developmental timing of Dlgh1 ablation may be critical for observing Dlgh1-dependent functional effects. We propose that T lymphocytes construct functionally unique Dlgh1 AB/Lck/p38 and Dlgh1/WASp complexes as a mechanism to specifically direct proximal TCR signals towards distinct cellular responses.

The dissertation of Oscar Silva is approved.

Jonathan Braun

David G. Brooks

Donald B. Kohn

M. Carrie Miceli, Committee Chair

University of California, Los Angeles

2013

To my wife, family and friends:

Chanel for being my companion and ultimate supporter through it all

My parents for instilling a relentless work ethic and drive to strive for better

Emmanuel and Rene for brotherly love and encouragement

Gustavo and Lizandro for keeping me grounded and entertained

TABLE OF CONTENTS

LIST OF FIGURES

LIST OF TABLES

Chapter 2

LIST OF ABBREVIATIONS

Ab	antibody
ADAP	adhesion and degranulation promoting adaptor protein
AP-1	activator protein 1
BSA	bovine serum albumin
Ca^{+2}	calcium ion
CARMA1	Caspase recruitment domain-containing MAGUK protein 1
CD	cluster of differentiation
DAG	diacylglycerol
Dlgh1	discs large homolog 1
EDTA	ethylenediamine tetra-acetic acid
ELISA	enzyme-linked immunoabsorbant assay
EL-4	CD8-CD4- thymoma cell line
EG.7	EL-4 cell line constitutively expressing $OVA_{257-263}$
ERK	extracellular signal regulated kinase
FCS	fetal calf serum
GADS	Grb2-related adapter protein
GFP	green fluorescent protein
Grb2	growth factor receptor-bound protein 2
GUK	guanylate kinase
hr	hour(s)
HRP	horseradish peroxidase
IFNγ	interferon gamma
IL	interleukin
IP3	inositol 1,4,5-triphosphate
Itk	IL2-inducible T cell kinase
JNK	c-Jun N-terminal kinase
LAT	linker of activated T cells
M	molar
mAb	monocloncal antibody
MAGUK	membrane associated guanylate kinase
MAPK	mitogen activated protein kinase

MFI	mean fluorescence intensity
MHC	major histocompatibility
min	minute(s)
mg	milligram(s)
mL	milliliter(s)
mM	millimolar
MTOC	microtubule organizing center
MSCV	murine stem cell virus
Nck	non-catalytic region of tyrosine kinase adaptor protein
NFAT	nuclear factor of activated T cells
NFκB	nuclear factor kappa-B
nM	nanomolar
nm	nanometer
NP-40	nonylphenoxypolyethoxyethanol
PBS	Phosphate buffered saline
PCR	polymerase chain reaction
PDZ	Post-synaptic density/Drosophila disc large tumor suppressor/Zonula occudens-1 protein
PFA	paraformaldehyde
PIP2	phosphatidylinositol 4,5-bisphosphate
PIP3	phosphatidylinositol 3,4,5-triphosphate
PLCγ1	phospholipase C-γ1
PKCθ	protein kinase C theta
s	second(s)
SDS-PAGE	sodium dodecyl sulfate-polyarilamide gel electrophoresis
SH2	Src homolog 2
SH3	Src homolog 3
SLP-76	Src homolog 2 domain-containing leukocyte phosphoprotein of 76 kDa
TBS	Tris-buffered saline
TCR	T cell receptor
Th	T helper
TNE	Tris HCl, NP-40, EDTA
TNF	tumor necrosis factor

Tween-20	Polyoxyethylene (20) sorbitan monolaurate
U	unit(s)
ZAP70	zeta-chain associated protein kinase 70
μg	microgram(s)
μL	microliter (s)
μM	micromolar

ACKNOWLEDGEMENTS

First of all, I would like to thank my mentor, Carrie Miceli, for her guidance and encouragement throughout my time in her lab. She has been nothing but supportive, optimistic and motivating. Her love for science and life is unmistakable, and her holiday parties are second to none. I would also like to thank my committee members, Jonathan Braun, David G. Brooks and Donald B. Kohn for their input, time and guidance. They are exemplary scientists and great role models to have.

I would like to thank everyone in the Miceli lab, past and present. Tamar, Lisa and Scot for showing me the ropes when I first arrived. Jillian, Genevieve and Derek for keeping the party going. Also, a big thanks and "un abrazo" to Gustavo and Lizandro for checking in on me from time to time and making me take time off work to watch the 49ers games.

To my parents and brothers for their support, love and encouragement. To my grandparents and godmother for helping my parents care for me and my brothers. And lastly, to my loving wife Chanel. Thank you for sharing every single step in this journey with me. For understanding my long hours and crazy work schedule. For baking dozens and dozens of cupcakes for everyone in the lab. For encouraging me to be better. You are the love of my life and I could not have done this without you.

I would like to acknowledge my funding sources throughout the years. The Medical Scientist Training Program (NIH NIGMS T32-GM08042), a Research Supplement to Promote Diversity in Health-Related Research (NIH NIAID AI067253), and the Microbial Pathogenesis Training Grant (NIH NIAID T32-AI067253). Also, I received financial support to present my graduate work at the 98th and 100th Annual Meeting of the American Association of Immunologists (AAI) from FASEB MARC.

Chapters 2 and 5 are versions of what will be first author or co-first author publications. Chapter 3 and 4 are published or versions of co-authored manuscripts. The author directing each project is indicated in bold.

CHAPTER 2. Dlgh1 splice variants regulate p38-dependent and –independent CTL effector functions.

Authors. Silva O, Crocetti JA, Humphries LA and **Miceli MC**.

CHAPTER 3. Dlgh1 tyrosine phosphorylation mediates TCR-dependent p38 and NFAT activation.

Authors. Crocetti JA, Silva O, Humphries LA and **Miceli MC**.

CHAPTER 4. Characterization of *In Vivo* Dlg1 Deletion on T Cell Development and Function.

Authors. Humphries LA, Shaffer MH, Sacirbegovic F, Tomassian T, McMahon KA, Humbert PO, Silva O, Round JL, Takamiya K, Huganir RL, Burkhardt JK, Russell SM, **Miceli MC**

Chapter 4 is reprinted from *PLOS One*, 2012, 7(9): e45276

CHAPTER 5. Acute dlgh1 knockout prevents optimal T cell activation and proinflammatory cytokine production

Authors. Silva O, Crocetti JA, Burkhardt JK and **Miceli MC**.

VITA

2000	Salutatorian Bellarmine College Preparatory San Jose, California
2001	CRC Freshman Chemistry Award Santa Clara University Santa Clara, California
2002	American Chemical Society Polyed Award Santa Clara University Santa Clara, California
2003	UCSD MSTP Summer Undergraduate Research Fellowship University of California, San Diego San Diego, California
2004	Sigma Xi, National Scientific Research Honor Society Phi Lambda Upsilon, National Chemistry Honor Society Professor Joseph F. Deck Award in Chemistry Santa Clara University Santa Clara, California
2004	UCSF Summer Research Training Program Fellowship University of California, San Francisco San Francisco, California
2004	B.S., Chemistry and Psychology, Cum Laude Santa Clara University Santa Clara, California
2006	Admitted to Medical Scientist Training Program David Geffen School of Medicine University of California, Los Angeles Los Angeles, California
2008	Joined Program in Microbiology, Immunology and Molecular Genetics
2008-2010	NIH NIAID Research Supplement to Promote Diversity in Health-Related Research
2011	American Association of Immunologists (AAI) Trainee Abstract Award
2011	AAI/FASEB MARC Travel Award

2011	UCLA MIMG Departmental Retreat Outstanding Oral Presentation Award
2011-2013	UCLA Microbial Pathogenesis Training Grant
2013	AAI/FASEB MARC Travel Award
2013	American Association of Immunologists Trainee Abstract Award

PUBLICATIONS

Carrasco MR, Brown RT, Serafimona IM, and **Silva O** (2003). Synthesis of N-Fmoc-O-(N'-Boc-N'-methyl)-aminohomoserine, an Amino Acid for the Facile Preparation of Neoglycopeptides. *Journal of Organic Chemistry*. 68(1): 195-197.

Carrasco MR, **Silva O**, Rawls KA, Sweeny MS, and Lombardo AA (2006). Chemoselective Alkylation of N-Alkylaminooxy-Containing Peptides. *Organic Letters*. 8(16): 3529-3532.

Tomassian T, Humphries LA, Liu SD, **Silva O**, Brooks DG, and Miceli MC (2011). Caveolin-1 Orchestrates TCR Synaptic Polarity, Signal Specificity and Function in CD8 T cells. *Journal of Immunology*. 187(6): 2993-3002.

Humphries LA, Shaffer MH, Sacirbegovic F, Tomassian T, McMahon KA, Humbert PO, **Silva O**, Round JL, Takamiya K, Huganir RL, Burkhardt JK, Russell SM, Miceli MC (2012). Characterization of *In Vivo* Dlg1 Deletion on T Cell Development and Function. *PLOS One*. 7(9): e45276.

Kendall GC, Mokhonova EI, Moran M, Sejbuk NE, Wang DW, **Silva O**, Wang RT, Lu QL, Damoiseaux R, Spencer MJ, Nelson SF, Miceli MC (2012). Dantrolene Enhances Antisense-Mediated Exon Skipping in Human and Mouse Models of Duchenne Muscular Dystrophy. *Science Translational Medicine*. 4, 164ra160.

PRESENTATIONS

Silva O, Humphries LA, Crocetti JA, Miceli MC (2011). Discs Large Homolog 1 Splice Variants Couple T Cell Receptor Engagement to Distinct T Cell Effector Functions. Presented at the American Association of Immunologists (AAI) 98th Annual Meeting, San Francisco, California.

Silva O, Crocetti JA, Humphries LA, Miceli MC (2013). Discs Large Homolog 1 Splice Variants Regulate p38-Dependent and –Independent CTL Effector Functions. Presented at the American Association of Immunologists (AAI) 100th Annual Meeting, Honolulu, Hawaii.

CHAPTER ONE

Introduction

The immune system is a collection of cells, structures and proteins that protect organisms against disease. Two distinct but interconnected immune networks exist in humans and other jawed vertebrates to allow for the detection and discrimination of microorganisms and malignant cells from healthy tissue – the innate and adaptive immune networks. Innate immunity provides organisms with a rapid but non-specific first line of defense, which is often sufficient to eliminate invading pathogens. By recognizing pathogenic association molecular patterns (PAMPs), which are common to many microorganisms, macrophages, neutrophils and dendritic cells (DCs) ingest and destroy pathogens before major clinical symptoms develop (1). However, when these innate immune cells are evaded or overwhelmed an adaptive immune response is required to eliminate pathogenic intruders. This adaptive immune response is dependent on T lymphocyte activation and the generation of an arsenal of effector cells that specifically recognize pathogenic antigens and target pathogens for destruction.

T lymphocyte activation occurs when the T cell receptor (TCR) recognizes antigenic peptide bound to membrane associated major histocompatibility complex (MHC) on the surface of antigen presenting cells (APCs) (2). Primary T cell activation, often referred to as T cell priming, occurs in secondary lymphoid tissues where activated, antigen-loaded DCs enter and present antigen and co-stimulatory molecules to circulating naïve CD8+ and CD4+ T cells. Depending on the activation status of the DCs, the antigenic peptide presented and the local inflammatory milieu, naïve T cells receive signals to differentiate and expand into effector T cells (3-5). In the case of CD8+ T cells, priming induces the generation of cytotoxic T lymphocytes (CTLs) with the ability to recognize infected cells and induce proinflammatory cytokine production and targeted cell killing via lytic granule-dependent mechanisms (6). On the other hand, CD4+ T cell priming may induce the differentiation of multiple effectors, including T helper 1 (Th1)

and T follicular helper (Tfh) cells. Th1 cells promote macrophage activation via production of interferon-γ (IFNγ), while Tfh cells activate B cells and promote germinal center (GC) formation, leading to the generation of high-affinity antibody producing plasma cells (7). Through the coordinated response of CD8+ and CD4+ T cells the adaptive immune system eradicates pathogens that evade the innate immune system. Furthermore, the adaptive immune system provides immunological memory, which is long-lasting protection against the same microorganism through the generation of long-lived lymphocytes that can become quickly reactivated upon re-exposure to pathogenic antigen (8).

T lymphocytes provide a means to combat and protect organisms from pathogenic assaults through the execution of a series of complex and precise cellular outcomes. These include T cell differentiation, proliferation, cytokine production, cell-mediated cytotoxicity and memory generation. The development and execution of these diverse cellular processes depends on the ability to selectively activate, integrate and tune the numerous signal transduction pathways activated downstream of the T cell receptor (9, 10). Thus, knowing how T cell signaling is choreographed is critical to understanding how these particular functional outcomes are elicited. This dissertation explores the molecular mechanism by which the scaffold protein *Discs large homolog 1 (Dlgh1)* specifically channels proximal TCR signals to trigger distinct T cell functional outcomes.

SCAFFOLD PROTEINS DIRECT T CELL RECEPTOR SIGNALING

T cell receptor signaling is initiated when TCRs, coreceptors (CD8/CD4) and co-stimulatory receptors (CD28/ICOS) ligate peptide-MHC and costimulatory molecules. This ligation event leads to the phosphorylation of the proximal TCR tyrosine kinases

Lck and Fyn. Once phosphorylated, Lck and Fyn phosphorylate immunoreceptor tyrosine-based activation motifs (ITAMs) found in CD3 ε, δ, and ζ of the TCR complex. Phosphorylated ITAMs then serve as docking sites for the Syk family tyrosine kinase ZAP70, which is phosphorylated by Lck. Once activated, ZAP70 and Lck can phosphorylate a number of scaffold and effector molecules leading to the activation of the actin cytoskeleton, integrins, mitogen activated protein kinases (MAPK) and transcription factors, ultimately leading to a diverse array of T cell functional outcomes (11).

During T cell signaling a dynamic cellular process of actin-mediated reorganization occurs where T cell receptors, intracellular signaling molecules and cytoskeletal components are recruited and positioned into a polarized macromolecular structure facing the APC. This molecular platform, often referred to as the immunological synapse (IS), provides a new landscape for the concentration, selective assembly and maintenance of signaling complexes (12). Thus, the IS can promote the formation and reorganization of new and old signaling complexes, which couple Lck and ZAP70 to the activation of MAPKs p38, JNK, and ERK, and transcription factors NFAT, NFκB and AP-1, allowing for gene regulation and protein production. Conversely, the immunological synapse can also dampen and terminate TCR signaling by directing TCR internalization, transducer ubiquitination and inhibitory receptor recruitment (13). Thus, the coordination and integration of these opposing activities may allow the synapse to “fine tune” TCR signal transduction leading to precise control over cellular outcomes. Finally, the immunological synapse also allows for the reorientation of the microtubule-organizing center (MTOC) and the polarized trafficking of cytokines, cytolytic granules and fate determinants, promoting direction secretion of cytokines, targeted cell killing and asymmetric division, respectively (8, 14, 15).

Scaffold proteins have emerged as key molecular intermediates coupling proximal TCR kinases to intracellular signaling pathways, thus having the potential to govern T cell functional outcomes. Scaffold proteins are multi-domain proteins with no inherent enzymatic activity, but can assemble, localize and insulate effector proteins critical for signal transduction pathways (16). Two of the most extensively studied scaffolds in T cells are LAT and SLP-76. Both of these scaffolds are tyrosine phosphorylated by ZAP70 and form an early TCR signaling complex critical for the initiation of many downstream signal transduction pathways in developing and mature T cells. This is emphasized by blocks in T cell development in germline deficient LAT and SLP-76 mice, and defects in peripheral T cell responses in conditional knockout mice (17-19). Phosphorylation of these scaffolds allows for the formation of multi-protein complexes with other adaptors and effector molecules such as Grb2, GADS, PLCγ1, Itk, Nck, Vav1 and ADAP. The presence of Vav1 and Nck in this LAT/SLP-76 complex allows for the activation of Cdc42 and WASp leading to actin polymerization and cytoskeletal reorganization, while ADAP facilitates the movement of the MTOC to the immune synapse via the plus-end microtubule motor protein dynein (20, 21). Activation of PLCγ1 by Itk in this LAT/SLP-76 complex allows for the catalytic conversion of PIP2 into IP3 and DAG, leading to intracellular Ca^{+2} release, and the recruitment and activation of PKCθ and Ras. This in turn results in MAPK and transcription factor activation, leading to the transcription of genes critical for T cell proliferation, differentiation, survival and effector function (11).

Despite the tremendous progress in the understanding of LAT, SLP-76 and the downstream pathways activated by TCR engagement, the mechanisms by which TCR-proximal kinase activity is *selectively* directed toward a discrete subset of these downstream pathways to effect particular cellular outcomes has been poorly

characterized until recently. It is now appreciated that the membrane associated guanylate kinase (MAGUK) scaffolds Dlgh1 (also known as SAP97) and CARMA1 (Caspase recruitment domain-containing MAGUK protein 1) bifurcate proximal TCR signals to independently control the MAPKs p38 and JNK, and the transcription factors NFAT and NFκB, respectively (22). Such signal specificity could allow T cells precise control over cellular functions.

DLGH1: A MOLECULAR CONDUIT GUIDING TCR SIGNAL SPECIFICITY

MAGUKs are a ubiquitous class of multi-domain scaffold proteins found at interfaces of cell:cell contact. Initially found to control signal transduction and cellular polarity in epithelial and neuronal cells, Dlgh1 has been demonstrated to localize to the T cell:APC contact site during antigen recognition and associate with proximal TCR tyrosine kinase Lck (23-25). Like other MAGUK scaffolds Dlgh1 has several modular domains important for protein-protein interactions; Dlgh1 contains three PDZ domains, a SH3 domain and a catalytically-inactive guanylate kinase (GUK) domain. In addition to these core MAGUK domains Dlgh1 has at least four areas of alternative splicing, one within the 5'UTR that regulates *dlgh1* translation and three within coding regions (Figure 1-1) (26). The first area of alternative splicing within a coding region is at the N-terminus where a recently identified CXCα palmitoylation domain or L27β oligomerization domain can be expressed (27). The next area of splicing is upstream of the first PDZ domain where the proline-rich i1A and/or i1B domains can be expressed. Finally, splicing occurs between the SH3 and GUK domains in an area often referred to as the HOOK domain. Within this region i2, i3, i4, and/or i5 can be expressed (28, 29).

During antigen recognition, the modular domains of Dlgh1 allow it to co-localize with synaptic actin, translocate into sphingolipid-rich microdomains within the

immunological synapse (IS), and associate with Lck and ZAP70 (23, 30). At the IS Dlgh1 mediates the *alternative p38 pathway* by assembling a molecular complex that channels proximal tyrosine Lck and ZAP70 kinase activity toward MAPK p38 activation (Figure 1-2). Specifically, the binding of Lck and ZAP70 to Dlgh1 allows for Lck-mediated phosphorylation of ZAP70. Once activated, ZAP70 directly phosphorylates p38 on tyrosine 323 (Y323), permitting p38 autophosphorylation on threonine 180 (T180), completing p38 activation and enabling p38 to phosphorylate discrete downstream targets (31). Indeed, Dlgh1-mediated alternative p38 activation selectively affects transcription factor NFAT, but not NFκB, via the direct or indirect phosphorylation of the transactivating domain of NFAT, leading to NFAT-dependent transcription (32, 33). Consequently, Dlgh1 provides T lymphocytes with signal specificity by coupling a fraction of the proximal TCR tyrosine kinase activity toward the activation of a specific MAPK and transcription factor, possibly leading to the transcriptional activation of a discrete set of genes important for particular T cell functions (see Chapter 2 and 3).

T CELL EFFECTOR FUNCTIONS ARE CONTROLLED BY DLGH1

In addition to binding p38 and selectively regulating NFAT-dependent transcription, Dlgh1 also associates with the cytoskeletal regulators WASp and Ezrin, and controls antigen-induced F-actin polymerization, TCR and lipid raft clustering, and MTOC focusing at the IS (23, 34, 35). Given the involvement of Dlgh1 in regulating T cell transcriptional activation and T cell polarity, our lab has proposed that Dlgh1 could play a critical role in T cell development, fate determination and effector function. Indeed, utilizing siRNA-mediated knockdown methodologies others have found a role for Dlgh1 in regulating T cell signaling in human antigen-experienced CD8+ and CD4+ T cells, and suppressor function in human CD4+CD25+ regulatory T cells (33, 36). Further, we have

found that Dlgh1 knockdown in primary murine CD8+ effector T cells disrupts TCR-induced cytokine production and contact-dependent cytolysis (23). Despite the role of Dlgh1 in regulating these T cell effector functions, the molecular mechanism by which Dlgh1 controls these responses is unclear. Dlgh1 ligands p38, WASp and Ezrin have been implicated in participating in processes that affect T regulatory suppressor function, cytokine production and cytotoxicity, however their relative contribution to Dlgh1-mediated functions has not been explored (34, 37-40). Also, it is uncertain if Dlgh1-medited cytoskeletal reorganization and alternative p38 activation are discrete or dependent pathways. This dissertation explores these unanswered questions, focusing on the molecular mechanisms by which Dlgh1 couples TCR engagement to CD8+ effector functions (Chapter 2 and 3).

DLGH1 REGULATION: POSSIBLE ROUTES FOR "TUNING" T CELL SIGNALING AND EFFECTOR FUNCTIONS

Despite having no inherent enzymatic activity, Dlgh1 is dynamically regulated by alternative splicing, phosphorylation, ubiquitination, and intramolecular interactions (28, 41-43). These modifications alter Dlgh1 localization, conformation, abundance and molecular composition. Such changes may have critical effects on Dlgh1-mediated T cell effector functions, and thus may be excellent targets for modulating Dlgh1 activity in T lymphocytes.

Alternative splicing of Dlgh1 generates unique Dlgh1 scaffolds with different functional properties in polarized epithelial and neuronal cells. In epithelial cells, Dlgh1 splice variants differentially localize within the cell depending on the expression of the i2 or i3 domains. Dlgh1 i3-containing proteins localize to sites of cell-cell contact, while Dlgh1 i2-containing proteins disperse throughout the cell, including the nucleus (35). In

addition to regulating Dlgh1 location, alternative splicing of Dlgh1 also regulates cellular function. In neuronal cells, alternative splicing of Dlgh1 differentially affects AMPA receptor-mediated excitatory postsynaptic currents (AMPAR EPSCs), which are important for learning and memory. Specifically, Dlgh1 splice variants expressing the N-terminal CXCα palmitoylation domain promote AMPAR EPSCs, while those expressing the L27β oligomerization domain do not. This may be a common mechanism of functional regulation among the discs large protein family as the exchange of the CXCα and L27β domains of Dlgh4 (also known as SAP95) had a similar effect on AMPAR EPSCs (27). As alternative splicing differentially controls Dlgh1 localization and cellular function in epithelial and neuron cells, two polarized cells types that have similarities to polarized lymphocytes (44), alternative splicing of Dlgh1 in T cells was explored as a possible mechanism of Dlgh1 regulation. Specifically, I determined what Dlgh1 protein variants were expressed in T cells due to alternative splicing, and assessed their role in controlling Dlgh1-mediated TCR signal specificity and effector function in CD8+ T cells (Chapter 2).

Phosphorylation dynamically regulates MAGUK protein complexes. For example, in resting T cells, CARMA1, a MAGUK family member, is initially autoinhibited due to intramolecular interactions. Upon TCR engagement, CARMA1 relocates to the immunological synapse where it associates with phosphorylated PDK1, generated via CD28 coreceptor engagement, and PKCθ, generated through the LAT/SLP76/PLCγ1 complex. Within this complex, PDK1 phosphorylates PKCθ, which in turn phosphorylates CARMA1 to relieve intramolecular autoinhibition. This allows CARMA1 to oligomerize, associate with MALT1 and Bcl10, and lead to MAPK JNK2 and IKK activation, promoting NFκB nuclear translocation and NFκB-dependent transcription (45). Dlgh1 has been demonstrated to be tyrosine phosphorylated in T lymphocytes,

however the functional relevance of this phosphorylation event has not been explored (24). Numerous studies in epithelial and neuronal cells have demonstrated that Dlgh1 phosphorylation alters Dlgh1 location (42, 46), protein abundance (47, 48) and function (49). Thus, we explored the possibility that phosphorylation of Dlgh1, like phosphorylation of CARMA1, may serve as a molecular "switch" that allows for the opening or positioning of the Dlgh1 scaffold to promote Dlgh1-mediated signaling (Chapter 3).

MOVING TOWARDS IN VIVO DLGH1 T CELL FUNCTIONALITY: DEVELOPMENT OF DLGH1 KNOCKOUT MICE

While we and others have defined a role for Dlgh1 in T cell signaling, cytoskeletal reorganization and effector responses, the majority of these studies have utilized siRNA-mediated knockdown methodologies which have inherit limitations. Namely, siRNA-mediated knockdown is usually transient, confines studies to activated T cells and precludes the evaluation of T cell development. Thus, to build on and extend the current understanding of Dlgh1 as a molecular scaffold that guides TCR signal specificity and cellular function, we, in collaboration with the Russell and Burkhardt laboratories developed three independent *dlgh1*-knockout mouse strains. Because mice harboring germline *dlgh1*-null mutations show several developmental abnormalities and die perinatally (50, 51) we generated mice in which *dlgh1* expression was specifically deleted in the hematopoietic compartment. Utilizing these mice we assessed the role of Dlgh1 in T cell development and peripheral T cell signaling, cytoskeletal reorganization, proliferation and cytokine production (Chapter 4). Furthermore, we also developed an inducible Dlgh1 knockout mouse model that allowed us to assess the functional

consequences of Dlgh1 deletion in mature peripheral T lymphocytes, once proper T cell development had occurred (Chapter 5).

AIMS OF DISSERTATION

This dissertation explores the molecular mechanisms of Dlgh1 regulation in CD8+ T cells and investigates the role of Dlgh1 in T cell activation and effector function in Dlgh1 knockout mice. Chapter 2 explores the post-transcriptional regulation of Dlgh1 via alternative splicing. Specifically investigating the role of Dlgh1 alternative splice variants in guiding TCR signal specificity to control p38-dependent and -independent CD8+ CTL effector functions. Chapter 3 assesses Dlgh1 tyrosine phosphorylation as a method to control the alternative p38 pathway in CD8+ T cells. Chapters 4 and 5 explore the functional role of Dlgh1 in T lymphocytes utilizing various Dlgh1 knockout mouse models.

Figure 1-1. Dlgh1 is a multi-domain protein with several sites of alternative splicing. Dlgh1 contains the following core MAGUK domains: three PDZ domains, one SH3 domain, and one GUK domain. Dlgh1 is unique among other MAGUK proteins because it has multiple known sites of alternative splicing. The first site is at the N-terminus where an L27β oligomerzation or CXCα palmitoylation domain can be expressed. The second site of alternative splicing is upstream of the first PDZ domain. Here the proline-rich i1A/i1B domains can be expressed. The last site of splicing is between the SH3 and GUK domains, often referred to as the HOOK domain. Within this region the i2, i3, i4 and or i5 exons can be expressed.

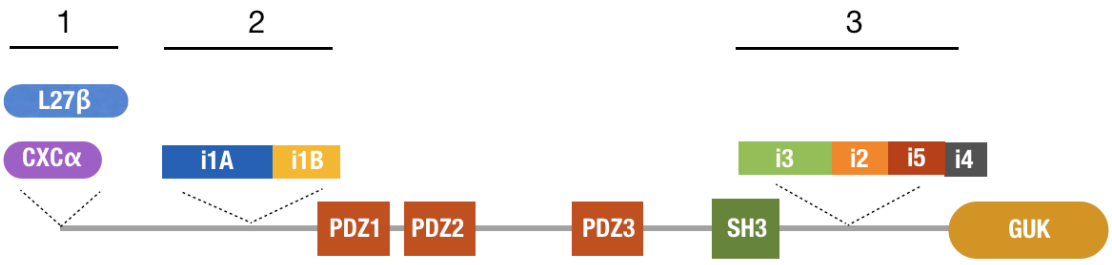
1
2
3
L27β
CXCα
i1A
i1B
i3
i2
i5
i4
PDZ1
PDZ2
PDZ3
SH3
GUK

Figure 1-2. Dlgh1 mediates the alternative p38 pathway.

TCR engagement leads to the recruitment of Dlgh1 to the TCR complex. At the TCR, Dlgh1 binds Lck allowing for activation of ZAP70. Once activated, ZAP70 can phosphorylate Dlgh1-partnered p38 on tyrosine 323 (Y323) enabling p38 autophosphorylation on threonine 180 (T180). This results in serine 54 phosphorylation of the transactivating domain of NFAT, leading to induction of NFAT responsive genes.

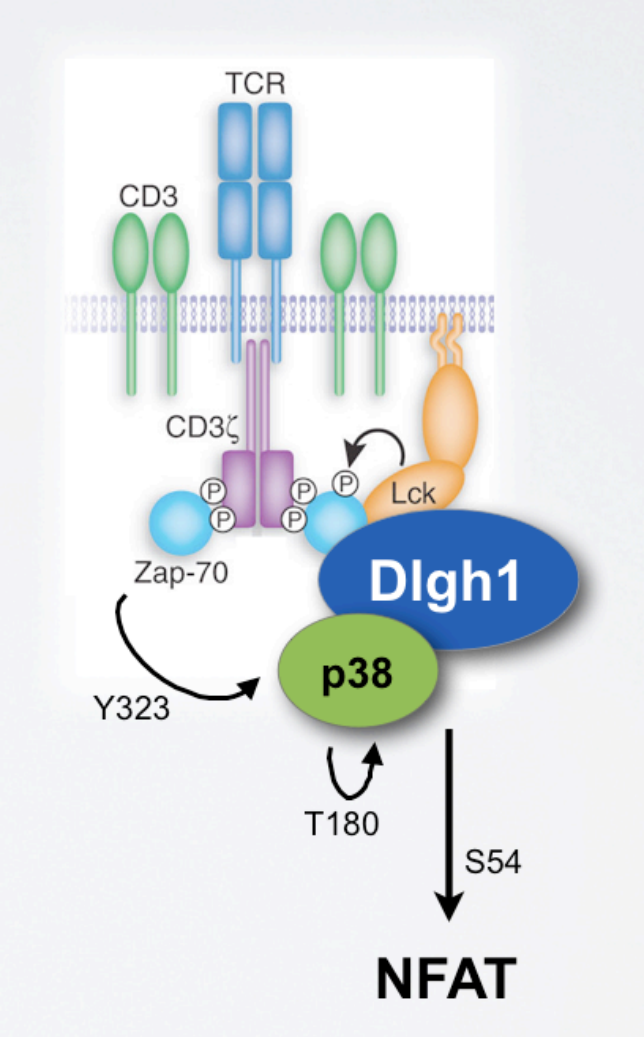

Adapted from Lineberry N and Fathman CG. Nature Immunology (2006) 7:369-370

REFERENCES

1. Blander JM SL (2012) Beyong pattern recognition: five immune checkpoints for scaling the microbial threat. *Nature Immunology Reviews* 12(3):215-225.

2. Rosenthal AS & Shevach EM (1973) Function of macrophages in antigen recognition by guinea pig T lymphocytes. I. Requirement for histocompatible macrophages and lymphocytes. *The Journal of experimental medicine* 138(5):1194-1212.

3. Joshi NS*, et al.* (2007) Inflammation directs memory precursor and short-lived effector CD8(+) T cell fates via the graded expression of T-bet transcription factor. *Immunity* 27(2):281-295.

4. King CG*, et al.* (2012) T cell affinity regulates asymmetric division, effector cell differentiation, and tissue pathology. *Immunity* 37(4):709-720.

5. Corse E, Gottschalk RA, & Allison JP (2011) Strength of TCR-Peptide/MHC Interactions and In Vivo T Cell Responses. *Journal of immunology (Baltimore, Md : 1950)* 186(9):5039-5045.

6. Zhang N & Bevan MJ (2011) CD8+ T Cells: Foot Soldiers of the Immune System. *Immunity* 35(2):161-168.

7. Nakayamada S, Takahashi H, Kanno Y, & O'Shea JJ (2012) Helper T cell diversity and plasticity. *Current opinion in immunology* 24(3):297-302.

8. Chang JT*, et al.* (2007) Asymmetric T lymphocyte division in the initiation of adaptive immune responses. *Science* 315(5819):1687-1691.

9. Guy CS*, et al.* (2013) Distinct TCR signaling pathways drive proliferation and cytokine production in T cells. *Nature Immunology* 14(3):262-270.

10. Guy CS & Vignali DAA (2009) Organization of proximal signal initiation at the TCR:CD3 complex. *Immunological reviews* 232(1):7-21.

11. Smith-Garvin JE, Koretzky GA, & Jordan MS (2009) T cell activation. *Annu Rev Immunol* 27:591-619.

12. Grakoui A*, et al.* (1999) The immunological synapse: a molecular machine controlling T cell activation. *Science* 285(5425):221-227.

13. Lee K-H*, et al.* (2003) The immunological synapse balances T cell receptor signaling and degradation. *Science* 302(5648):1218-1222.

14. Huse M, Quann EJ, & Davis MM (2008) Shouts, whispers and the kiss of death: directional secretion in T cells. *Nat Immunol* 9(10):1105-1111.

15. Stinchcombe JC, Majorovits E, Bossi G, Fuller S, & Griffiths GM (2006) Centrosome polarization delivers secretory granules to the immunological synapse. *Nature* 443(7110):462-465.

16. Shaw AS & Filbert EL (2009) Scaffold proteins and immune-cell signalling. *Nat Rev Immunol* 9(1):47-56.

17. Kadlecek TA*, et al.* (1998) Differential requirements for ZAP-70 in TCR signaling and T cell development. *Journal of immunology (Baltimore, Md : 1950)* 161(9):4688-4694.

18. Zhang W*, et al.* (1999) Essential role of LAT in T cell development. *Immunity* 10(3):323-332.

19. Wu GF*, et al.* (2011) Conditional deletion of SLP-76 in mature T cells abrogates peripheral immune responses. *European journal of immunology* 41(7):2064-2073.

20. Combs J*, et al.* (2006) Recruitment of dynein to the Jurkat immunological synapse. *Proceedings of the National Academy of Sciences of the United States of America* 103(40):14883-14888.

21. Zeng R*, et al.* (2003) SLP-76 coordinates Nck-dependent Wiskott-Aldrich syndrome protein recruitment with Vav-1/Cdc42-dependent Wiskott-Aldrich syndrome protein activation at the T cell-APC contact site. 171(3):1360-1368.

22. Rebeaud F, Hailfinger S, & Thome M (2007) Dlgh1 and Carma1 MAGUK proteins contribute to signal specificity downstream of TCR activation. *Trends Immunol* 28(5):196-200.

23. Round JL*, et al.* (2005) Dlgh1 coordinates actin polymerization, synaptic T cell receptor and lipid raft aggregation, and effector function in T cells. *J Exp Med* 201(3):419-430.

24. Hanada T, Lin L, Chandy KG, Oh SS, & Chishti AH (1997) Human homologue of the Drosophila discs large tumor suppressor binds to p56lck tyrosine kinase and Shaker type Kv1.3 potassium channel in T lymphocytes. *J Biol Chem* 272(43):26899-26904.

25. Dimitratos SD, Woods DF, Stathakis DG, & Bryant PJ (1999) Signaling pathways are focused at specialized regions of the plasma membrane by scaffolding proteins of the MAGUK family. 21(11):912-921.

26. Cavatorta AL*, et al.* (2011) Regulation of translational efficiency by different splice variants of the Disc large 1 oncosuppressor 5'-UTR. *The FEBS journal* 278(14):2596-2608.

27. Schlüter OM, Xu W, & Malenka RC (2006) Alternative N-terminal domains of PSD-95 and SAP97 govern activity-dependent regulation of synaptic AMPA receptor function. *Neuron* 51(1):99-111.

28. McLaughlin M, *et al.* (2002) The distribution and function of alternatively spliced insertions in hDlg. *J Biol Chem* 277(8):6406-6412.

29. Godreau D, Vranckx R, Maguy A, Goyenvalle C, & Hatem SN (2003) Different isoforms of synapse-associated protein, SAP97, are expressed in the heart and have distinct effects on the voltage-gated K+ channel Kv1.5. *J Biol Chem* 278(47):47046-47052.

30. Xavier R, *et al.* (2004) Discs large (Dlg1) complexes in lymphocyte activation. *J Cell Biol* 166(2):173-178.

31. Mittelstadt PR, Yamaguchi H, Appella E, & Ashwell JD (2009) T Cell Receptor-mediated Activation of p38 by Mono-phosphorylation of the Activation Loop Results in Altered Substrate Specificity. *Journal of Biological Chemistry* 284(23):15469-15474.

32. Round JL, *et al.* (2007) Scaffold protein Dlgh1 coordinates alternative p38 kinase activation, directing T cell receptor signals toward NFAT but not NF-kappaB transcription factors. *Nat Immunol* 8(2):154-161.

33. Zanin-Zhorov A, *et al.* (2012) Scaffold protein Disc large homolog 1 is required for T-cell receptor-induced activation of regulatory T-cell function. *Proceedings of the National Academy of Sciences of the United States of America* 109(5):1625-1630.

34. Lasserre R, *et al.* (2010) Ezrin tunes T-cell activation by controlling Dlg1 and microtubule positioning at the immunological synapse. *EMBO J.*

35. Lue RA, Brandin E, Chan EP, & Branton D (1996) Two independent domains of hDlg are sufficient for subcellular targeting: the PDZ1-2 conformational unit and an alternatively spliced domain. *J Cell Biol* 135(4):1125-1137.

36. Adachi K & Davis MM (2011) T-cell receptor ligation induces distinct signaling pathways in naive vs. antigen-experienced T cells. *Proceedings of the National Academy of Sciences of the United States of America* 108(4):1549-1554.

37. Jirmanova L, Sarma DN, Jankovic D, Mittelstadt PR, & Ashwell JD (2009) Genetic disruption of p38alpha Tyr323 phosphorylation prevents T-cell receptor-mediated p38alpha activation and impairs interferon-gamma production. *Blood* 113(10):2229-2237.

38. Morales-Tirado V, *et al.* (2004) Cutting edge: selective requirement for the Wiskott-Aldrich syndrome protein in cytokine, but not chemokine, secretion by CD4+ T cells. *J Immunol* 173(2):726-730.

39. De Meester J, Calvez R, Valitutti S, & Dupré L (2010) The Wiskott-Aldrich syndrome protein regulates CTL cytotoxicity and is required for efficient killing of B cell lymphoma targets. *Journal of Leukocyte Biology* 88(5):1031-1040.

40. Marangoni F*, et al.* (2007) WASP regulates suppressor activity of human and murine CD4(+)CD25(+)FOXP3(+) natural regulatory T cells. *J Exp Med* 204(2):369-380.

41. Narayan N, Massimi P, & Banks L (2008) CDK phosphorylation of the discs large tumour suppressor controls its localisation and stability. *J Cell Sci* 122(Pt 1):65-74.

42. Massimi P, Narayan N, Cuenda A, & Banks L (2006) Phosphorylation of the discs large tumour suppressor protein controls its membrane localisation and enhances its susceptibility to HPV E6-induced degradation. *Oncogene* 25(31):4276-4285.

43. Marcette J, Hood IV, Johnston CA, Doe CQ, & Prehoda KE (2009) Allosteric control of regulated scaffolding in membrane-associated guanylate kinases. *Biochemistry* 48(42):10014-10019.

44. Nelson WJ (2003) Adaptation of core mechanisms to generate cell polarity. *Nature* 422(6933):766-774.

45. Rawlings DJ, Sommer K, & Moreno-García ME (2006) The CARMA1 signalosome links the signalling machinery of adaptive and innate immunity in lymphocytes. 6(11):799-812.

46. Koh YH, Popova E, Thomas U, Griffith LC, & Budnik V (1999) Regulation of DLG localization at synapses by CaMKII-dependent phosphorylation. *Cell* 98(3):353-363.

47. Mantovani F, Massimi P, & Banks L (2001) Proteasome-mediated regulation of the hDlg tumour suppressor protein. *J Cell Sci* 114(Pt 23):4285-4292.

48. Mantovani F & Banks L (2003) Regulation of the discs large tumor suppressor by a phosphorylation-dependent interaction with the beta-TrCP ubiquitin ligase receptor. *J Biol Chem* 278(43):42477-42486.

49. Mauceri D, Gardoni F, Marcello E, & Di Luca M (2007) Dual role of CaMKII-dependent SAP97 phosphorylation in mediating trafficking and insertion of NMDA receptor subunit NR2A. *J Neurochem* 100(4):1032-1046.

50. Caruana G & Bernstein A (2001) Craniofacial dysmorphogenesis including cleft palate in mice with an insertional mutation in the discs large gene. *Mol Cell Biol* 21(5):1475-1483.

51. Mahoney ZX*, et al.* (2006) Discs-large homolog 1 regulates smooth muscle orientation in the mouse ureter. *Proceedings of the National Academy of Sciences of the United States of America* 103(52):19872-19877.

CHAPTER TWO

Dlgh1 splice variants regulate p38-dependent and –independent CTL effector functions

ABSTRACT

CD8+ cytotoxic T lymphocytes (CTLs) mediate lytic factor degranulation and production of proinflammatory cytokines. Here we investigated how Discs large homolog 1 (Dlgh1) alternative splice variants serve as molecular conduits to drive these distinct CTL responses. We discovered that at least two distinct Dlgh1 protein variants exist in T cells due to alternative splicing: Dlgh1 L27β-i1Ai1B-i3i5 (Dlgh1 AB) and Dlgh1-L27β-i1B-i3i5 (Dlgh1 B). Dlgh1 AB, but not Dlgh1 B was found to control p38-dependent proinflammatory cytokine production by binding Lck, promoting p38 phosphorylation and enhancing T cell receptor (TCR)-induced IFNγ and TNFα gene expression. In contrast, both Dlgh1 AB and Dlgh1 B enhanced antigen-induced degranulation, which was found to be largely p38-independent as pharmacological inhibition of p38 had little effect on actin polymerization, granzyme B exocytosis or degranulation. Finally, the SH3-domain of Dlgh1 and the actin regulator WASp were found to be necessary for Dlgh1-mediated degranulation. These results demonstrate that CD8+ CTLs express unique Dlgh1 scaffolds with differential capacities to nucleate p38-dependent and –independent pathways to promote TCR-induced proinflammatory cytokine production and degranulation.

INTRODUCTION

CD8+ cytotoxic T lymphocytes (CTLs) are critical components of the adaptive immune response due to their ability to induce lytic factor degranulation and proinflammatory cytokine production. Although the combinatorial use of these two functions is often required to efficiently clear intracellular pathogens, these CTL activities are not always coordinately invoked (1). In fact, these effector functions can be selectively inhibited during chronic viral infection, suggesting that signaling complexes downstream of the T cell receptor (TCR) may be uniquely formed to guide degranulation and proinflammatory cytokine production (2). How proximal TCR signals are specifically channeled to produce precise cellular behaviors is just beginning to be elucidated (3).

Scaffold proteins couple extracellular receptors to intracellular signaling pathways, and therefore have the potential to manipulate functional outcomes of receptor engagement (4). Discs large homolog 1 (Dlgh1), a membrane associated guanylate kinase (MAGUK) scaffold protein, localizes to the immunological synapse (IS) during T cell activation where it regulates cytoskeletal and transcriptional activities (5). Dlgh1 mediates the alternative p38 pathway by directing TCR proximal tyrosine kinases Lck and ZAP70 toward p38 activation and NFAT-dependent transcription (6). Cytoskeletally, Dlgh1 associates with WASp, Ezrin and GAKIN, and promotes actin polymerization, TCR and lipid raft reorganization, MTOC dynamics, and CTL cytotoxicity (5-9). These activities are hypothesized to require specific Dlgh1 domains that allow for binding, recruitment and juxtaposition of these signaling and cytoskeletal mediators.

Dlgh1 is a multi-domain protein with three PSD95/Dlg/ZO-1 (PDZ) domains, a Src homology 3 (SH3) domain and a catalytically-inactive guanylate kinase (GUK) domain. In addition to these constant MAGUK domains Dlgh1 has at least four areas of alternative splicing, one within the 5'UTR that regulates *dlgh1* translation and three

within coding regions (10-14). Upstream of PDZ1, i1A and/or i1B can be spliced into Dlgh1. Between SH3 and GUK, often referred to as the HOOK domain, exons i2, i3, i4 and/or i5 can be expressed (12). Finally, either a recently identified CXCα palmitoylation domain or the L27β oligomerization domain can be alternatively spliced at the N-terminus (11). Despite having described functions in epithelial, neuronal and cardiac cells, to our knowledge there have been no reports on Dlgh1 splice variants in any hematopoietic cell type (11, 13, 15).

Here we report that mouse CD8+ T cells utilize Dlgh1 splice variants as molecular conduits to guide degranulation and transcriptional activation of proinflammatory cytokines. We discovered that at least two Dlgh1 protein variants exist in T cells due to alternative splicing: Dlgh1 L27β-i1Ai1B-i3i5 (Dlgh1 AB) and Dlgh1-L27β-i1B-i3i5 (Dlgh1 B). We found that both Dlgh1 AB and Dlgh1 B were capable of actin-mediated, p38-independent degranulation, and that this activity depended on the SH3-domain of Dlgh1 and WASp. However, only Dlgh1 AB drove proinflammatory cytokines production by binding Lck, promoting alternative p38 activation and downstream NFAT-mediated upregulation of IFNγ and TNFα gene expression. Our results provide insight into how CTLs may form distinct molecular platforms required to nucleate signaling pathways for specific CTL effector functions.

MATERIALS and METHODS

Mice

OT-1 TCR transgenic mice (16) were maintained and used in accordance with the University of California Los Angeles Chancellor's Animal Research Committee

Antibodies and Reagents

For primary T cell stimulations and re-stimulations anti-CD3, clone 145-2C11 (BD 553057) and anti-CD28, clone 37.51 (BD 553295) were used. For immunoprecipitations and immunoblotting Mouse anti-Dlg1 (BD 610875), Rabbit anti-p38, clone C20 (Santa Cruz Biotechnology sc-535), Mouse anti-Lck, clone 3A5 (Santa Cruz Biotechnology sc-433), Mouse anti-WASp, clone B-9 (Santa Cruz Biotechnology, sc-13139), Rabbit anti-phospho-p38 (T180/Y182), clone D3F9 (Cell Signaling 4511), Donkey Anti-Mouse IgG-HRP (Jackson ImmunoResearch 715-035-150), and Donkey-Anti-Rabbit IgG-HRP (Santa Cruz Biotechnology sc-2305) were used. For flow cytometry, Rat anti-CD8b-PE, clone H35-17.2 (BD 550798), Alexa Fluor647 Mouse anti-p38 MAPK (pT180/pY182), clone 36 (BD 612595), Rat anti-IFNγ-APC, clone XMG1.2 (BD 554413), Rat anti-IL-2-APC, clone JES6-5H4 (BD 554429), Rat anti-CD107a-APC, clone 1D4B (BD 560646), Alexa Fluor647 Phalloidin (Molecular Probes, Invitrogen A22287), and Alexa Fluor647 AffiniPure F(ab)2 Donkey Anti-Mouse IgG (Jackson ImmunoResearch 715-606-150) were used. For inhibitors studies Insolution SB203580 (Calbiochem 559398), cytochalasin D (Sigma C8273) and DMSO (Sigma D2650) were used. For antigen experiments $OVA_{257-264}$ peptide from AnaSpec (#60193) was used.

Cell Culture

Spleen and lymph node cells were obtained from 8- to 14-week old OT-1 TCR transgenic

mice. These mice have CD8+ T cell that recognize $OVA_{257-264}$ in the context of H-$2K^b$. CD8+ cells were sorted using CD8a (Ly-2) microbeads (Miltenyi 130-049-401). Sorted CD8+ T cells were stimulated in vitro with plate-bound anti-CD3/anti-CD28 or MEF.B7.OVA antigen presenting cells for 48-72 hrs in complete media composed of RPMI 1640 medium with 10% FCS, sodium pyruvate, 50nM β-meraptoethanol, penicillin, streptomycin and glutamine followed by expansion in rIL-2 (100U/mL) for an additional 3-4 days to generate primary mouse CTLs. BI-141 murine T cell hybridoma cells were maintained in complete media. OT-1 hybridoma T cells were maintained as in (17). MEF.B7.OVA cells stably expressing H-$2K^b$, B7.1, and $OVA_{257-264}$ where maintained as in (5). H-$2K^b$ EG.7 cells constitutively expressing $OVA_{257-264}$ and EL-4 cells were maintained in as in (18)

DNA Constructs

Retroviral constructs pMSCV-GFP-Puro (MGP) and pMSCV-IRES-GFP (MIG) have been previously described (19, 20). GFP was removed from the MGP construct and replaced with dsRED using the *BglII* and *NotI* restriction sites, this vector was named MRP. The Invitrogen Block-IT miR RNAi Designer was used to predict siRNA sequences against WASp or specific Dlgh1 regions: L27β, i1A, i1B, i3 and 3′UTR. These sequences were cloned into the MGP or MRP microRNA-based knockdown vectors using a previous published strategy and the sequences can be found in Table 2-1 (21). MGP constructs were renamed miR-control, miR L27β, miR i1A, miR i1A*, miR i1B, miR i3, and miR i3*. The MRP constructs were renamed Control, Dlgh1 KD (miR 3′UTR), WASp KD 1 and WASp KD 2. To generate MIG-Dlgh1 splice variant constructs we first PCR amplified Dlgh1 L27β-i1Ai1B-i2i5 from the pSport vector used in (6) and cloned it into MIG using the *XhoI* and *EcoRI* restriction sites. Next, we took cDNA from primary antigen-

experienced CD8+ OT-1 TCR transgenic T cells and amplified either N-terminal Dlgh1 fragments containing the i1A/i1B splice region or C-terminal Dlgh1 fragments containing the i2/i3/i4/i5 splice region and cloned these fragments into the MIG-Dlgh1 L27β-i1A-i1B i2i5 construct using either *XhoI/BstBI* (N-terminal fragments) or *BstBI/EcoRI* (C-terminal fragments) restriction sites. Note, the BstBI restriction site was chosen because it was within Dlgh1 and divided Dlgh1 into two fragments (approximately 1700bp and 1100bp) with different splicing regions in each. The clones were screened using i1A/i1B and i2/i3/i4/i5 RT-PCR primer sets and sent out for sequencing to confirm the splice variant combinations. Once all four possible Dlgh1 splice variant combinations were cloned into MIG, Dlgh1 L27β-i1Ai1B-i3i5 (Dlgh1 AB) and Dlgh1-L27β-i1B-i3i5 (Dlgh1 B) were cloned into pGEX 4T-1 using *EcoRI* and *SalI* restriction sites. To generate Dlgh1 i1B truncations we used Dlgh1-L27β-i1B-i3i5 as a template and used a *XhoI* forward primer and different *EcoRI* reverse primers that terminated the Dlgh1 sequence at various lengths. The primers set used for Dlgh1 truncation synthesis can be found in Table 2-2.

Retrovirus Production and Infections

293T cells were transfected with pCL-Eco and either knockdown or overexpression constructs. Transfection was performed with TransIT 293 (Mirus 2705) per manufacturer's instructions. After 48 hrs, viral supernatant was harvested, 0.45µm filtered and used to infect activated primary OT-1 cells or T cell-lines via spin infection in the presence of polybrene (8µg/mL) at 1250*g* for 90 mins at room temperature. For primary cell infections, T cells were infected after 48-72 hrs of stimulation with anti-CD3/anti-CD28. Two spin-infections were performed on cells 24 hrs apart. Infected primary T cells were used for functional assays 24-48 hrs after the last spin-infection.

GST-precipitations, Immunoprecipitations and Immunoblotting

For GST precipitation assays, lysates from stimulated or unstimulated OT-1 hybridoma cells were incubated for 2 hrs at 4°C with purified GST-alone or GST-Dlgh1 fusion proteins. GST-precipitates were washed and then run on SDS-PAGE. Stimulated OT-1 hybridoma lysates were generated by incubating 4 x10^7 cells with anti-CD3 and anti-CD28 followed by antibody crosslinking using donkey anti-hamster secondary for 15 mins at 37°C. Cells were lysed using IP Lysis buffer (Pierce) in the presence of protease and phosphatase inhibitors (Pierce) and cleared by centrifugation. For immunoprecipitations, lysates from stimulated or unstimulated OT-1 T cell hybridoma cells were first pre-cleared by incubation with 20µL 50% (vol/vol) protein G sepharose (GE Healthcare 17-51320-01) in PBS for 2 hrs at 4°C. Sepharose beads were removed and cleared lysates were incubated with 2µg anti-Dlgh1 for 1 hr at 4°C. 40µL of 50% (vol/vol) protein G sepharose slurry in PBS was added and allowed to incubate overnight at 4°C. Immunoprecipiates were washed to remove unbound proteins and analyzed via SDS-PAGE. For all other protein isolations, cells were lysed on ice with TNE buffer (50mM Tris pH 6.8, 1% NP-40, and 20mM EDTA) containing 1X protease inhibitor cocktail (Pierce 87786) and cleared by centrifugation. Proteins were separated by SDS-PAGE and transferred to nitrocellulose. Membranes, blocked with TBS plus 5% milk and 0.1% Tween-20, were incubated with primary antibodies (1:1000) overnight at 4°C, followed by incubation with HRP-conjugated secondary antibodies (1:5000) for either 4 hours (Dlgh1 blots) or 1 hour (all others) at room temperature. Signals were detected by enhanced chemiluminescence reagents (Western Lightening *Plus*-ECL; Pierce NEL104001EA).

RT-PCR and qPCR

T cells were stimulated with platebound anti-CD3 (2μg/mL) and anti-CD28 (2μg/mL) antibodies or left unstimulated. RNA was isolated using TRIZOL reagent. RNA (2.0 μg) was reverse-transcribed using Superscript III (Invitrogen) according to the manufacture's instructions with oligo(dT) primer in 20uL reactions. cDNA was diluted 1:5 with DEPC-H20 and used for subsequent RT-PCR and qPCR analysis. For RT-PCR, 2.0μL of cDNA was used for PCR amplification with annealing temperatures of 62°C and 58°C for the i1A/i1B and i2/i3 primer sets respectfully. For qPCR, Sybrgreen-based quantitative PCR analysis was performed on the iCycler BioRad instrument according to the manufacturer's instructions (Bio-Rad). Amplification conditions were: 95°C for 3 minutes, followed by 40 cycles of 95°C for 30 s and 60°C for 30 s. For all experiments, mRNA was normalized to L32. Primers used for RT-PCR and qPCR analysis can be found in Table 2-2.

DNA Sequencing

PCR products from RT-PCRs were gel extracted using the QIAquick Gel Extraction kit by QIAGEN. Purified products were sequenced by Sanger sequencing (Laragen Sequencing and Genotyping Service; Culver City, CA)

ELISAs

To detect protein expression of IFNγ, TNFα, IL-2, and Granzyme B in the supernatant of restimulated CTLs ELISAs were performed with cytokine- and lytic factor-specific Ready-Set-Go kits from eBioscience (88-7334, 88-7324, 88-7024, 88-8022) and carried out according to the manufacturer's instructions

Degranulation

Primary mouse OT-1 CTLs or OT-1 hybridoma T cells and EG.7 target cells were co-cultured (1:1) in 200μL of OT-1 hyridoma media in 96-well plates at 37°C, in the presence of 1.0μL CD107a-APC, 1.0μL GolgiPLUG and 1.0μL GolgiSTOP. Cells were harvested, surface stained with CD8b-PE in FACS buffer, washed, fixed in 2% paraformaldehyde and then analyzed using a BD FACS-Calibur

Actin Polymerization

Primary mouse OT-1 CTLs were briefly spun onto adherent MEF.B7.OVA cells in 12-well plates and placed in an incubator for 5 or 15 minutes. Cells were placed on ice and ice cold PBS was added. Cells were quickly harvested, spun down and resuspended in 200μL of BD Cytofix/Cytoperm (BD Bioscience) for overnight fixation and permeabilization at 4°C. Cells were then washed in BD Permeabilization wash solution, stained for 1 hr with Alexa Fluor 647 phalloidin (0.3 units) and CD8b-PE (1:200) in 200μL BD Permeabilization wash solution, washed and fixed in 2% paraformaldhehyde. Data was collected using a BD FACS-Calibur.

Intracellular Phospho-p38

For intracellular phospho-p38 analysis, T cells were stimulated with plate-bound anti-CD3 (5μg/mL) and anti-CD28 (20μg/mL) by quickly spin-contacting the cells to plates. After the stimulation, cells were immediately fixed in 4% paraformaldehyde for 15 minutes on ice. Cells were then harvested, washed with FACS buffer (PBS + 3% FBS + 0.1% sodium azide), and permeabilized with ice cold methanol overnight at 4°C. Cells were then stained with Alexa Fluor647 Mouse anti-p38 MAPK (pT180/pY182) for 30 mins at room temperature, washed and immediately analyzed using a BD FACS-Calibur.

Intracellular Cytokines

Primary mouse OT-1 CTLs were restimulated with either platebound anti-CD3 (2µg/mL) and anti-CD28 (2µg/mL) antibodies, EG.7 cells, or EL-4 cells pulsed with various concentrations of $OVA_{257-264}$ peptide for 4 hrs in the presence of GolgiPLUG (BD 555029). Cells were surface stained with CD8b-PE in FACS wash buffer (PBS + 3% FCS + 0.1% sodium azide) prior to overnight fixation and permeabilization with BD Cytofix/Cytoperm (BD 51-2090KZ) at 4°C. Cells were then washed in BD Permeabilization wash solution, stained for 30 mins with IFNγ-APC or IL-2-APC, washed and data collected using a BD FACS-Calibur.

Intracellular Dlgh1 and WASp

For intracellular Dlgh1 and WASp analysis, T cells were fixed and permeabilized with the Foxp3 Fixation/Permeabilization buffer set (eBioscience 00-5523-00), washed and stained for 30 mins at 4°C with primary antibodies (Dlgh1 or WASp at 1:1000). Cells were washed, stained for 30 mins at 4°C with Alexa Fluor647 AffiniPure F(ab)2 Donkey Anti-Mouse IgG (1:5000). Cells were then washed, fixed in 2% paraformaldehyde and analyzed with a BD FACS-Caliber.

Statistical Analysis

Standard deviation was calculated using Numbers (Apple). Statistical significance was determined by performing a two-tailed t test. p values < 0.05 were considered significant

RESULTS

T cells Express Two Distinct Dlgh1 Protein Variants Due to Alternative Splicing

To investigate if alternative splicing of *dlgh1* occurs in T cells we developed PCR primers that flanked the i1A/i1B or i2/i3/i4/i5 splicing regions (Figure 2-1A). We preformed RT-PCR on cDNA obtained from murine T cells, followed by DNA sequencing of individual PCR products. Assessing the i1A/i1B region we observed two RT-PCR products in all T cells surveyed, which based on size and DNA sequencing were found to be the i1B-only and i1Ai1B exon combinations (Figure 2-1B, top). All T cells surveyed also expressed the i3i5 and i2i5 splice combinations (Figure 2-1B, middle). Finally, all T cells expressed L27β (Figure 2-1B, bottom); CXCα was not assessed. Based on these results, we concluded that at least four possible *dlgh1* transcripts were expressed in T cells, with differences being in the inclusion of i1A and the inclusion of i3 or i2 (Figure 2-2B). Similar results were also seen in other hematopoietic and non-hematopoietic cells (Figure 2-2C).

To determine which *dlgh1* transcripts were expressed on the protein level, all four possible splice variant combinations were cloned into a retroviral vector and used to infect hybridoma T cells which were analyzed for Dlgh1 protein expression via SDS-PAGE. Comparing migration distances of the overexpressed Dlgh1 variants to endogenous Dlgh1 which runs as a protein doublet (Dlgh1-130kDa and Dlgh1-120 kDa), Dlgh1-130kDa corresponded best to Dlgh1 L27β-i1Ai1B-i3i5 or Dlgh1 L27β-i1Ai1B-i2i5, while Dlgh1-120kDa corresponded best to Dlgh1 L27β-i1B-i3i5 (Figure 2-1C). To determine which of these Dlgh1 variants were endogenously expressed, we selectively targeted L27β, i1A, i1B and i3 for knockdown. We were unable to target i2 as it was only 36 bp. Targeting L27β, i1B or i3 completely ablated Dlgh1 protein levels, indicating that all protein variants of Dlgh1 in T cells expressed these exons. Interestingly, when i1A was

targeted a selective loss of Dlgh1-130kDa was observed, indicating that Dlgh1-130kDa contained i1A, while Dlgh1-120kDa did not (Figure 2-1D). Similar results were also observed in 3T3 fibroblasts (Figure 2-2D). Taken together, these data demonstrated that at least two protein variants of Dlgh1 are expressed in T cells due to alternative splicing: Dlgh1-L27β-i1Ai1B-i3i5 (Dlgh1 AB) and Dlgh1-L27β-i1B-i3i5 (Dlgh1 B) (Figure 2-1E).

Dlgh1 Splice Variants Differentially Regulate the Alternative p38 Pathway

Dlgh1 AB differs from Dlgh1 B by the presence of the proline-rich i1A domain (Figure 2-2A). The i1A domain is predicted to bind the SH3-domain of Lck, which we previously showed to be necessary for Dlgh1 association (5, 22). To determine if the i1A-domain was required for this association we performed GST-pulldown assays. We found that both Dlgh1 AB and Dlgh1 B pulled-down the PDZ binding protein p38, but only Dlgh1 AB pulled-down Lck (Figure 2-3A). Lck activity is required for ZAP70-mediated alternative p38 phosphorylation leading to NFAT-dependent transcription (6). Accordingly, overexpression of Dlgh1 AB enhanced NFATc1 gene expression, while Dlgh1 B did not (Figure 2-3B). This enhanced NFATc1 gene expression was prevented by pharmacological inhibition of p38 activity using SB203580. Further, overexpression of Dlgh1 AB or Dlgh1 B did not greatly affect IkBα gene expression (Figure 2-3B), despite recent findings indicating that Dlgh1 negatively regulates NFκB via PTEN stabilization and inhibition of Akt in human regulatory T cells (Tregs) (23). To directly assess the role of Dlgh1 splice variants in p38 activation we measured p38 phosphorylation (T180/Y182) in response to CD3/CD28 crosslinking. We generated stable *dlgh1* knockdown OT-1 hybridoma T cells in which the 3'UTR of *dlgh1* transcripts was targeted, allowing for selective re-expression of Dlgh1 AB or Dlgh1 B (Figure 3-5C). We found Dlgh1 AB enhanced, while Dlgh1 B inhibited TCR-induced p38 phosphorylation, despite

both Dlgh1 variants co-immunoprecipitating p38 (Figure 2-3C). Collectively, these results demonstrate that Dlgh1 AB, but not Dlgh1 B, promotes alternative p38 activation through association with Lck.

Dlgh1 AB Promotes p38-Dependent Transcription of Proinflammatory Cytokines

The alternative p38 pathway controls T cell mediated autoimmunity and inflammation (6, 24-26). Thus we hypothesized that Dlgh1 splice variants may have differential impacts on proinflammatory cytokine production in murine CD8+ CTLs. Overexpression of Dlgh1 AB in primary CD8+ OT-1 T cells selectively upregulated TCR-induced IFNγ and TNFα gene expression, while not interfering with IL-2 or granzyme B. In contrast, Dlgh1 B overexpression did not enhance IFNγ, TNFα, IL-2 or granzyme B expression (Figure 2-4B). Furthermore, pharmacological inhibition of p38 activity prevented the enhanced proinflammatory gene expression seen with Dlgh1 AB overexpression (Figure 2-5B).

Additionally, specific knockdown of Dlgh1 AB reduced IFNγ and TNFα expression to levels equivalent to total Dlgh1 knockdown, while again not affecting IL-2 or granzyme B expression (Figure 2-6C). Similar results were seen with intracellular cytokine analysis, as Dlgh1 knockdown prevented optimal IFNγ production, but did not affect IL-2 in response to anti-CD3/anti-CD28 (Figure 2-7B). Production of IFNγ was also defective in response to antigen at various concentrations (Figure 2-7C). Knockdown of Dlgh1 AB also reduced intracellular p38 phosphorylation (T180/Y182) to levels similar to total Dlgh1 knockdown (Figure 2-6E, Figure 2-6F). Collectively, these results demonstrate that Dlgh1 AB selectively promotes p38-dependent proinflammatory cytokine gene expression, while Dlgh1 B does not. Furthermore, these data provide support for a mechanism by which TCR signal specificity provided by the Dlgh1 AB/p38/NFAT

signalosome is translated into a precise cellular behavior, production of proinflammatory cytokines.

Dlgh1 AB and Dlgh1 B Support p38-Independent Degranulation

In addition to producing proinflammtory cytokines CD8+ CTLs also mediate lytic factor degranulation to execute contact-dependent cytotoxicity. We previously demonstrated that Dlgh1 is required for optimal CD8+ T cell cytotoxicity (5), however the mechanism of action was not explored. While assessing the role of Dlgh1 splice variants in proinflammatory cytokine production, we observed Dlgh1 knockdown prevented optimal secretion of lytic factor granzyme B, in addition to IL-2, despite unaltered TCR-induced gene expression of either (Figure 2-6C, Figure 2-6D). Interestingly, this defect was only seen when both Dlgh1 AB and Dlgh1 B were knocked-down and not when Dlgh1 AB was specifically targeted. Based on these data we hypothesized that either Dlgh1 B was specifically mediating lytic factor degranulation, and possibly IL-2 secretion, or that low amounts of either Dlgh1 AB or Dlgh1 B was sufficient to maintain this activity. To further investigate the possibility that Dlgh1 was controlling lytic factor degranulation we decided to assess the ability of OT-1 hybridoma T cells selectively re-expressing Dlgh1 AB or Dlgh1 B (Figure 2-5C) to degranulate and expose CD107a/LAMP-1 in response to antigen ($OVA_{257-264}$). We found Dlgh1 knockdown prevented optimal degranulation, while re-expression of Dlgh1 AB or Dlgh1 B rescued and enhanced antigen-induced degranulation (Figure 2-8A).

Because Dlgh1 B cannot support alternative p38 activity or IFNγ transcriptional activation (Figure 2-3, Figure 2-5) we hypothesized that Dlgh1-mediated degranulation may be p38-independent. Pretreatment of OT-1 hybridoma T cells selectively re-expressing Dlgh1 AB or Dlgh1 B with various concentrations of SB203580 had no

appreciable effect on Dlgh1-mediated degranulation (Figure 2-8B). Similar results were also observed in primary OT-1 CTLs, as p38 inhibition did not greatly affect degranulation or granzyme B secretion (Figure 2-9). In contrast, pretreatment with the actin inhibitor cytochalasin D at various concentrations did reduce degranulation, indicating that polymerization of actin was required for degranulation (Figure 2-8B).

The Actin Regulator WASp and the SH3-Domain of Dlgh1 are Required for Degranulation

CD8+ CTL degranulation requires actin-mediated cytoskeletal reorganization to allow for polarized delivery of the MTOC and lytic granules to the IS (27). To explore the requirement for particular Dlgh1 splice variants in antigen-induced actin polymerization we specifically targeted Dlgh1 AB in primary OT-1 CTLs and found Dlgh1 AB knockdown had no effect on actin polymerization, while total Dlgh1 knockdown did (Figure 2-6B, Figure 2-10B). These results suggested that actin polymerization, like degranulation, may be p38-independent. Accordingly, pretreatment of primary OT-1 CTLs with SB203580 had no affect on antigen-induced actin polymerization (Figure 2-10C).

To explore the molecular basis of Dlgh1-mediated p38-independent, actin-dependent degranulation we decided to generate OT-1 hybridoma T cells that selectively expressed Dlgh1 B variants or truncations to test their ability to promote degranulation, as many cytoskeletal effectors are known to associate with the C-terminal half of Dlgh1 (Figure 2-11). In cells expressing equivalent intracellular protein levels of these truncations or variants, the replacement of i3 with i2 had no effect on Dlgh1-mediated degranulation. Furthermore, deletion of the GUK and HOOK domains still allowed for Dlgh1-mediated degranulation. However once the SH3-domain of Dlgh1 was deleted the ability to rescue antigen-induced degranulation was lost (Figure 2-8C). This data

suggested a Dlgh1-SH3 associated ligand may be responsible for Dlgh1-mediated degranulation.

We previously mapped the WASp binding site to the SH3 domain of Dlgh1 (6). Thus we hypothesized WASp may be the cytoskeletal intermediate promoting Dlgh1-mediated degranulation, as WASp promotes F-actin polymerization and lytic granule release in murine T cells (28). Knockdown of WASp with two different target sequences significantly prevented antigen-induced degranulation (Figure 2-8E). Furthermore, WASp knockdown in OT-1 hybridoma T cells selectively re-expressing Dlgh1 AB or Dlgh1 B prevented the enhanced antigen-induced degranulation seen with Dlgh1 re-expression (Figure 2-8F). These data show that WASp and the SH3-domain of Dlgh1 are required for degranulation, suggesting that Dlgh1-mediated degranulation is WASp-dependent.

DISCUSSION

Dlgh1 serves as a conduit for TCR proximal kinases Lck and ZAP70 to promote p38 phosphorylation and selective activation of the transcription factor NFAT (6, 23, 29). This study extends these findings by demonstrating that Dlgh1 AB, but not Dlgh1 B, forms the molecular platform for alternative p38 activity by binding Lck and promoting p38 phosphorylation (Figure 2-3). Further, the signal specificity generated by Dlgh1 AB/p38 is functionally translated into the transcriptional activation of proinflammatory cytokines IFNγ and TNFα, but not IL-2 in murine CD8+ T cells (Figure 2-4 and Figure 2-6). Similar results have been demonstrated in T cells from p38 knockin mice in which Y323, the critical tyrosine residue phosphorylated by Dlgh1-associated ZAP70 in the alternative p38 pathway, is replaced with phenylalanine. Specifically, T cells from p38 Y323F mice stimulated with anti-CD3/anti-CD28 showed decreased intracellular protein levels of IFNγ and TNFα, while IL-2 levels were unaffected (26). Taken together, these findings demonstrate that the signal specificity provided by Dlgh1 AB/p38 can lead to at least one discrete cellular function, production of proinflammatory cytokines.

NFATc2 is a downstream target of alternative p38 activation, as Dlgh1 knockdown and p38 inhibition prevents serine 54 phosphorylation of NFATc2 (6). Our current results demonstrate that not all NFAT-dependent genes are affected by Dlgh1 knockdown, as IL-2 transcription was not affected (Figure 2-4, Figure 2-6). These results suggest that other transcription factors can compensate for the loss of NFATc2 and maintain IL-2 transcription. One possible transcription factor that could have compensated is NFATc1. NFATc1 does not have a serine residue in its transactivation domain like NFATc2, and while IL-2 production is diminished in NFATc2/NFATc1 double knockout T cells, NFATc2 knockout T cells have no appreciable defects in IL-2 transcription (30, 31). Besides NFATc1, NFκB could also compensate as genetic

disruption of the NFκB signaling pathway results in a reduction of TCR-induced IL-2 production (32). In line with our previously published data, Dlgh1 overexpression did not reduce transcriptional activation of the NFκB-responsive gene IκBα, despite recent evidence that shows Dlgh1 knockdown in human Tregs enhances NFκB activation (23). We hypothesize differences in T cell subtype or between human and mouse systems may account for these discrepancies. Despite the precise molecular details of why IL-2 transcription was not affected, it is clear that the Dlgh1 AB/p38 pathway mediates the transcriptional activation of only a subset of CD8+ effector genes. A more through analysis of genes regulated by the Dlgh1AB/p38 pathway in T cells would be very informative to determine the global cellular affect of Dlgh1 AB/p38-mediated signaling.

In this study we show that Dlgh1 splice variants promote p38-independent lytic factor degranulation. Furthermore, we provide evidence that i3, HOOK and GUK are not required for Dlgh1-mediated degranulation, indicating that GUK-associated GAKIN and i3-associated Ezrin are not required for Dlgh1-mediated degranulation. These results suggest that the Ezrin binding site located within PDZ1/PDZ2 of Dlgh1 may have a more important functional role than previously thought, and may be regulating microtubule anchoring and p38/NFAT activation downstream of actin polymerization and immune synapse formation. Thus, we hypothesize that Dlgh1 and Dlgh1-associated WASp are promoting degranulation by aiding in establishing early synaptic polarity, providing a site for the recruitment and anchoring of the MTOC and lytic granules to the mature IS.

Polarity proteins and cytoskeletal regulators have been suggested to work cooperatively to control lytic factor degranulation and cytotoxicity in CD8+ T lymphocytes (33). Dlgh1, a member of the ancestral Scribble polarity network, and WASp have both been demonstrated to be required for optimal contact-dependent cytotoxicity (5, 34). Furthermore, both control key processes required for lytic factor

degranulation including lytic synapse formation, actin polymerization, and MTOC dynamics (5, 9, 35-37). We propose that the Dlgh1-SH3 binding partner WASp is required for Dlgh1-mediated degranulation, as a Dlgh1 truncation lacking the SH3 domain is incapable of supporting Dlgh1-mediated degranulation and knockdown of WASp diminishes the enhanced degranulation seen with Dlgh1 re-expression (Figure 2-8).

WASp activity is regulated by two hierarchial mechanisms, allostery and oligomerization (38). WASp is held in an autoinhibited "closed" state by intra- or intermolecular interactions between the VCA and GBD domains. Distruption of VCA-GBD interaction results in "opening" and activation of WASp. Dlgh1-SH3 may pry open WASp by binding its proline rich domain, like other SH3-containing proteins (38). Alternatively, Dlgh1 may drive WASp activation via Fyn-mediated tyrosine phosphorylation at Y293, as Dlgh family members bind Fyn via PDZ3, a domain adjacent to the WASp binding site (39, 40). Dlgh1 may also regulate WASp via oligomerization and clustering, as Dlgh1 forms homo and hetero-oligomers and induces clustering of lipid rafts and TCRs (41, 42). These mechanisms of WASp regulation are not mutually exclusive but rather synergistic, resulting in possible hyperactivation of WASp by Dlgh1. Future experiments assessing these possible mechanisms of WASp activation will be very informative. Furthermore, it would interesting to speculate if similar WASp-dependent processes are controlling Dlgh1-mediated directional secretion of IL-2, as WASp has been shown to specifically affect the secretion of cytokines, but not chemokines (43).

In summary, alternative splicing of *dlgh1* in murine CD8+ T cells provides molecular scaffolds for p38-independent degranulation and p38-dependent proinflammatory cytokine production. Understanding how CTL functions are mediated by discrete signaling complexes may allow for rational design of therapeutics seeking to

inhibit particular pathways while leaving others intact. Such design may be particular useful in combating human disease. In particular melanoma, as resistance to adoptive cell transfer therapy has been suggested to be cased in part by excessive T-cell mediated proinflammatory cytokine production (44).

Figure 2-1. T lymphocytes express two Dlgh1 protein variants due to alternative splicing: Dlgh1 AB and Dlgh1 B.

(A). Schematic of the analyzed areas of splicing in Dlgh1.

(B). RT-PCR of cDNA from different murine T cells (CD8 = purified unstimulated primary OT-1 CD8+ T cell; CTL = OT-1 CD8+ T cell stimulated with CD3/CD28 and expanded in rIL-2; OT-1H = OT-1 hybridoma T cell line; BI-141 hybridoma T cell line) using primers that flank the i1A/i1B (*top*) or i2/i3/i4/i5 (*middle*) splice region. Primers that lie within L27β were also used (*bottom*)

(C). BI-141 T cells infected with viruses encoding different Dlgh1 splice variants were analyzed via protein immunoblotting for Dlgh1; Lck was used as a loading control.

(D). BI-141 T cells infected with knockdown viruses targeting L27β, i1A, i1B or i3 were analyzed via protein immunoblotting for Dlgh1; Lck was used as a loading control.

(E). Schematic of the two predominant Dlgh1 protein variants expressed in T cells.

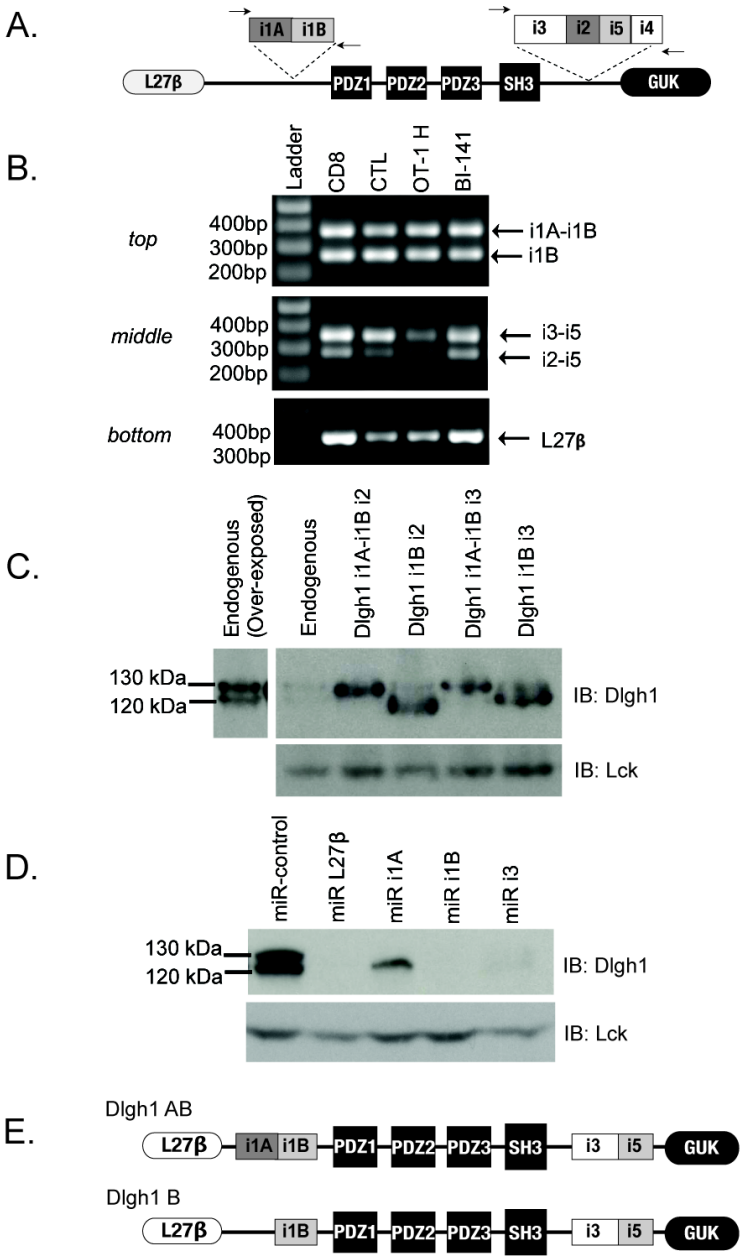
A.
i1A
i1B
i3
i2
i5
i4
L27β
PDZ1
PDZ2
PDZ3
SH3
GUK
B.
Ladder
CD8
CTL
OT-1 H
BI-141
top
400bp
300bp
200bp
i1A-i1B
i1B
middle
400bp
300bp
200bp
i3-i5
i2-i5
bottom
400bp
300bp
L27β
C.
Endogenous (Over-exposed)
Endogenous
Dlgh1 i1A-i1B i2
Dlgh1 i1B i2
Dlgh1 i1A-i1B i3
Dlgh1 i1B i3
130 kDa
120 kDa
IB: Dlgh1
IB: Lck
D.
miR-control
miR L27β
miR i1A
miR i1B
miR i3
130 kDa
120 kDa
IB: Dlgh1
IB: Lck
E.
Dlgh1 AB
L27β
i1A
i1B
PDZ1
PDZ2
PDZ3
SH3
i3
i5
GUK
Dlgh1 B
L27β
i1B
PDZ1
PDZ2
PDZ3
SH3
i3
i5
GUK

Figure 2-2. Dlgh1 Alternative Splice Variants in Hematopoietic and Non-Hematopoietic Cells.

(A). Nucleotide lengths of alternatively splice *dlgh1* exons and encoded amino acid sequences.

(B). Schematic representation of four possible *dlgh1* transcripts expressed in T cells due to alternative splicing.

(C). RT-PCR of cDNA from different murine hematopoietic and non-hematopoietic cells (A20 B cell line, WeHi B cell line; RAW267 macrophage cell line; 3T3 fibroblasts) using primers that flanks the i1A/i1B (left) and i2/i3/i4/i5 (right) splicing regions.

(D). 3T3 fibroblasts infected with miR-based knockdown viruses targeting specific regions of Dlgh1 and analyzed for Dlgh1 protein expression via immunoblotting; p38 was used as a loading control.

A.

Exon	Length (bp)	Amino Acid Sequence encoded
i1A	99bp	**P**TEAV**PP**SS**P**IV**P**VT**P**AL**P**V**P**AESTVV**P**SA**P**Q
i1B	54bp	AN**PPP**VLNTDSLET**P**TY
i3	102bp	QSFNDKRKKNLFSRKFPFYKNKDQSEQETSDADQ
i2	36bp	EIPDDMGSKGLK
i5	39bp	HVTSNASDSESSY
i4	39bp	LILITDEYGCSKG

B.

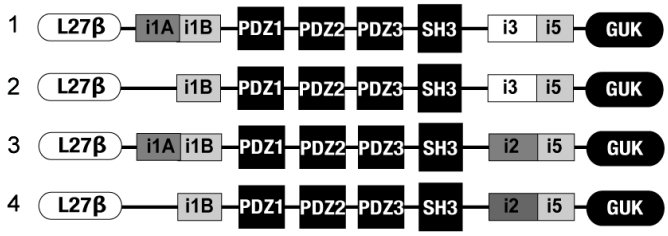

C.

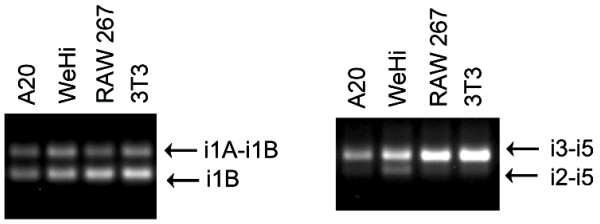

D.

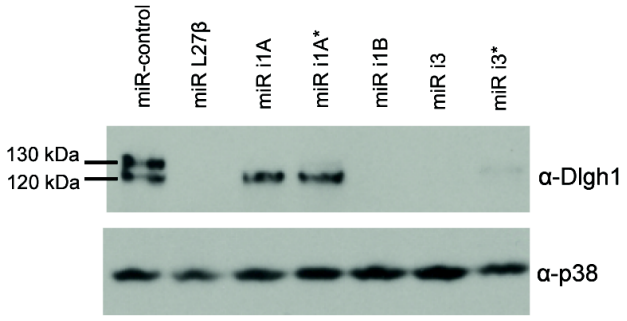

Figure 2-3. Dlgh1 AB binds Lck and promotes p38-dependent NFAT transcriptional activation and p38 phosphorylation, while Dlgh1 B does not.

(A). GST-fusion proteins of Dlgh1 AB and Dlgh1 B or GST-alone were purified and incubated with protein lysate from OT-1 hybridoma T cells that were unstimulated (0′) or stimulated (15′ mins) with anti-CD3/anti-CD28. Associated proteins were analyzed via SDS-PAGE and immunoblotted for Lck, p38 and Dlgh1.

(B). BI-141 T cells overexpressing Dlgh1 AB or Dlgh1 B were pretreated with SB203580 or carrier for 30 mins and then stimulated with anti-CD3/anti-CD28 for 2hrs or left unstimulated. RNA was isolated for qPCR. mRNA was normalized to L32 and fold-increase in mRNA expression vs. unstimulated samples is shown. Error bars represent SD of samples analyzed in triplicate. Data are representative of three independent experiments.

(C). OT-1 hybridoma T cells expressing endogenous Dlgh1 or selectively re-expressing Dlgh1 AB or Dlgh1 B were left unstimulated (-) or stimulated with anti-CD3/anti-CD28 (+) for 15 mins, followed by immunoprecipitation with anti-Dlgh1 and assessment of p38 T180/Y182 phosphorylation. Data is representative of three independent experiments.

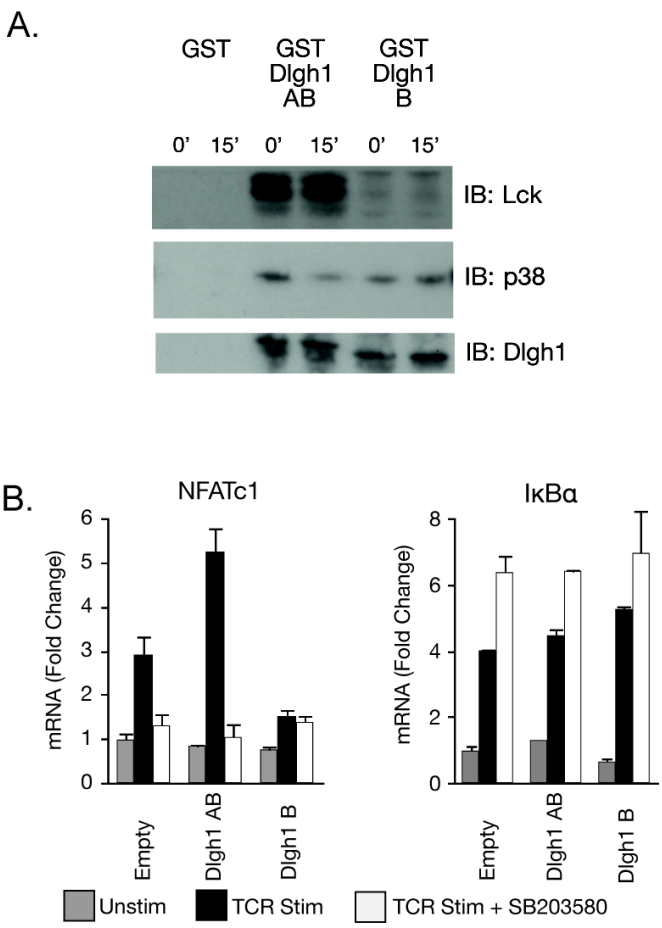
A.
GST
GST Dlgh1 AB
GST Dlgh1 B
0' 15' 0' 15' 0' 15'
IB: Lck
IB: p38
IB: Dlgh1
B.
NFATc1
IκBα
mRNA (Fold Change)
Empty
Dlgh1 AB
Dlgh1 B
Unstim
TCR Stim
TCR Stim + SB203580
C.
IP:
Endogenous Dlgh1
Dlgh1 AB
Dlgh1 B
CD3/CD28:
p-p38 (T180/Y182)
p38

Figure 2-4. Dlgh1 AB overexpression selectively enhances TCR-induced transcription of IFNγ and TNFα but not IL-2 or granzyme B, while Dlgh1 B does not.
(A-B). Purified primary OT-1 CD8+ T cells were stimulated with anti-CD3/anti-CD28 for 48 hrs, followed by infection with Dlgh1-viruses. Cells were restimulated with anti-CD3/anti-CD28 for 4hrs or left unstimulated. RNA was isolated for qPCR analysis. mRNA was normalized to L32 and fold-increase in mRNA expression vs. unstimulated samples is shown. Error bars represent SD of samples analyzed in triplicate. Data are representative of three independent experiments

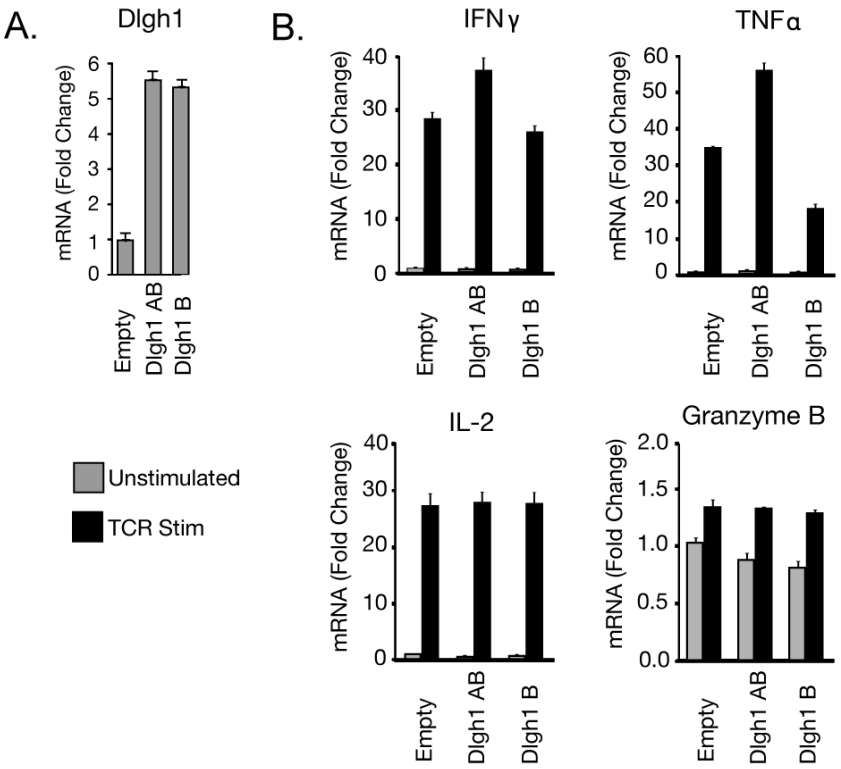
A.
Dlgh1
mRNA (Fold Change)
0
1
2
3
4
5
6
Empty
Dlgh1 AB
Dlgh1 B
Unstimulated
TCR Stim
B.
IFNγ
TNFα
IL-2
Granzyme B
mRNA (Fold Change)
0
10
20
30
40
50
60
0.0
0.5
1.0
1.5
2.0
Empty
Dlgh1 AB
Dlgh1 B

Figure 2-5. Dlgh1 AB Promotes p38-Dependent Transcription of IFNγ.

(A-B). BI-141 hybridoma T cells were infected with Dlgh1-viruses to overexpress Dlgh1 splice variants.

(A). Cells were analyzed via protein immunoblotting for Dlgh1; Lck was used as a loading control.

(B). Cells were pretreated with 10μM SB203580 or carrier (DMSO) for 30 minutes. Cells were stimulated with anti-CD3/anti-CD28 for 2hrs or left unstimulated. RNA was isolated for qPCR analysis.

(C-D). OT-1 hybridoma T cells were infected with the indicated Dlgh1 re-expression (**bold**) and/or Dlgh1 knockdown (KD) viruses. The Dlgh1 knockdown (Dlgh1 KD) construct targets the 3'UTR of *dlgh1* allowing for re-expression of specific Dlgh1 splice variants.

(C). Cells were analyzed via protein immunoblotting for Dlgh1; p38 was used as a loading control.

(D). Cells were stimulated with anti-CD3/anti-CD28 or left unstimulated. RNA was isolated for qPCR analysis. For all qPCR data, mRNA was normalized to L32 and fold-increase in mRNA expression vs. unstimulated samples is shown. Error bars represent SD of samples analyzed in triplicate. Data are representative of at least two independent experiments.

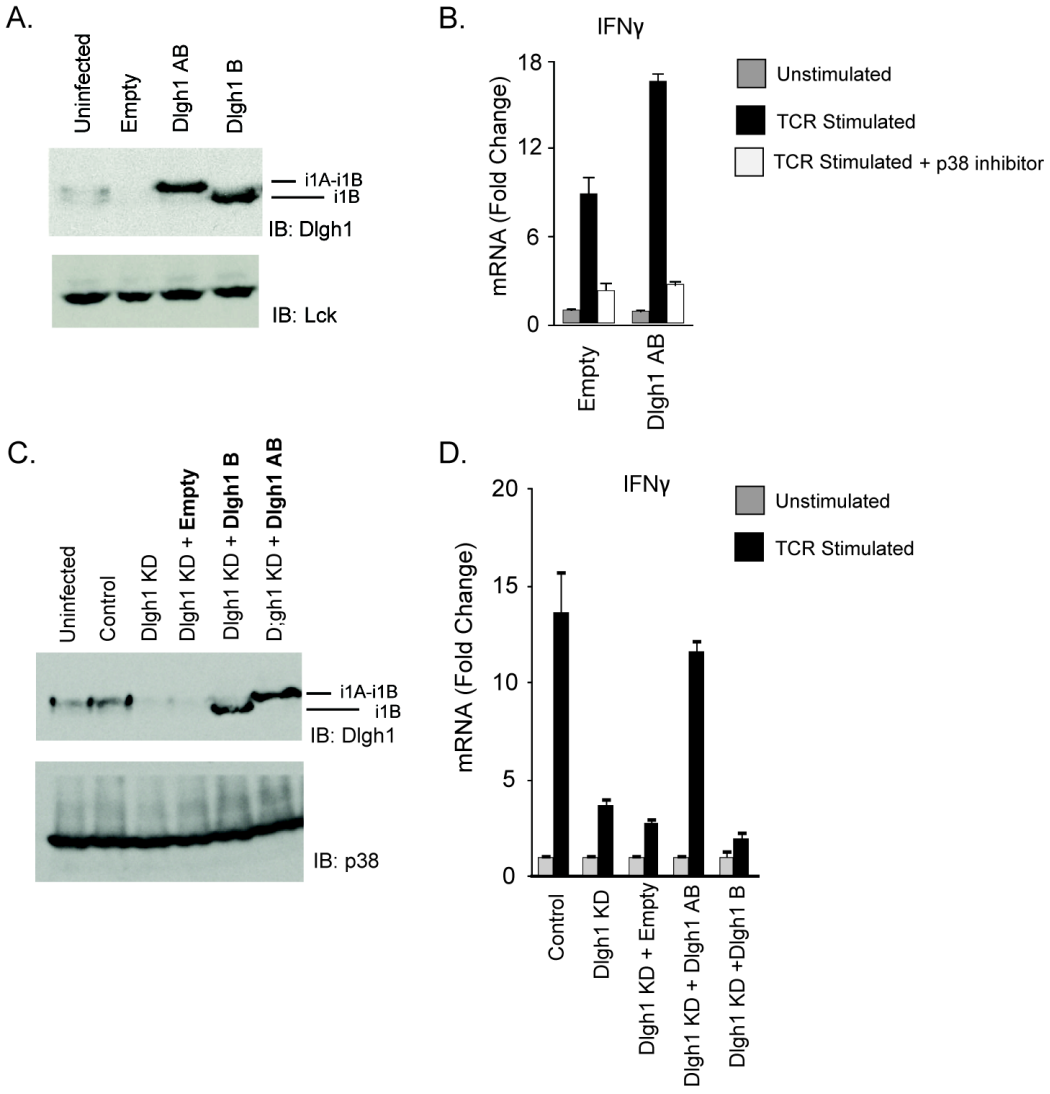
A.
Uninfected
Empty
Dlgh1 AB
Dlgh1 B
i1A-i1B
i1B
IB: Dlgh1
IB: Lck
B.
IFNγ
mRNA (Fold Change)
18
12
6
0
Empty
Dlgh1 AB
Unstimulated
TCR Stimulated
TCR Stimulated + p38 inhibitor
C.
Uninfected
Control
Dlgh1 KD
Dlgh1 KD + Empty
Dlgh1 KD + Dlgh1 B
D;gh1 KD + Dlgh1 AB
i1A-i1B
i1B
IB: Dlgh1
IB: p38
D.
IFNγ
mRNA (Fold Change)
20
15
10
5
0
Control
Dlgh1 KD
Dlgh1 KD + Empty
Dlgh1 KD + Dlgh1 AB
Dlgh1 KD +Dlgh1 B
Unstimulated
TCR Stimulated

Figure 2-6. Dlgh1 AB Knockdown Diminishes p38 Phosphorylation and Transcription of IFNγ and TNFα but not IL-2 or granzyme B, while total Dlgh1 Knockdown Also Prevents Effector Molecule Secretion and Actin Polymerization.

(A). Schematic representation of Dlgh1 variants targeted for knockdown using miR-based knockdown viruses.

(B-F) Purified primary OT-1 CD8+ T cells were stimulated with anti-CD3/anti-CD28 for 48 hrs, followed by infection with miR-based viruses.

(B). Cells were restimulated with MEF.B7.OVA cells for 15 mins and assessed for actin polymerization by intracellular phalloidin staining. The change in actin polymerization relative to miR-control was quantified as ΔMFI (%), where ΔMFI = stimulated MFI - unstimulated MFI for each condition, and where miR-control is set to 100%. Analysis was done on CD8+GFP+ cells. Error bars represent SD of means from four independent experiments

(C) Cells were restimulated with anti-CD3/anti-CD28 for 4hrs or left unstimulated. RNA was isolated for qPCR analysis. mRNA was normalized to L32 and the fold-increase in mRNA expression vs. unstimulated samples is shown. Error bars represent SD of samples analyzed in triplicate. Data are representative of at least three independent experiments.

(D) Cells were restimulated with anti-CD3/anti-CD28 for 48 hours and supernatants collected for ELISA analysis. Error bars represent SD of samples analyzed in triplicate. Data are representative of three independent experiments.

(E-F) Cells were restimulated with anti-CD3/anti-CD28 for 30 mins and stained intracellularly for phospho-p38 (T180/Y182). (E) CD8+GFP+ cells were gated and histograms of phosphorylated p38 is shown. The filled grey histogram represents the

miR-control unstimulated condtion, while the solid lines are the from the indicated stimulated conditions.

(F) The percentage of p38 phosphorylation relative to the miR-control is quantified as ΔMFI (%), where ΔMFI = stim MFI - unstim MFI for each condition, and where miR-control is set to 100%. Error bars represent SD of means from three independent experiments.

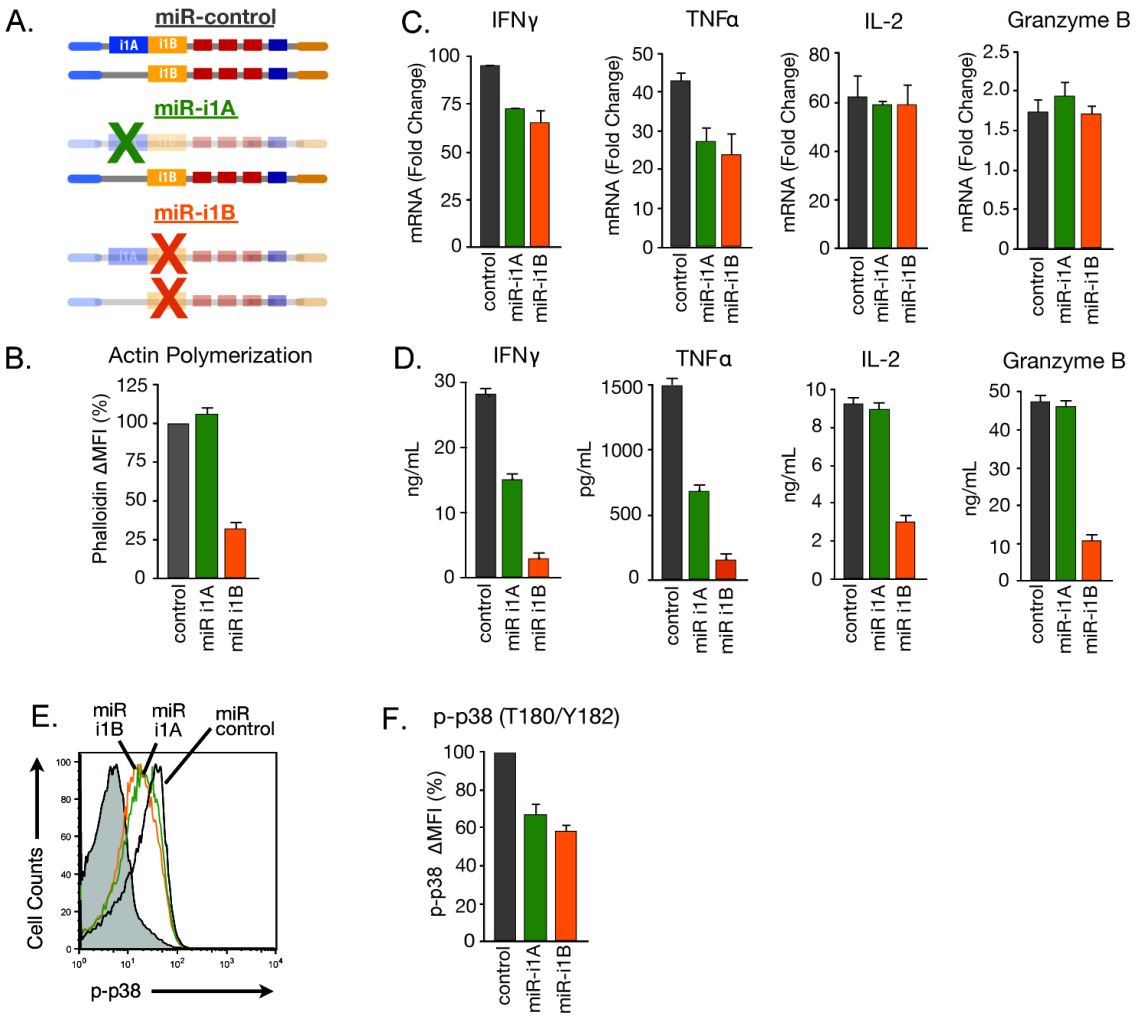
A.
miR-control
i1A
i1B
i1B
miR-i1A
i1B
miR-i1B
B.
Actin Polymerization
Phalloidin ΔMFI (%)
125
100
75
50
25
0
control
miR i1A
miR i1B
C.
IFNγ
TNFα
IL-2
Granzyme B
mRNA (Fold Change)
control
miR-i1A
miR-i1B
D.
IFNγ
TNFα
IL-2
Granzyme B
ng/mL
pg/mL
control
miR i1A
miR i1B
E.
miR i1B
miR i1A
miR control
Cell Counts
p-p38
F.
p-p38 (T180/Y182)
p-p38 ΔMFI (%)
control
miR-i1A
miR-i1B

Figure 2-7. Dlgh1 Knockdown Prevents Optimal Intracellular IFNγ Production.

(A-D) Purified primary OT-1 CD8+ T cells were stimulated with anti-CD3/anti-CD28 for 48 hrs, followed by infection with miR-based knockdown viruses.

(A) Cells were analyzed via protein immunoblotting for Dlgh1 knockdown; Lck was used as a loading control.

(B) Cells were restimulated with anti-CD3/anti-CD28 for 4 hrs in the presence of GolgiPLUG and assessed for intracellular cytokines.

(C-D) Cells were restimulated with EG.7 cells or EL-4 cells pulsed with various concentrations of $OVA_{257-264}$ peptide for 4 hrs in the presence of GolgiPLUG and assessed for intracellular cytokines. (C) CD8+IFNγ+ (%MAX) was measured by setting the miR-control 200nM OVA condition to 100%. The average and SD of three independent experiments is shown.

(D) The average and SD MFI of IFNγ+ cells from three independent experiments is also shown.

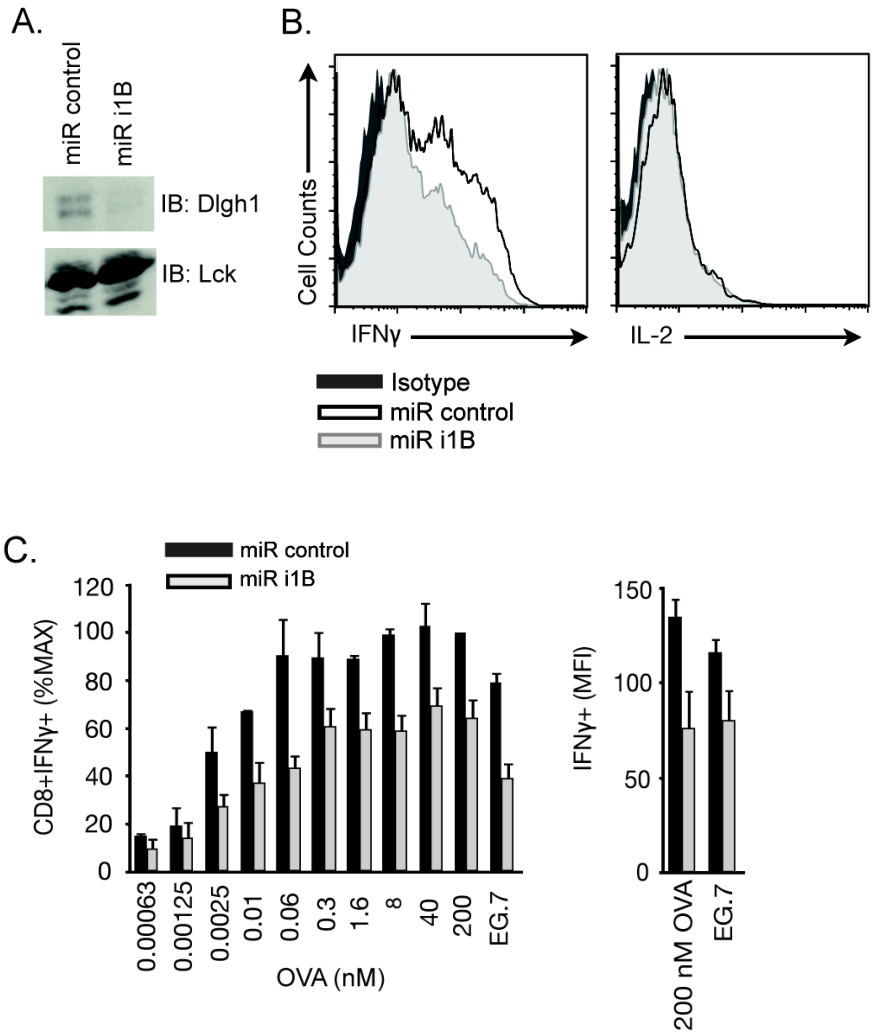
A.
miR control
miR i1B
IB: Dlgh1
IB: Lck
B.
Cell Counts
IFNγ
IL-2
Isotype
miR control
miR i1B
C.
miR control
miR i1B
CD8+IFNγ+ (%MAX)
120
100
80
60
40
20
0
0.00063
0.00125
0.0025
0.01
0.06
0.3
1.6
8
40
200
EG.7
OVA (nM)
IFNγ+ (MFI)
150
100
50
0
200 nM OVA
EG.7

Figure 2-8. Selective Re-expression of Dlgh1 AB or Dlgh1 B promotes p38-independent degranulation, which requires the SH3 domain of Dlgh1 and WASp.

(A-F) OT-1 hybridoma T cells were infected with re-expression (**bold**) and/or knockdown (KD) constructs.

(A, C, E, F) Cells were stimulated with EG.7 cells for 3hrs in the presence of anti-CD107a. Relative degranulation was measured by setting the percentage of CD8+CD107a+ in the miR-control stimulated condition to 100%. The average and SD of six (A) or three (C, E, F) independent experiments is shown. *P* values were calculated by *t* test. $^*P < 0.05$.

(B) Cells were pretreated with carrier (DMSO) or various concentrations of cytochalasin D or SB203580 for 1hr prior to stimulation with EG.7 cells for 3hrs in the presence of anti-CD107a. Relative degranulation was measured as above. Error bars represent SD of samples analyzed in triplicate. Data represents at least two independent experiments.

(D) Protein lysates from WASp knockdown cells were analyzed via SDS-PAGE and immunoblotting.

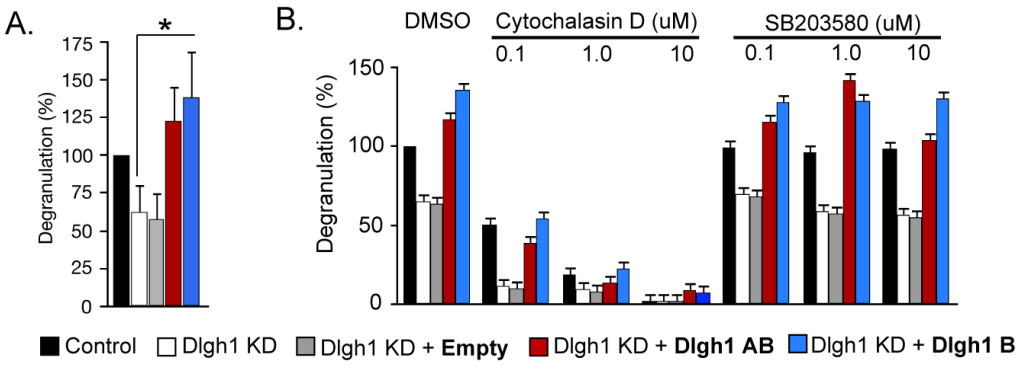
A.
B.
Degranulation (%)
DMSO
Cytochalasin D (uM)
SB203580 (uM)
0.1
1.0
10
Control
Dlgh1 KD
Dlgh1 KD + Empty
Dlgh1 KD + Dlgh1 AB
Dlgh1 KD + Dlgh1 B

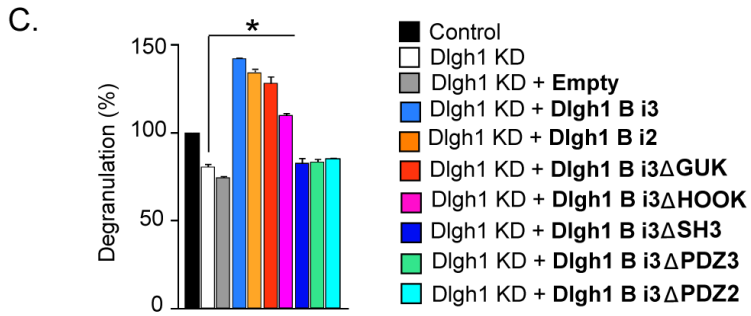
C.
Degranulation (%)
Control
Dlgh1 KD
Dlgh1 KD + Empty
Dlgh1 KD + Dlgh1 B i3
Dlgh1 KD + Dlgh1 B i2
Dlgh1 KD + Dlgh1 B i3ΔGUK
Dlgh1 KD + Dlgh1 B i3ΔHOOK
Dlgh1 KD + Dlgh1 B i3ΔSH3
Dlgh1 KD + Dlgh1 B i3ΔPDZ3
Dlgh1 KD + Dlgh1 B i3ΔPDZ2

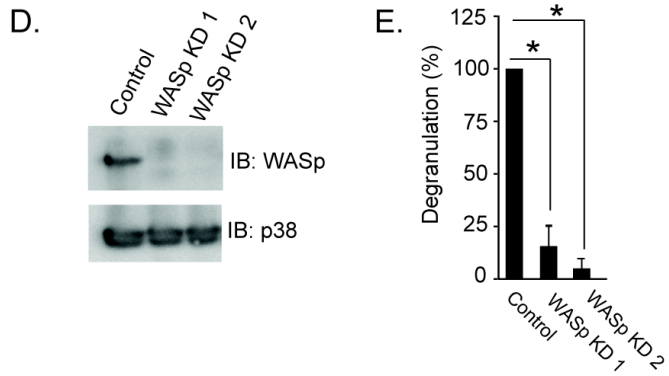
D.
Control
WASp KD 1
WASp KD 2
IB: WASp
IB: p38
E.
Degranulation (%)
Control
WASp KD 1
WASp KD 2

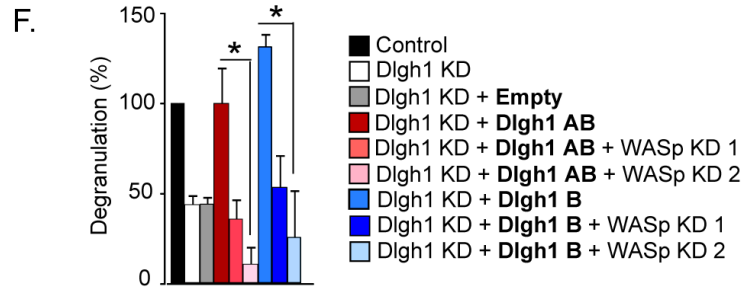
F.
Degranulation (%)
Control
Dlgh1 KD
Dlgh1 KD + Empty
Dlgh1 KD + Dlgh1 AB
Dlgh1 KD + Dlgh1 AB + WASp KD 1
Dlgh1 KD + Dlgh1 AB + WASp KD 2
Dlgh1 KD + Dlgh1 B
Dlgh1 KD + Dlgh1 B + WASp KD 1
Dlgh1 KD + Dlgh1 B + WASp KD 2

Figure 2-9. CTL Degranulation and Granzyme B Secretion in Primary CD8+ OT-1 T Cells are Not Greatly Affected by p38 Inhibition.

(A) Primary mouse CD8+ OT-1 CTLs were pretreated with carrier (DMSO) or various concentrations of cytochalasin D (0.1, 1.0, 10 μM) or SB203580 (0.1, 1.0, 10 μM) for 1 hour prior to stimulation with EG.7 cells for 3 hours in the presence of anti-CD107a. Relative degranulation was measured by setting the percentage of CD8+CD107a+ in the stimulated DMSO condition to 100%. Error bars represent standard deviations of samples analyzed in triplicate. Data are representative of at least two independent experiments.

(B) Primary mouse CD8+ OT-1 CTLs were pretreated with carrier (DMSO) or various concentrations of SB203580 (0.625, 1.25, 2.5, 5, 10 μM) for 1 hour prior to stimulation with anti-CD3/anti-CD28 for 48 hrs. Supernatants were collected and analyzed via ELISA. Error bars represent standard deviations of samples analyzed in triplicate. Data are representative of at least two independent experiments.

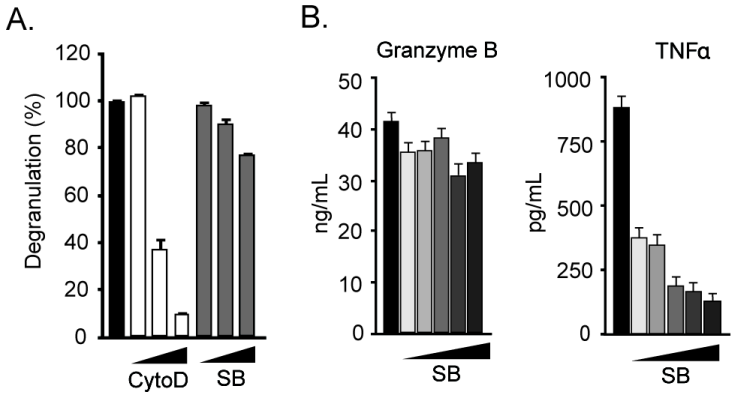
A.
B.
Degranulation (%)
120
100
80
60
40
20
0
CytoD
SB
Granzyme B
ng/mL
50
40
30
20
10
0
SB
TNFα
pg/mL
1000
750
500
250
0
SB

Figure 2-10. Dlgh1 Knockdown Perturbs p38-Independent Actin Polymerization.

(A-B) Primary OT-1 CD8+ T cells were infected with miR-based knockdown viruses.

(A) Cells were sorted based on GFP positivity and analyzed for Dlgh1 protein expression via immunoblotting; Lck was visualized as a loading control.

(B) Cells were restimulated with MEF.B7.OVA cells for 5 or 15 minutes and assessed for actin polymerization by intracellular phalloidin staining. Histograms of intracellular phalloidin for each condition are representative of four independent experiments.

(C) Primary mouse OT-1 CTLs were pretreated with 10μM SB203580 or carrier (DMSO) for 30 minutes. Cells were then stimulated with MEF.B7.OVA cells for 15 minutes and assessed for actin polymerization by intracellular phalloidin staining. The change in actin polymerization relative to DMSO was quantified as ΔMFI (%), where ΔMFI = stimulated MFI - unstimulated MFI for each condition, and where DMSO was set to 100%. Analysis was done on CD8+GFP+ cells. Error bars represent SD of means from three independent experiments.

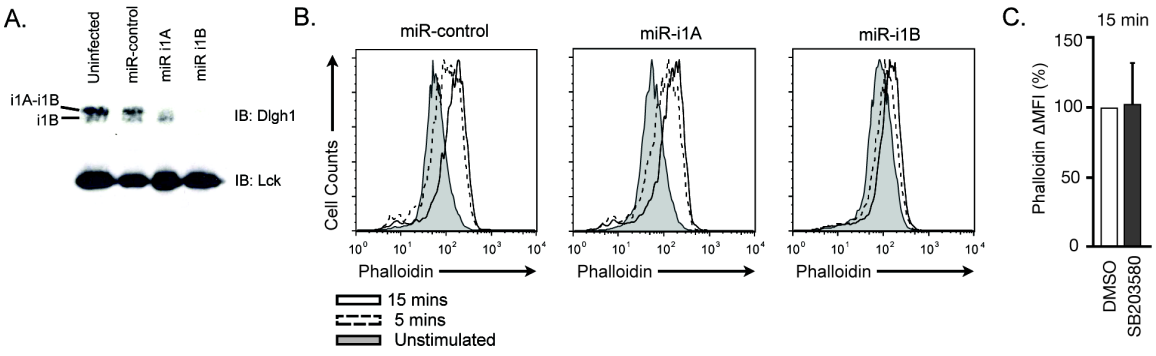
A.
Uninfected
miR-control
miR i1A
miR i1B
i1A-i1B
i1B
IB: Dlgh1
IB: Lck
B.
miR-control
miR-i1A
miR-i1B
Cell Counts
Phalloidin
15 mins
5 mins
Unstimulated
C.
15 min
Phalloidin ΔMFI (%)
150
100
50
0
DMSO
SB203580

Figure 2-11. OT-1 hybridoma T cell lines.

(A) Schematic representation of Dlgh1 i1B truncations and variants that were re-expressed in OT-1 hybridoma T cells.

(B-E) OT-1 hybridoma T cells were infected with the indicated Dlgh1 re-expression (**bold**) and/or knockdown (KD) viruses. The Dlgh1 knockdown (Dlgh1 KD) construct targets the 3'UTR of *dlgh1* allowing for re-expression of specific Dlgh1 variants.

(B) Cells were analyzed via SDS-PAGE and immunoblotted for Dlgh1 to visualize Dlgh1 i1B truncations/variants.

(C-E) The indicated cells were analyzed for intracellular Dlgh1 (C, E) or WASp (D) protein levels via flow cytometry; geometric mean fluorescent intensities are graphed.

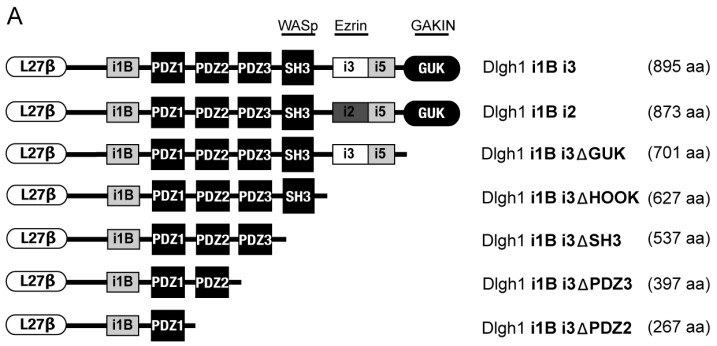
A
WASp
Ezrin
GAKIN
L27β
i1B
PDZ1
PDZ2
PDZ3
SH3
i3
i5
GUK
i2
Dlgh1 i1B i3 (895 aa)
Dlgh1 i1B i2 (873 aa)
Dlgh1 i1B i3ΔGUK (701 aa)
Dlgh1 i1B i3ΔHOOK (627 aa)
Dlgh1 i1B i3ΔSH3 (537 aa)
Dlgh1 i1B i3ΔPDZ3 (397 aa)
Dlgh1 i1B i3ΔPDZ2 (267 aa)

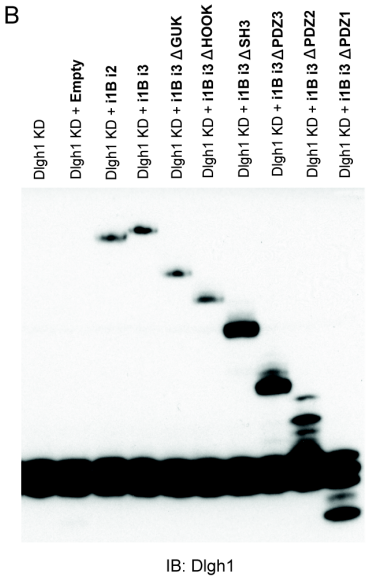
B
Dlgh1 KD
Dlgh1 KD + Empty
Dlgh1 KD + i1B i2
Dlgh1 KD + i1B i3
Dlgh1 KD + i1B i3 ΔGUK
Dlgh1 KD + i1B i3 ΔHOOK
Dlgh1 KD + i1B i3 ΔSH3
Dlgh1 KD + i1B i3 ΔPDZ3
Dlgh1 KD + i1B i3 ΔPDZ2
Dlgh1 KD + i1B i3 ΔPDZ1
IB: Dlgh1

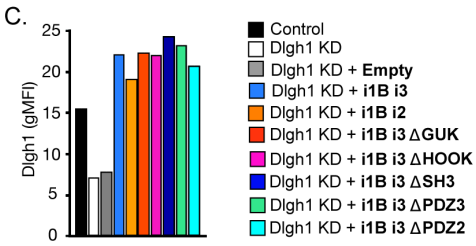
C.
Dlgh1 (gMFI)
25
20
15
10
5
0
Control
Dlgh1 KD
Dlgh1 KD + Empty
Dlgh1 KD + i1B i3
Dlgh1 KD + i1B i2
Dlgh1 KD + i1B i3 ΔGUK
Dlgh1 KD + i1B i3 ΔHOOK
Dlgh1 KD + i1B i3 ΔSH3
Dlgh1 KD + i1B i3 ΔPDZ3
Dlgh1 KD + i1B i3 ΔPDZ2

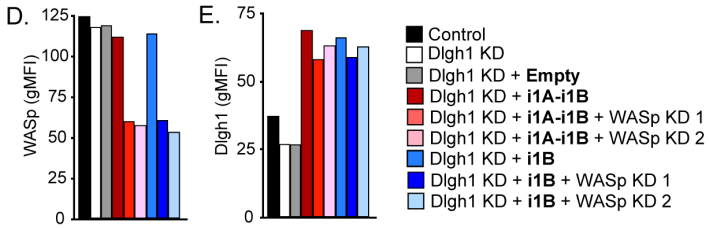
D.
WASp (gMFI)
125
100
75
50
25
0
E.
Dlgh1 (gMFI)
75
50
25
0
Control
Dlgh1 KD
Dlgh1 KD + Empty
Dlgh1 KD + i1A-i1B
Dlgh1 KD + i1A-i1B + WASp KD 1
Dlgh1 KD + i1A-i1B + WASp KD 2
Dlgh1 KD + i1B
Dlgh1 KD + i1B + WASp KD 1
Dlgh1 KD + i1B + WASp KD 2

Table 2-1. Knockdown Sequences

Construct	**Anti-Sense Sequence**
miR-control	GTCTCCACGCGCAGTACATTT
miR-L27β	TTCCATAGAGCGGGTTATTAA
mIR-i1A	CCAGTCCCTGCTGAGAGTACT
miR-i1A*	TCCCTGCTGAGAGTACTGTCG
miR-i1B	AGCTTAGAGACACCAACTTAT
miR-i3	AAGAACCTCTTTTCCCGAAAA
miR-i3*	GAACCTCTTTTCCCGAAAATT
Dlgh1 KD (targets 3'UTR of *dlgh1*)	GTCCTCCACACTGACACAGAT
WASp KD1	TGTGTGCTTCGTGAAGGATA
WASp KD 2	ACCCTCAGAAGTCCTACTTCA

Table 2-2. RT-PCR primers, qPCR primers, and cloning primers

RT-PCR Primer	**Sequence**
Forward i1A/i1B	CGGTATCAGGATGAAGAGGTA
Reverse i1A/i1B	CCCCTTTCAAGTGTGATTTCC
Forward i2/i3/i4/i5	CAGGCAGGTCACCCCAGA
Reverse i2/i3/i4/i5	GGTCCTAATATGATGACTGGTCGGG
qPCR Primer	**Sequence**
Forward NFATc1	GCCTCGTATCAGTGGGCGAAG
Reverse NFATc1	CGAAGCTCGTATGGACCA
Forward IκBα	CTGCAGGCCACCAACTACAA
Reverse IκBα	CAGCACCCAAAGTCACCAAGT
Forward IFNγ	GTCAACAACCCACAGGTCCAG
Reverse IFNγ	CCTTTTCCGCTTCCTGAGG
Forward TNFα	AATGGCCTCCCTCTCATCAGT
Reverse TNFα	GCTACAGGCTTGTCACTCGAATT
Forward IL-2	CCTGAGCAGGATGGAGAATTACA
Reverse IL-2	TCCAGAACATGCCGCAGAG
Forward Granzyme B	AAACGTGCTTCCTTTCGGG
Reverse Granzyme B	GAAACTATGCCTGCAGCCACT
Forward Dlgh1	AGATCGCATCATATCGGTGAA
Reverse Dlgh1	TCAAAACGACTGTACTCTTCGG
Forward L32	AAGCGAAACTGGCGGAAAC
Reverse L32	TAACCGATGTTGGGCATCAG
Cloning Primers	**Sequences**
Forward XhoI Dlgh1	ATCGCAATTGCACGAGCATGCCGGTCCGGAAGGAAGATACC
Reverse EcoRI Dlgh1	ATTCGTGAATTCACTTCATAGCTTTTCTTTCGCTGGGTCCCAGATGTA
Forward BstI Dlgh1	GGGTCTCTTCGAACCAGCCAGAAG
Reverse BstI Dlgh1	CTTCTGGCTGGTTCGAAGAGACCC
Forward EcoRI Dlgh1	TATGAATTCCTGCCGGTCCGG
Reverse SalI Dlgh1	ACTGTCGACACTTCATAGCTTTTCTTTCGCTGGGTC
Reverse EcoRI Dlgh1 ΔGUK	TCATTGGAATTCTTTTCATTCTTGTTGATTCACTGGCTCATA
Reverse EcoRI Dlgh1 ΔHOOK	TCATTGGAATTCTTTTCAGAATTTGACCGTTTTTAATCGGGC
Reverse EcoRI Dlgh1 ΔSH3	TCATTGGAATTCTTTTCAACTGACACTGCTATTCATCATCTG
Reverse EcoRI Dlgh1 ΔPDZ3	TCATTGGAATTTTCATCCAGCTTCTTTTAATGCCTCCAC
Reverse EcoRI Dlgh1 ΔPDZ2	TCATTGGAATTCTTTTCATCCAGCTTCTTTTAATGCCTCCAC

REFERENCES

1. Hufford MM, Kim TS, Sun J, & Braciale TJ (2011) Antiviral CD8+ T cell effector activities in situ are regulated by target cell type. *The Journal of experimental medicine* 208(1):167-180.

2. Agnellini P*, et al.* (2007) Impaired NFAT nuclear translocation results in split exhaustion of virus-specific CD8+ T cell functions during chronic viral infection. *Proceedings of the National Academy of Sciences of the United States of America* 104(11):4565-4570.

3. Guy CS*, et al.* (2013) Distinct TCR signaling pathways drive proliferation and cytokine production in T cells. *Nature Immunology* 14(3):262-270.

4. Rebeaud F, Hailfinger S, & Thome M (2007) Dlgh1 and Carma1 MAGUK proteins contribute to signal specificity downstream of TCR activation. *Trends Immunol* 28(5):196-200.

5. Round JL*, et al.* (2005) Dlgh1 coordinates actin polymerization, synaptic T cell receptor and lipid raft aggregation, and effector function in T cells. *J Exp Med* 201(3):419-430.

6. Round JL*, et al.* (2007) Scaffold protein Dlgh1 coordinates alternative p38 kinase activation, directing T cell receptor signals toward NFAT but not NF-kappaB transcription factors. *Nat Immunol* 8(2):154-161.

7. Hanada T, Lin L, Tibaldi EV, Reinherz EL, & Chishti AH (2000) GAKIN, a novel kinesin-like protein associates with the human homologue of the Drosophila discs large tumor suppressor in T lymphocytes. *J Biol Chem* 275(37):28774-28784.

8. Xavier R*, et al.* (2004) Discs large (Dlg1) complexes in lymphocyte activation. *J Cell Biol* 166(2):173-178.

9. Lasserre R*, et al.* (2010) Ezrin tunes T-cell activation by controlling Dlg1 and microtubule positioning at the immunological synapse. *EMBO J* 29(14):2301-2314.

10. Cavatorta AL*, et al.* (2011) Regulation of translational efficiency by different splice variants of the Disc large 1 oncosuppressor 5'UTR. *The FEBS journal* 278(14):2596-2608.

11. Schlüter OM, Xu W, & Malenka RC (2006) Alternative N-terminal domains of PSD-95 and SAP97 govern activity-dependent regulation of synaptic AMPA receptor function. *Neuron* 51(1):99-111.

12. McLaughlin M*, et al.* (2002) The distribution and function of alternatively spliced insertions in hDlg. *J Biol Chem* 277(8):6406-6412.

13. Godreau D, Vranckx R, Maguy A, Goyenvalle C, & Hatem SN (2003) Different isoforms of synapse-associated protein, SAP97, are expressed in the heart and have distinct effects on the voltage-gated K+ channel Kv1.5. *J Biol Chem* 278(47):47046-47052.

14. Lue RA, Brandin E, Chan EP, & Branton D (1996) Two independent domains of hDlg are sufficient for subcellular targeting: the PDZ1-2 conformational unit and an alternatively spliced domain. *J Cell Biol* 135(4):1125-1137.

15. Hanada T, Takeuchi A, Sondarva G, & Chishti AH (2003) Protein 4.1-mediated membrane targeting of human discs large in epithelial cells. *J Biol Chem* 278(36):34445-34450.

16. Hogquist KA*, et al.* (1994) T cell receptor antagonist peptides induce positive selection. *Cell* 76(1):17-27.

17. Stotz SH, Bolliger L, Carbone FR, & Palmer E (1999) T cell receptor (TCR) antagonism without a negative signal: evidence from T cell hybridomas expressing two independent TCRs. *J Exp Med* 189(2):253-264.

18. Moore MW, Carbone FR, & Bevan MJ (1988) Introduction of soluble protein into the class I pathway of antigen processing and presentation. *Cell* 54(6):777-785.

19. O'Connell RM*, et al.* (2008) Sustained expression of microRNA-155 in hematopoietic stem cells causes a myeloproliferative disorder. *J Exp Med* 205(3):585-594.

20. Park S-G*, et al.* (2009) The kinase PDK1 integrates T cell antigen receptor and CD28 coreceptor signaling to induce NF-κB and activate T cells. *Nat Immunol* 10(2):158-166.

21. O'Connell R, Chaudhuri A, Rao D, & Baltimore D (2009) Inositol phosphatase SHIP1 is a primary target of miR-155. *Proc Natl Acad Sci USA* 106(17):7113-7118.

22. Hanada T, Lin L, Chandy KG, Oh SS, & Chishti AH (1997) Human homologue of the Drosophila discs large tumor suppressor binds to p56lck tyrosine kinase and Shaker type Kv1.3 potassium channel in T lymphocytes. *J Biol Chem* 272(43):26899-26904.

23. Zanin-Zhorov A*, et al.* (2012) Scaffold protein Disc-Large Homolog 1 is required for T cell receptor-induced activation of regulatory T cell function. *Proc Natl Acad Sci USA* 109(5):1625-1630.

24. Jirmanova L, Giardino Torchia ML, Sarma ND, Mittelstadt PR, & Ashwell JD (2011) Lack of the T cell-specific alternative p38 activation pathway reduces autoimmunity and inflammation. *Blood* 118(12):3280-3289.

25. López-Santalla M*, et al.* (2011) Tyr323-dependent p38 activation is associated with rheumatoid arthritis and correlates with disease activity. *Arthritis and rheumatism* 63(7):1833-1842.

26. Jirmanova L, Sarma D, Jankovic D, Mittelstadt P, & Ashwell J (2008) Genetic disruption of p38α Tyr-323 phosphorylation prevents TCR-mediated p38α activation and impairs IFNγ production. *Blood* 113(10): 2229-2237.

27. Huse M, Quann EJ, & Davis MM (2008) Shouts, whispers and the kiss of death: directional secretion in T cells. *Nat Immunol* 9(10):1105-1111.

28. Nikolov NP*, et al.* (2010) Systemic autoimmunity and defective Fas ligand secretion in the absence of the Wiskott-Aldrich syndrome protein. 116(5):740-747.

29. Adachi K & Davis MM (2011) T-cell receptor ligation induces distinct signaling pathways in naive vs. antigen-experienced T cells. *Proceedings of the National Academy of Sciences of the United States of America* 108(4):1549-1554.

30. Hodge MR*, et al.* (1996) Hyperproliferation and dysregulation of IL-4 expression in NF-ATp-deficient mice. *Immunity* 4(4):397-405.

31. Peng SL, Gerth AJ, Ranger AM, & Glimcher LH (2001) NFATc1 and NFATc2 together control both T and B cell activation and differentiation. *Immunity* 14(1):13-20.

32. Li Q & Verma IM (2002) NF-kappaB regulation in the immune system. *Nature reviews Immunology* 2(10):725-734.

33. Stinchcombe J & Griffiths G (2007) Secretory mechanisms in cell-mediated cytotoxicity. *Annual Reviews* 23:495-517.

34. Orange JS*, et al.* (2002) Wiskott-Aldrich syndrome protein is required for NK cell cytotoxicity and colocalizes with actin to NK cell-activating immunologic synapses. 99(17):11351-11356.

35. Ludford-Menting MJ*, et al.* (2005) A network of PDZ-containing proteins regulates T cell polarity and morphology during migration and immunological synapse formation. *Immunity* 22(6):737-748.

36. De Meester J, Calvez R, Valitutti S, & Dupré L (2010) The Wiskott-Aldrich syndrome protein regulates CTL cytotoxicity and is required for efficient killing of B cell lymphoma targets. *Journal of Leukocyte Biology* 88(5):1031-1040.

37. Calvez R*, et al.* (2011) The Wiskott-Aldrich syndrome protein permits assembly of a focused immunological synapse enabling sustained T-cell receptor signaling. *Haematologica* 96(10):1415-1423.

38. Padrick SB*, et al.* (2008) Hierarchical regulation of WASP/WAVE proteins. 32(3):426-438.

39. Padrick SB & Rosen MK (2010) Physical mechanisms of signal integration by WASP family proteins. 79:707-735.

40. Tezuka T, Umemori H, Akiyama T, Nakanishi S, & Yamamoto T (1999) PSD-95 promotes Fyn-mediated tyrosine phosphorylation of the N-methyl-D-aspartate receptor subunit NR2A. 96(2):435-440.

41. Feng W, Long J-F, Fan J-S, Suetake T, & Zhang M (2004) The tetrameric L27 domain complex as an organization platform for supramolecular assemblies. *Nat Struct Mol Biol* 11(5):475-480.

42. Nakagawa T*, et al.* (2004) Quaternary structure, protein dynamics, and synaptic function of SAP97 controlled by L27 domain interactions. *Neuron* 44(3):453-467.

43. Morales-Tirado V*, et al.* (2004) Cutting edge: selective requirement for the Wiskott-Aldrich syndrome protein in cytokine, but not chemokine, secretion by CD4+ T cells. *J Immunol* 173(2):726-730.

44. Landsberg J*, et al.* (2012) Melanomas resist T-cell therapy through inflammation-induced reversible dedifferentiation. *Nature* 490(7420):412-416.

CHAPTER THREE

Dlgh1 tyrosine phosphorylation mediates TCR-dependent p38 and NFAT activation

ABSTRACT

Discs Large Homolog 1 (Dlgh1) acts as a key point of control downstream of the T cell receptor (TCR) by regulating p38-dependent NFAT activation and proinflammatory cytokine production. Upon TCR stimulation, Dlgh1 forms a complex with Lck, Zap70 and p38 facilitating the direct phosphorylation of p38 by Zap70, known as the alternative p38 pathway. However, the molecular mechanism by which Dlgh1 coordinates the alternative p38 pathway remains unknown. Here we report that TCR-induced Dlgh1 phosphorylation was required to license Dlgh1-mediated activation of the alternative p38 pathway. Specifically, we demonstrate that Dlgh1 is tyrosine phosphorylated in response to TCR stimulation, and that Lck, not Zap70 is responsible for Dlgh1 phosphorylation. Additionally, we identify Dlgh1 Tyr222 as a major site of Lck-mediated Dlgh1 phosphorylation. T cells expressing Dlgh1 scaffolds in which Tyr222 is mutated to Phe (Y222F) are unable to coordinate TCR-induced activation of the alternative p38 pathway and demonstrate decreased NFAT activation and production of proinflammatory cytokines IFNγ and TNFα, but not IL-2. Overall, these data demonstrate that TCR-induced phosphorylation of Dlgh1 at Tyr222 by Lck is a crucial step in Dlgh1-mediated p38 and NFAT activation and the production of proinflammatory cytokines downstream of the T cell receptor. Our study is the first to demonstrate that Dlgh1 tyrosine phosphorylation plays a critical role in TCR signaling, and positions Dlgh1 phosphorylation as a point of control essential for activation of p38-dependent events in response to TCR engagement.

INTRODUCTION

CD8+ cytotoxic T lymphocytes (CTLs) play a vital role in the adaptive immune response through their ability to mediate contact-dependent lysis and produce proinflammatory cytokines. Both of these CTL effector functions require T cell activation triggering through engagement of the T cell receptor (TCR) by cognate antigen complexes presented on the surface of antigen presenting cells. TCR triggering is coupled to downstream effector functions through the activation and recruitment of TCR proximal tyrosine kinases (PTKs) Lck and Zap70 which initiate downstream signaling networks including mitogen activated protein kinase (MAPK) pathways p38, JNK and ERK. Transcription factors activated by these signaling networks, including NFAT and NFκB, control the gene expression which in turn determines the magnitude and duration of T cell responses including: proliferation, differentiation, effector function and memory formation (1, 2).

Recent studies have revealed a previously unappreciated amount of functional heterogeneity in CD8+ T cell populations demonstrating that proximal signals initiated through the TCR are coupled to a particular subset of possible downstream pathways leading to discrete functional responses (3, 4). Scaffold proteins have emerged as key points of control that couple proximal signal transducers to particular signaling and cytoskeletal networks through the formation multi-component signalosomes (5-8). Discs Large Homolog 1 (Dlgh1) is a founding member of the MAGUK family of protein scaffolds. Structurally, Dlgh1 contains various modular domains required for specific protein-protein interactions including: three PDZ domains, an SH3 domain and a catalytically inactive guanylate kinase domain which are common to all MAGUK family members. Additionally, Dlgh1 contains an L27 oligomerization domain, an N terminal proline rich region and a C terminal HOOK domain not seen in other MAGUK family

members. Interestingly, these Dlgh1-specific domains are all known to be regions of alternative splicing hypothesized to yield Dlgh1 scaffolds capable of facilitating a unique subset of Dlgh1 functions (9, 10).

Like many scaffold proteins, Dlgh1 forms various intramolecular interactions creating a closed conformation hypothesized to impact its function by masking ligand binding sites or affecting the juxtaposition of existing ligands (11, 12). In other systems, scaffold protein structure and function are controlled through a series of phosphorylation and/or ligand binding events that lead to the gradual unfolding of the scaffold into an active conformation (13-15). These phosphorylation events are hypothesized to provide molecular memory by creating a primed or "open" scaffold capable of binding new ligands; endowing the scaffold with novel and/or heightened functionality upon secondary stimulation.

In response to TCR activation, Dlgh1 localizes to the immunologic synapse (IS) where it acts as a master regulator of polarity and promotes antigen-dependent cytoskeletal events including: actin polymerization, TCR micro-domain and lipid raft reorganization, receptor clustering, MTOC dynamics, and contact-dependent lysis in differentiated CD8+ effector cells (5, 16-18). Additionally, Dlgh1 mediates T cell-specific signal transduction by directing the activity of TCR-proximal tyrosine kinases Lck and Zap70 toward the alternative p38 signal transduction pathway (6, 19). This pathway is unique to lymphocytes and independent of the canonical p38 pathway which is activated in response to environmental stress, and is mediated by the three-tiered MAPK cascade culminating in activation of p38 through direct phosphorylation at T180 and Y182 by MKK4 and/or MKK6 (19, 20).

We and others have demonstrated that Dlgh1 coordinates the TCR-induced alternative p38 pathway and activation of its downstream targets through interactions

with PTKs Lck and Zap70 and p38 MAPK (5, 6, 18). This Dlgh1-mediated complex directs alternative p38 activation by facilitating Lck-dependent activation of Zap70 and subsequent Zap70-mediated phosphorylation of p38 at Tyr323. Phosphorylation of p38 at Tyr323 is unique to the alternative p38 pathway, and allows p38 to dimerize and transphosphorylate at T180 in the p38 activation loop yielding a fully active kinase (6, 19, 21, 22). Ablation of the alternative p38 pathway through the loss of Dlgh1, a p38 Y323F knockin mutation or addition of p38 inhibitors leads to decreased NFAT-dependent transcription, and impaired production of pro-inflammatory cytokines IFNγ and TNFα. Interestingly, the Dlgh1-mediated alternative p38 pathway does not lead to decreases in IL-2 production or NFκB-dependent transcription (6, 16, 23, 24). In fact, recent studies in human T cells suggest that Dlgh1 might act as an antagonist to NFκB activation through association and stabilization of PTEN (25). Together these studies position Dlgh1 as a major point of control downstream of the TCR required for optimal activation of the alternative p38 pathway and downstream p38-dependent functions. However, the sequence of molecular events governing Dlgh1-mediated alternative p38 activation remains largely unknown.

In this report we demonstrate that TCR-induced Dlgh1 tyrosine phosphorylation licenses the Dlgh1 scaffold to coordinate the alternative p38 pathway. Specifically, we establish that Dlgh1 is tyrosine phosphorylated in response to TCR stimulation and identify Dlgh1 Tyr222 as a major site of Lck-mediated Dlgh1 phosphorylation. In addition, we provide evidence that phosphorylation of Dlgh1 at Tyr222 is required for coordination of the alternative p38 pathway, activation of NFAT-dependent transcription and production of pro-inflammatory cytokines IFNγ and TNFα, but not IL-2. Collectively these data provide evidence that TCR-induced Dlgh1 tyrosine

phosphorylation is an essential molecular event required for the Dlgh1-mediated alternative p38 pathway and selective production of TNFα and IFNγ, but not IL-2.

MATERIALS AND METHODS

In Vitro Kinase Assays

OT1 hybridoma cells ($40x10^6$) were incubated with anti-CD3 and anti-CD28 antibody followed by crosslinking with donkey anti-hamster secondary for 15 mins at 37°C. Cells were lysed using IP Lysis buffer (Pierce) in the presence of protease and phosphatase inhibitors (Pierce). Resulting lysates were cleared by centrifugation and incubated with wild type or Y222F GST-Dlgh1 fusion proteins. Complexes were pulled down using glutathione sepharose slurry and beads were washed with kinase buffer (Cell Signaling) with protease and phosphatase inhibitors. Kinase assays were incubated at 30°C for 30 mins in 50µl kinase buffer in the presence or absence of 50µM ATP (Cell Signaling). Alternatively, wild type or Y222F GST-Dlgh1 fusion proteins were bound to glutathione sepharose beads and incubated with recombinant Lck or Zap70 (Active Motif) in 50µl kinase buffer in the presence or absence of 50µM ATP at 30°C for 30 mins.

Dlgh1 Knockdown and Expression

Stable Dlgh1 knockdown lines were created in both OT1 and BI-141 hybridomas using a mIR-155 based retroviral knockdown vector (see Chapter 2). Anti-sense sequences specific for the 3'UTR region of Dlgh1 were cloned in to the mIR-155-based knockdown vector. Virus was produced by transfecting $4x10^6$ 293T cells with 50µg of knockdown vector and 50µg of pCL-Eco packaging vector (Mirus). Resulting viral supernatant was used to spin infect OT1 or BI-141 hybridomas for 90 mins at 1250*g* on two consecutive days. Cells were allowed to rest for a day then assessed for Dlgh1 knockdown. Stable lines were maintained in media supplemented with 25µg/mL puromycin (Invitrogen). Dlgh1 was re-introduced in to these cell lines using an MSCV-based retroviral vector expressing wild type or Y222F Dlgh1 using the same viral production and transduction methods

used for the knockdown virus. Cells were assessed for equal re-expression of Dlgh1 on the mRNA and protein levels.

Flow Cytometry

For measurement of Dlgh1 $1x10^6$ cells were fixed and permeablized using FoxP3 staining buffer set (eBioscience 00-5523-00) according to the manufacturer's instructions. Dlgh1 was detected using αDlgh1 antibody (BD Biosciences 610875) at 1:1000 followed by Alexa Fluor 647-conjugated donkey anti-mouse IgG F(ab')2 (Jackson Immunoresearch 715-606-150) at 1:1000. For measurement of p38 phosphorylation in primary CD8+ T cells, 24hrs after retroviral transduction, cells were pooled and counted and were placed in fresh media at a concentration of $2x10^6$ cells per ml. Cells were allowed to rest for 4hrs at 37°C in 6-well dishes at volume of 2mls per well and were transferred to 12-well plates coated with 5µg anti-CD3 (clone 145-2C11; BD 553057) and 20µg anti-CD28 (clone 37.51; BD 553295) with a final volume of 1ml per well ($2x10^6$ cells) and incubated for 5 mins or 15 mins at 37°C to stimulate. Cells were fixed in paraformaldehyde (4% final concentration) for 30 mins followed by permeablization using the FoxP3 staining buffer set (eBioscience 00-5523-00) according to manufacturer's instructions. Phosphorylated p38 T180/Y182 was detected using Alexa Fluor 647 conjugated phosphorylated p38 antibody (T180/Y182; BD Phosflow 612595) at 1:20. Events were collected using FACSCalibur (BD Biosciences) and analyzed using FlowJo software.

Immunoprecipitation and Immunoblotting

For immunoprecipitation, lysates were incubated with 20µl 50% (volume/volume) protein G sepharose slurry in PBS (GE Healthcare 17-5132-01) for 2 hrs at 4°C to pre-clear. Sepharose beads were removed and cleared lysates were incubated with 2µg

αDlgh1 antibody (BD Biosciences 610875) or IgG1κ control antibody (BD Pharmingen 554121) for 1hr at 4°C followed by the addition of 40µl 50% protein G sepharose slurry in PBS and incubation over night at 4°C. Immunoblotting was performed using antibodies directed against Dlgh1 (BD Biosciences 610875), phosphotyrosine (clone 4G10), p38 (clone C20; Santa Cruz SC535), GST (Cell Signaling 2625) or phosphorylated p38 (T180/Y182 clone D3F9; Cell Signaling 4511). Blots were imaged using ECL Plus Western Blotting Substrate (Pierce 32132) or LiCor Odyssey Imaging System.

RNA Isolation

Cells were re-suspended in 1ml TRIzol reagent (Invitrogen). Chloroform (200µl) was added and samples were shaken vigorously and then centrifuged at 12,000*g* for 15min. The top layer was transferred to a new tube and 500µl isopropanol was added, followed by centrifugation for 15min at 12,000g. The pellet was washed once in 70% ethanol and then dissolved in RNase free water.

Reverse Transcription and Quantitative PCR

For quantitative PCR, RNA was quantified 2µg RNA was reverse-transcribed using Superscript II reverse transcriptase (Invitrogen) according to the manufacturer's instructions using random hexamer and oligo$(dT)_{20}$ as primers. The iCycler thermocycler was used for quantitative PCR analysis according to manufacturer's instructions (BioRad). A final volume of 25µl was used for each quantitative PCR reactions containing the following: Taq polymerase (Invitrogen), 1X Taq buffer (Stratagene), 125µM dNTP, SYBR Green I (Molecular Probes) and fluorescein (BioRad) with cDNA as a template. The following gene-specific primers were used for amplification: L32F-5´-AAG CGAAACTGGCGGAAAC-3´, L32(R)-5´-TAACCGATGTTGGGCATCAG-3´, NFATc1(F)-

5´-GCCTCGTAT CAGTGGGCGAAG-3´, NFATc1(R)-5´-CGAAGCTCGTATGGACCA-3´, IκBα(F)-5´-CTGCAGGCCACCAACTACAA-3´, IκBα(R)-5´-CAGCACCCAAAGTCACCAAGT-3´, IFNγ(F)-5´-GTCAAC AACCCACAGGTCCAG-3´, IFNγ(R)-5´-CCTTTTCCGCTTCCTGAGG-3´, TNFα(F)-5´-AATGGCCTCCCTCTCATCAGT-3´, TNFα(R)-5´-GCTACAGGCTTGTCACTCGAATT-3´. Amplification conditions were 94°C for 3min followed by 40 cycles of 94°C for 30sec, 61°C for 30sec, 72°C for 30sec. All quantitative PCR products were normalized to L32 ribosomal protein quantitative PCR products to correct for differences in template input to determine relative mRNA levels.

Statistical Methods

Standard deviation was calculated using Microsoft Excel. Statistical significance was obtained with a two-sided student t-test assuming equal variances.

RESULTS

Dlgh1 is Tyrosine Phosphorylated in Response to TCR Stimulation

Tyrosine phosphorylation is a well-documented mechanism to regulate scaffold protein folding and ligand binding (13-15). We have previously shown that Dlgh1 associates with at least two tyrosine kinases, Lck and Zap70, and that this association is required for TCR-induced Dlgh1-mediated signal transduction (6). To determine if Dlgh1 was phosphorylated by an associated kinase, we performed *in vitro* kinase assays using Dlgh1 complexes. Specifically, GST fusion proteins expressing full length Dlgh1 (GST-Dlgh1) were incubated with T cell lysates in order to form Dlgh1 signaling complexes. Upon addition of ATP to these complexes, a robust phosphotyrosine Dlgh1 (pY-Dlgh1) band was observed indicating that Dlgh1 was phosphorylated by at least one associated kinase (Figure 3-1A). In order to determine if this phosphorylation was TCR-induced, Dlgh1 was immunoprecipitated from resting or TCR-stimulated OT-1 T cells. An increased level of pY-Dlgh1 was observed in TCR-stimulated samples compared to resting samples suggesting that Dlgh1 tyrosine phosphorylation was TCR-induced (Figure 3-1B). Together these data demonstrate that Dlgh1 was tyrosine phosphorylated by at least one of its associated kinases, and that this phosphorylation was induced in intact T cells in response to TCR stimulation.

Tyr222 is a Major Site of TCR-induced Dlgh1 Phosphorylation

In order to gain insight into possible Dlgh1 tyrosine phosphorylation sites, we scanned the Dlgh1 protein sequence for YEEI motifs. This motif is a target for Lck phosphorylation, and once phosphorylated on the tyrosine, serves as optimal binding site motif for the SH2 domains of both Lck and Zap70 (26, 27) (Scansite 2.0). Of the 29 tyrosine residues present in full length Dlgh1 (GenBank: AAH57118.1), only one was part

of a YEEI motif. This motif was located in the linker region between the proline rich region and PDZ1 domain at positions 222-225 with the tyrosine at position 222 (Tyr222) (Figure 3-1C). The YEEI motif and the surrounding regions were highly conserved across species; consistent with the suggestion that Tyr222 may play a role in Dlgh1 function. To test this hypothesis we created GST-Dlgh1 fusion proteins in which Tyr222 is mutated to phenylalanine (Y222F) to disrupt phosphorylation at this position. Full length wild type (WT) orY222F GST-Dlgh1 fusion proteins were used to form complexes with T cell ligands and subsequently *in vitro* phosphorylated. Upon the addition of ATP, Y222F Dlgh1 consistently showed a 40% decrease in tyrosine phosphorylation signal relative to WT Dlgh1 demonstrating that Tyr222 is a major site, but not the only site of Dlgh1 tyrosine phosphorylation. (Figure 3-1D, 3-1E).

Phosphorylation of Dlgh1 is mediated by Lck, not Zap70

To determine which Dlgh1-bound kinase was responsible for Dlgh1 phosphorylation at Tyr 222 we incubated GST-Dlgh1 with T cell lysates to form Dlgh1 complexes. These complexes were *in vitro* phosphorylated by incubation with ATP in the presence or absence of src family kinase inhibitor PP2. A robust pY-Dlgh1 band was observed upon the addition of ATP which was completely blocked by the addition of PP2 (Figure 3-2A). Since Lck kinase activity is required for the activation of Zap70 these data demonstrate that Dlgh1 is phosphorylated by Lck, Zap70 or an unidentified Lck-dependent, Dlgh1-associated kinase. We incubated WT or Y222F GST-Dlgh1 fusion proteins with recombinant active Lck or Zap70 to determine if either of these kinases can directly phosphorylate Dlgh1. These experiments showed that rLck, but not rZap70 was able to directly phosphorylate Dlgh1 upon the addition of ATP. Further, phosphorylation of Y222F Dlgh1 by Lck was significantly reduced compared to WT Dlgh1 demonstrating

that Lck phosphorylates Tyr222 and at least on other unidentified tyrosine residue (Figure 3-2B, 3-2C). While rZap70 did not phosphorylate Dlgh1 it did phosphorylate GST-LAT demonstrating that the Zap70 kinase was active in our system (Figure 3-2B, 3-2C). Together these data identify Lck as the kinase responsible for Dlgh1 phosphorylation at Tyr222 and at least one other site.

Dlgh1 Tyr222 Facilitates Phosphorylation of Dlgh1-Bound p38

We and others have shown that juxtaposition of Lck, Zap70 and p38 by Dlgh1 is required for alternative p38 activation in T cells (6, 16, 25, 28). To assess the requirement of Dlgh1 Tyr222 in coordinating alternative p38 activation we formed Dlgh1 complexes by incubating WT or Y222F GST-Dlgh1 with T cell lysates and assessed the level of p38 phosphorylation (pY-p38) upon the addition of ATP. We observed a significant decrease in the amount of pY-p38 associated with Y222F Dlgh1 compared to WT providing evidence that Tyr222 is required to facilitate phosphorylation of Dlgh1-bound p38 (Figure 3-3A, 3-3B).

Phosphorylation of Dlgh1 Tyr222 Coordinates Alternative p38 Activation in CD8+ T cells

To assess the requirement for Dlgh1 Tyr222 phosphorylation in TCR-induced functions we created stable cell lines expressing predominately WT or Y222F Dlgh1. Briefly, Dlgh1 was knocked down in T cells using a miRNA-based retroviral vector specific for the 3' untranslated region (3'UTR) of Dlgh1. This process yielded stable cell lines expressing less than 10% the original amount of Dlgh1 protein. These lines were subsequently infected with an MSCV-based retrovirus expressing WT, Y222F or a control vector (Figure 3-4). The resulting cell lines expressed comparable amounts of WT or

Y222F Dlgh1 on both the mRNA and protein levels (Figure 3-4, Figure 3-5A, data not shown). Uninfected T cells or T cells expressing WT or Y222F Dlgh1 were stimulated through their TCR and the amount of Dlgh1-bound p-p38 (180/182) was assessed (Figure 3-5B). A low level of TCR-inducible p38 phosphorylation was present in the uninfected cells. This phosphorylation was significantly enhanced in cells expressing WT Dlgh1, but was completely absent in cells expressing Y222F Dlgh1. Similarly, overexpression of WT, but not Y222F Dlgh1 led to an increased level of TCR-induced p38 phosphorylation (T180/Y182) compared to control cells (Figure 3-5C, 3-5D). Together these experiments highlight an essential role for Dlgh1 Tyr222 in the regulation of TCR-induced alternative p38 activation in intact T cells.

Loss of Dlgh1 Ty222 Phosphorylation results in Decreased NFAT-, but not NFκB-dependent Expression

We and others have demonstrated that Dlgh1-mediated alternative p38 activation induces NFAT-, but not NFκB-dependent gene activation (6, 16, 25). To determine if Dlgh1 Ty222 plays a role in TCR-induced NFAT or NFκB activation, a panel of Dlgh1 knockdown and Dlgh1 re-expressing T cell lines were stimulated through their TCR and induction of *Nfatc1* (NFAT-dependent gene) and *Iκbα* (NFκB-dependent gene) was measured via quantitative PCR. In keeping with previous reports, T cells lacking Dlgh1 demonstrated impaired induction of *Nfatc1* upon TCR stimulation (Figure 3-6A) (6, 16, 25). Expression of WT Dlgh1 in Dlgh1 deficient cells was able to rescue *Nfatc1* expression while expression of Y222F Dlgh1 in these cells only further attenuated *Nfatc1* expression (Figure 3-6A). Dlgh1 knockdown or re-expression of WT or Y222F Dlgh1 had no significant effect on the level of *Ikba* induction upon TCR stimulation (Figure 3-6B). We further interrogated these findings in primary CD8+ T cells where expression of WT, but

not Y222F Dlgh1 was able to enhance TCR-dependent *Nfatc1* transcription while Dlgh1 expression has no significant effect on *Ikbα* transcription (Figure 3-6C, 3-6D).

Dlgh1 Tyr222 is required for optimal p38-dependent IFNγ and TNFα , but not IL-2 production

TCR induced alternative p38 activation has been shown to differentially regulate cytokine production. Specifically this the alternative p38 pathway leads to increased production of proinflammatory cytokines IFNγ and TNFα, while no affecting the levels of IL-2 production (6, 23, 24, 29, 30). In order to examine the requirement of Dlgh1 Tyr222 in TCR-induced cytokine production, a panel of Dlgh1 knockdown and re-expressing T cells were stimulated and their ability to upregulate cytokine gene transcription was measured. Dlgh1-deficient T cells demonstrated impaired induction of both IFNγ and TNFα transcription, but not IL-2 transcription compared to control cells (Figure 3-7A, 3-7C). Introduction of WT Dlgh1 was able to completely rescue the defect in TNFα and IFNγ transcription while introduction of Y222F Dlgh1 showed not significant increase in cytokine gene expression above the Dlgh1-deficient cells (Figure 3-7A, 3-7B). Re-expression of WT or Y222F Dlgh1 showed no significant change in the amount of IL-2 mRNA produced suggesting that Dlgh1 Tyr222 plays a role in differential regulation of cytokines (Figure 3-7C). To determine if a Dlgh1 Tyr222 was required for induction of cytokines in primary T cells, CD8+ T cells overexpressing WT or Y222F Dlgh1 were stimulated through their TCR and transcription of cytokine genes was assessed. In these experiments WT, but not Y222F Dlgh1 was able to enhance the production of both IFNγ and TNFα while neither had a significant effect on IL-2 production (Figure 3-7D-3-7F). In fact, cells overexpressing Y222F Dlgh1 demonstrated lower levels of proinflammatory cytokine production than control cells suggesting Dlgh1 Y222F might act as a dominant

negative. Together these results support a model where phosphorylation Lck-mediated phosphorylation of Dlgh1 at Tyr222 facilitates the alternative p38 pathway. Loss of this pathway leads to decreased NFAT-dependent gene transcription including the production of proinflammatory cytokines IFNγ and TNFα.

DISCUSSION

Dlgh1 is a scaffold protein required for TCR-induced alternative p38 activation, NFAT-dependent transcription and proinflammatory cytokine production (6, 16, 25). However, the mechanism(s) by which Dlgh1 specifically couples TCR engagement to this subset of signaling pathways and functions remains unclear. In this study, we characterize the role of Dlgh1 tyrosine phosphorylation in facilitating Dlgh1-mediated signaling events. We have demonstrated that Dlgh1 is phosphorylated in response to TCR stimulation by at least one bound kinase, and that Dlgh1 Tyr222 is a major site of Dlgh1 tyrosine phosphorylation. Additionally, we showed that Lck, but not Zap70 is able to directly phosphorylate Dlgh1, and that phosphorylation of Dlgh1 Tyr222 is mediated directly by Lck. Importantly, mutation of Dlgh1 on Tyr222 disrupts TCR-induced alternative p38 activation. Disruption of this pathway leads to decreased NFAT-dependent transcription including induction of proinflammatory cytokines IFNγ and TNFα, but not IL-2. Therefore, our studies provide evidence that Lck-mediated phosphorylation of Dlgh1 plays a vital role specifying signal transduction downstream of the TCR.

The Dlgh1 complex in T cells contains several tyrosine kinases, including proximal tyrosine kinases Lck and Zap70, which are thought to endow the Dlgh1 complex with kinase activity in response to TCR activation (5, 6, 18, 31). However, the tyrosine phosphorylation state of Dlgh1 itself had yet to be determined. We observed that Dlgh1 was robustly phosphorylated when Dlgh1 complexes were incubated with ATP, indicating that Dlgh1 was tyrosine phosphorylated, and that this phosphorylation was mediated by one or more Dlgh1-associated kinases (Figure 3-1A). Examination of Dlgh1 complexes in resting or TCR-stimulated T cells revealed that Dlgh1 tyrosine phosphorylation was TCR-inducible in intact T cells (Figure 3-1B). Interestingly, the top

band of the Dlgh1 doublet appeared to be preferentially phosphorylated, suggesting that a particular variant of Dlgh1 may be selectively phosphorylated. Experiments investigating this possibility are currently underway.

To further investigate the role of Dlgh1 tyrosine phosphorylation in TCR-mediated signaling we wanted to identify specific site(s) of Dlgh1 phosphorylation. To this end, we identified Tyr222 of Dlgh1 as a potential Lck-mediated phosphorylation site (26, 27) (Scansite 2.0, Figure 3-1C). This site is part of a YEEI motif known to be a target of Lck phosphorylation, and once phosphorylated forms a binding site that could associate with the SH2 domain of Lck or Zap70. We found that mutation of Dlgh1 Tyr222 to Phe (Y222F) led to a 40% decrease in Dlgh1 phosphorylation (Figure 3-1B). Since Dlgh1 is a large scaffold protein containing 29 tyrosine residues, a 40% decrease in phosphorylation suggested that Dlgh1 Tyr222 is a major site of phosphorylation (Figure 3-1C). Additionally, we demonstrated that Dlgh1 phosphorylation could be directly phosphorylated by Lck, but not Zap70 at several tyrosine residues, including Tyr222 (Figure 3-2B). Lck is thought to be associated with the N terminal proline-rich region of Dlgh1 via its SH3 domain immediately upstream of the Y222 phosphorylation site (5). Our data support a model where constitutively associated Lck becomes activated upon TCR stimulation allowing it to phosphorylate Dlgh1 at several tyrosines including Y222.

We and others have previously demonstrated that Dlgh1 coordinates the TCR-induced alternative p38 pathway through juxtaposition of Lck, Zap70 and p38 leading to NFAT-dependent transcription and production of proinflammatory cytokines (5, 6, 16, 23, 25). Here we provide evidence that phosphorylation of Dlgh1 at Tyr222 is critical for the activation of the alternative p38 pathway, and its subsequent downstream functions. Dlgh1 complexes formed with Dlgh1 Y222F in a cell free system were unable to phosphorylate p38 associated with the complex (Figure 3-3). Additionally, TCR-induced

p38 phosphorylation of Dlgh1-bound p38 was severely impaired in CD8+ T cells expressing Dlgh1 Y222F (Figure 3-5). We found that expression of Dlgh1 Y222F in T cells led to defective activation of NFAT-dependent genes including *Nfatc1* and proinflammatory cytokines *Ifng* and *Tnfa* while having no effect on the activation of NFκB-dependent gene *IkBa* or production of *Il2* (Figure 3-6, 3-7). These data positioned TCR-induced Dlgh1 phosphorylation at Tyr222 as a vital step in the alternative p38 pathway, specifying TCR signals toward NFAT-mediated genes and the production of proinflammatory cytokines.

Together our data support a model where loss of Dlgh1 Tyr222 phosphorylation disrupts the coordination of Lck and Zap70 kinase activity disallowing phosphorylation of Dlgh1-associated p38 leading to defective NFAT activation and proinflammatory cytokine production. Since Dlgh1 Tyr222 is part of a YEEI motif known to bind SH2 domains upon phosphorylation, one possible function of Dlgh1 Tyr222 phosphorylation is the creation of an SH2 binding site for Lck or Zap70 (26, 27) (Scansite 2.0, Figure 3-1). To this end, we have observed a modest decrease in Zap70 association with Dlgh1 Y222F compared to wild type; however the association is not consistently disrupted at a high level (data not shown). Since Zap70 has two SH2 domains known to bind in tandem, we hypothesize that Dlgh1 Tyr222 is one of two sites required for Zap70 association with Dlgh1. Therefore, disruption of a single SH2 binding site at Tyr222 might be sufficient to perturb the juxtaposition of Zap70 with Lck and p38 which is required for p38 activation but insufficient to completely ablate Zap70 association with Dlgh1. A second option is that phosphorylation of Dlgh1 Tyr222 leads to a conformational change in the Dlgh1 protein structure that exposes ligand binding sites and/or properly positions ligands relative to each other. Recent structural and biochemical studies have demonstrated that the Dlgh1 protein structure depends significantly on numerous intramolecular

interactions allowing Dlgh1 to exist in several conformational states from completely compact to fully extended (11, 12). Biochemical studies have demonstrated that Dlgh1 intramolecular interactions modulate the binding of GKAP to the GUK region of Dlgh1. Additionally, phosphorylation of MAGUK family member CARMA1 has been hypothesized to trigger a conformational change required for the proper assembly of the CARMA1 signalosome and activation of NFκB suggesting the phosphorylation may play a similar role in the formation of the Dlgh1 signalosome (14, 32). Experiments are currently underway to investigate these possibilities.

Our data place Tyr222 phosphorylation as a vital regulatory step in activation of p38, NFAT and pro-inflammatory cytokines downstream of the TCR. Recent studies have demonstrated that both qualitative and quantitative differences in the strength of the TCR interaction with antigen peptide::MHC complex can influence events downstream of the TCR (33). This signal strength model has been shown to translate into functional differences in mouse model of rheumatoid arthritis where 'optimal' TCR signal strength leads increased frequency and severity of disease (34). Additionally, over activation of the alternative p38 pathway in T cells has been correlated with increased severity of rheumatoid arthritis in humans (35). Given these data, it is interesting to imagine that TCR-induced phosphorylation of Dlgh1 occurs at times of high TCR stimulation acting as a molecular switch turning on p38 dependent functions including proinflammatory cytokine production. Given the dependence of autoimmune disorders including rheumatoid arthritis on the production of proinflammatory cytokines, pharmacologic inhibition of Dlgh1 phosphorylation could be an interesting option for more specific treatment of these diseases in the future.

Figure 3-1. Dlgh1 Tyr222 is phosphorylated by bound kinases in response to TCR-CD28 stimulation.

(A) GST-Dlgh1 was conjugated to glutathione sepharose beads and used to pull down ligands from T cell lysates; resulting complexes were washed and incubated 20 min with or without 10mM ATP and subsequently blotted using anti-phosphotyrosine (4G10) or anti-GST antibodies.

(B) OT-1 T cell hybridomas were left unstimulated (0') or stimulated with soluble anti-CD3 and anti-CD28 for 15 or 30 min; lysates were immunoprecipitated using anti-Dlgh1 or immunoglobulin control, immunoprecipitates were washed and immunoblotted with anti-phosphotyrosine (4G10) or anti-Dlgh1.

(C) Schematic of Dlgh1 domains depicting the location of tyrosine 222 relative to the other 29 tyrosine residues present in Dlgh1 (stars).

(D) Wild type (WT) or Tyr222 to Phe222 mutant (Y222F) GST-Dlgh1 was conjugated to glutathione sepharose beads and used to pull down ligands from T cell lysate; complexes subsequently washed and incubated for 20 min in the presence or absence of 10mM ATP then immunoblotted with anti-phosphotyrosine (4G10) or anti-GST (left). Blot was imaged (D, *left*) and quantitated (D, *right*) using the LiCor Odyssey system. Error bar represents S.D.; $^{**}p < 0.05$; n =3 independent experiments.

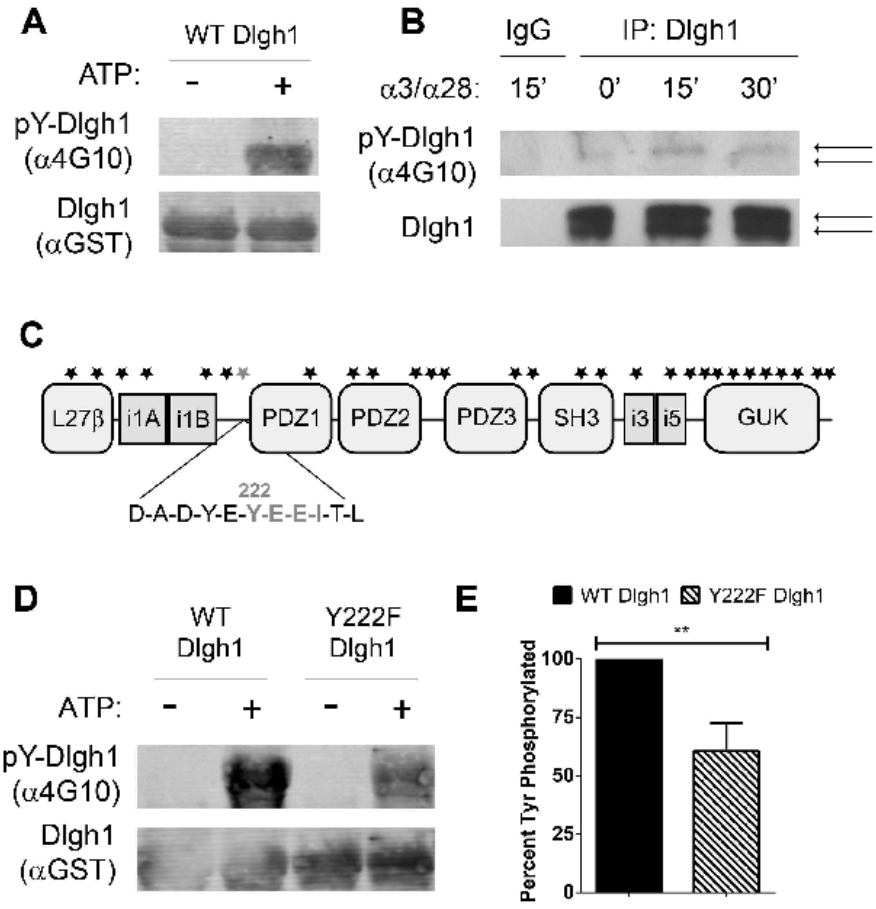
A
WT Dlgh1
ATP:
-
+
pY-Dlgh1
(α4G10)
Dlgh1
(αGST)
B
IgG
IP: Dlgh1
α3/α28:
15'
0'
15'
30'
pY-Dlgh1
(α4G10)
Dlgh1
C
L27β
i1A
i1B
PDZ1
PDZ2
PDZ3
SH3
i3
i5
GUK
222
D-A-D-Y-E-Y-E-E-I-T-L
D
WT
Dlgh1
Y222F
Dlgh1
ATP:
-
+
-
+
pY-Dlgh1
(α4G10)
Dlgh1
(αGST)
E
WT Dlgh1
Y222F Dlgh1
**
Percent Tyr Phosphorylated
100
75
50
25
0

Figure 3-2. Lck phosphorylates Dlgh1 at several sites including Tyr222.
(A) GST-Dlgh1 was conjugated to glutathione sepharose beads and used to pull down ligands from T cell lysates; complexes were washed and incubated for 20 min in the presence or absence of 10mM ATP and 10μM PP2; complexes were separated using SDS-PAGE and immunoblotted using anti-phosphotyrosine (4G10) or anti-GST.
(B-C) WT or Y222F GST-Dlgh1 fusion proteins were incubated for 20 min with 10mM ATP in the presence or absence of rLck or rZap70; samples were blotted using anti-phosphotyrosine (4G10) or anti-GST. Blots were imaged (B) and quantitated (C) using the LiCor Odyssey system. Error bars represent S.D.; **$p<0.05$; n=3 independent experiments.

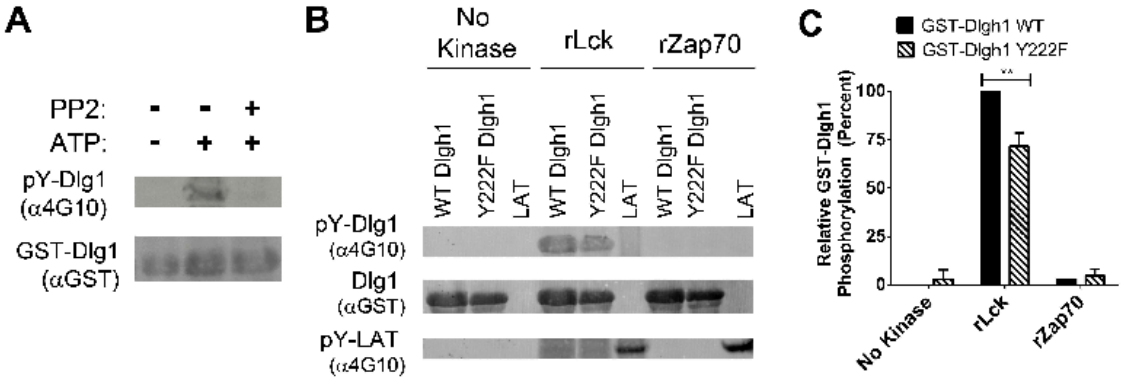
A
PP2: - - +
ATP: - + +
pY-Dlg1 (α4G10)
GST-Dlg1 (αGST)
B
No Kinase
rLck
rZap70
WT Dlgh1
Y222F Dlgh1
LAT
pY-Dlg1 (α4G10)
Dlg1 (αGST)
pY-LAT (α4G10)
C
GST-Dlgh1 WT
GST-Dlgh1 Y222F
Relative GST-Dlgh1 Phosphorylation (Percent)
100
75
50
25
0
**
No Kinase
rLck
rZap70

Figure 3-3. Dlgh1 Tyr222 is required for optimal p38 phosphorylation *in vitro*.
(A) WT or Y222F GST-Dlgh1 fusion proteins were conjugated to glutathione sepharose beads and used to pull down ligands from T cell lysates; complexes were washed and incubated for 20 min in the presence or absence of 10mM ATP; complexes were immunoblotted for pY-p38 (anti-4G10) or total p38 (anti-p38). Blots were quantitated using the LiCor Odyssey system (B). Error bars represent S.D.;** $p<0.05$; n=3 independent experiments.

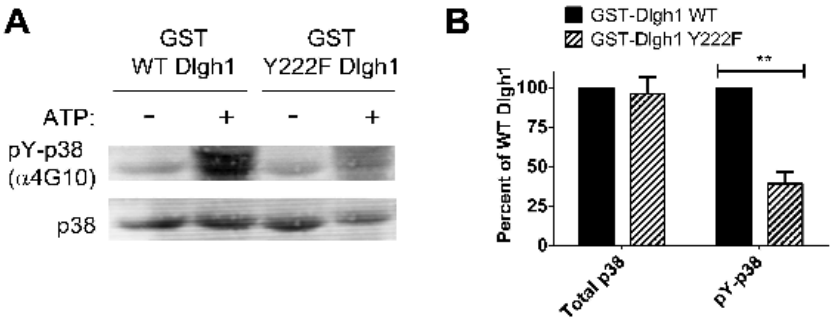
A
GST
WT Dlgh1
GST
Y222F Dlgh1
ATP:
-
+
-
+
pY-p38
(α4G10)
p38
B
GST-Dlgh1 WT
GST-Dlgh1 Y222F
**
Percent of WT Dlgh1
100
75
50
25
0
Total p38
pY-p38

Figure 3-4. Dlgh1 is knocked down and subsequently re-expressed to equal levels in various T cells.

(A) *Dlgh1*-specific qPCR of OT-1 hybridomas infected with a retroviral vector expressing a microRNA specific for the 3'UTR region of Dlgh1 (3'UTR) and subsequently infected with a retroviral vector expressing either full length wild type Dlgh1 (WT) or Dlgh1 Y222F (Y222F).

(B) Protein analysis of OT-1 hybridomas infected with a retroviral vector expressing a microRNA specific for the 3'UTR region of Dlgh1 (3'UTR) and subsequently infected with a retroviral vector expressing either full length wild type Dlgh1 (WT) or Dlgh1 Y222F (Y222F).

(C) *Dlgh1*-specific qPCR analysis of antigen experienced primary OT-1 T cells infected with retroviral vector expressing WT or Y222F Dlgh1 or empty control.

(D) Intracellular Dlgh1 analysis via flow cytometry of BI-141 cells infected with retroviral 3'UTR knock down vector followed by infection with retroviral vectors expressing WT or Y222F Dlgh1.

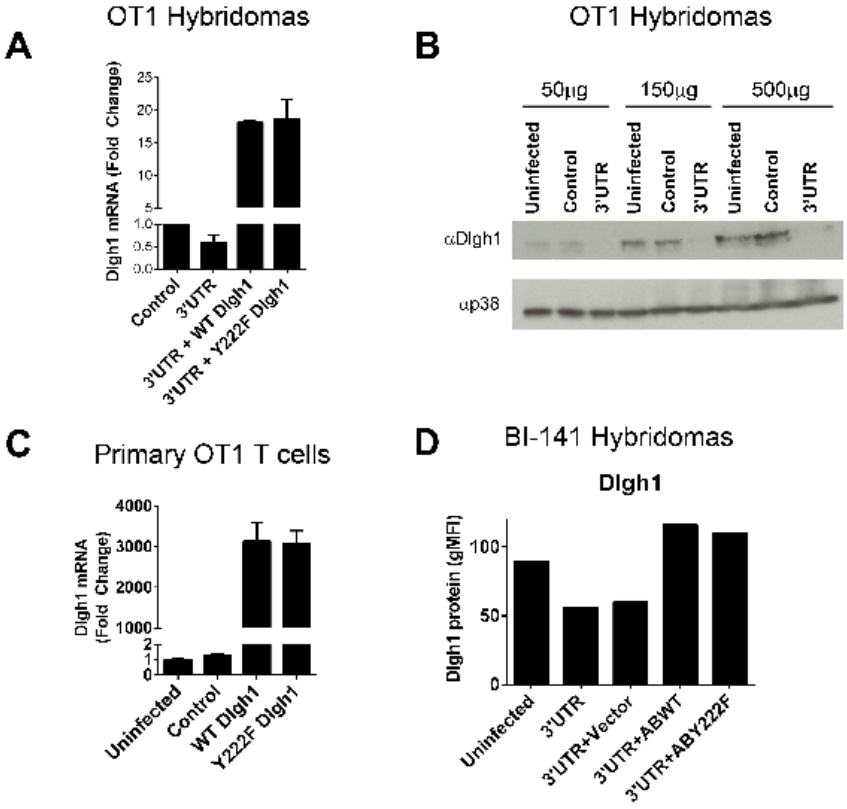
A
OT1 Hybridomas
Dlgh1 mRNA (Fold Change)
Control
3'UTR
3'UTR + WT Dlgh1
3'UTR + Y222F Dlgh1
B
OT1 Hybridomas
50µg
150µg
500µg
Uninfected
Control
3'UTR
αDlgh1
αp38
C
Primary OT1 T cells
Dlgh1 mRNA (Fold Change)
Uninfected
Control
WT Dlgh1
Y222F Dlgh1
D
BI-141 Hybridomas
Dlgh1
Dlgh1 protein (gMFI)
Uninfected
3'UTR
3'UTR+Vector
3'UTR+ABWT
3'UTR+ABY222F

Figure 3-5. Tyr222 of Dlgh1 coordinates TCR-induced alternative p38 activation in T cells.

(A) Endogenous Dlgh1 was knocked down in OT-1 T cell hybridomas using a mIR-based retroviral vector targeted to the 3' untranslated region of Dlgh1 (3'UTR) and WT or Y222F Dlgh1 was re-introduced into Dlgh1 deficient cells using an MSCV-based retroviral expression vector (3'UTR+WT or 3'UTR+Y222F); total cell lysates were immunoblotted with anti-Dlgh1 or anti-p38.

(B) Immunoblot analysis of lysates from uninfected OT-1 T cell hybridomas or WT or Y222F Dlgh1 re-expressing OT-1 T cell hybridomas left unstimulated or stimulated for 15 min with soluble anti-CD3 and anti-CD28; lysates were immunoprecipitated using anti-Dlgh1 or immunoglobulin control and immunoblotted with anti-pp38 T180/Y182, anti-p38 or anti-Dlgh1.

(C-D) Primary OT-1 T splenocytes stimulated for 2 days with plate-bound anti-CD3 and anti-CD28 and infected with MSCV-based retrovirus expressing either WT or Y222F Dlgh1

(C) Cells were permeablized using FoxP3 permeabilizing buffer for 15 minutes according to manufacturer's instructions. Cells were stained using anti-Dlgh1 at 1:100 for 45min and goat anti-mouse Alexa 647 1:100 for 30minutes.

(D) Cells were rested for 4hours at 37°C then stimulated on plate bound αCD3/αCD28 antibody for 15 minutes. Cells were fixed in 4% paraformaldehyde for 20minutes then permeabilized with FoxP3 staining kit according to manufacturer's instructions for 15 minutes and then stained with anti-pp38 T180/Y182 Alexa 647 for 40minutes.

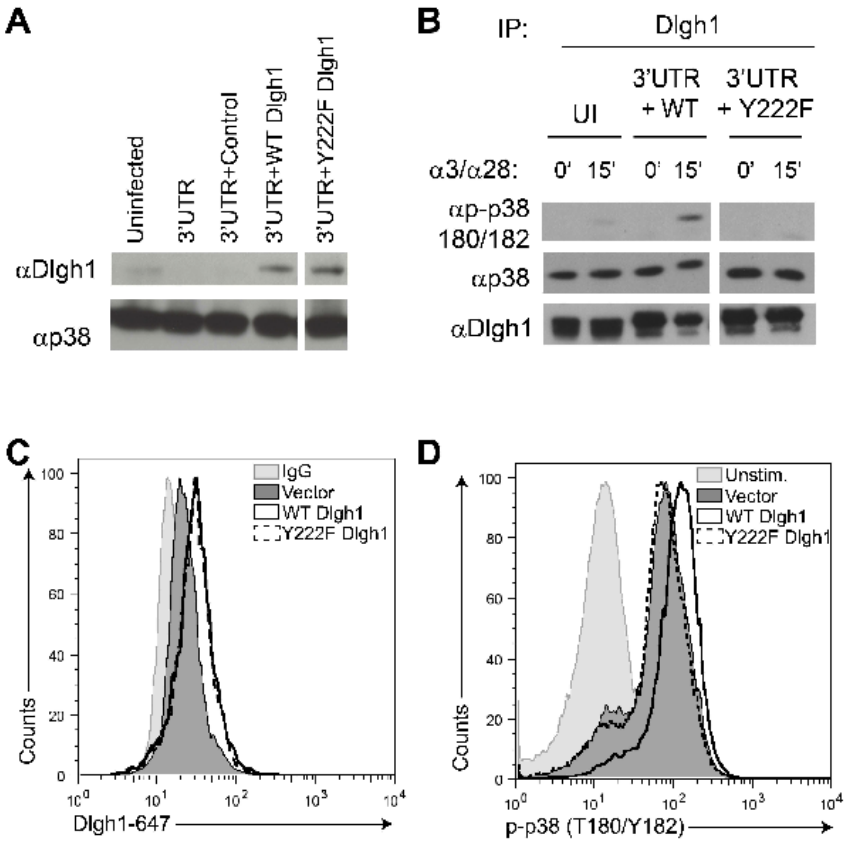
A
Uninfected
3'UTR
3'UTR+Control
3'UTR+WT Dlgh1
3'UTR+Y222F Dlgh1
αDlgh1
αp38
B
IP:
Dlgh1
UI
3'UTR + WT
3'UTR + Y222F
α3/α28:
0' 15' 0' 15' 0' 15'
αp-p38 180/182
αp38
αDlgh1
C
IgG
Vector
WT Dlgh1
Y222F Dlgh1
Counts
Dlgh1-647
D
Unstim.
Vector
WT Dlgh1
Y222F Dlgh1
Counts
p-p38 (T180/Y182)

Figure 3-6. Dlgh1 Tyr222 is required for TCR-mediated NFAT-, but not NFκB-dependent transcription.

(A-D) Quantitative PCR analysis of (A,C) *NFATc1* or (B,D) *IkBa* mRNA expression in (A,B) OT-1 T cell hybridomas where endogenous Dlgh1 has been knocked down using a mIR-based retroviral vector specific for the 3' untranslated region of Dlgh1 and wild-type (WT) or Y222F Dlgh1 has been re-expressed using an MSCV-based retroviral expression vector; or (C,D) primary OT-1 T splenocytes stimulated for 2 days with plate-bound anti-CD3 and anti-CD28 and infected with MSCV-based retrovirus expressing either WT or Y222F Dlgh1; (A-D) 72hrs after infection, cells were left unstimulated (solid bars) or re-stimulated with plate-bound 5ug/mL anti-CD3 and 5ug/mL anti-CD28 for 2hr (hashed bars). *Nfatc1* (A,C) and *Ikba* (B,D) were detected using gene-specific primers. **$p<0.05$; n=3 independent experiments. **$p<0.05$; n=3 independent experiments.

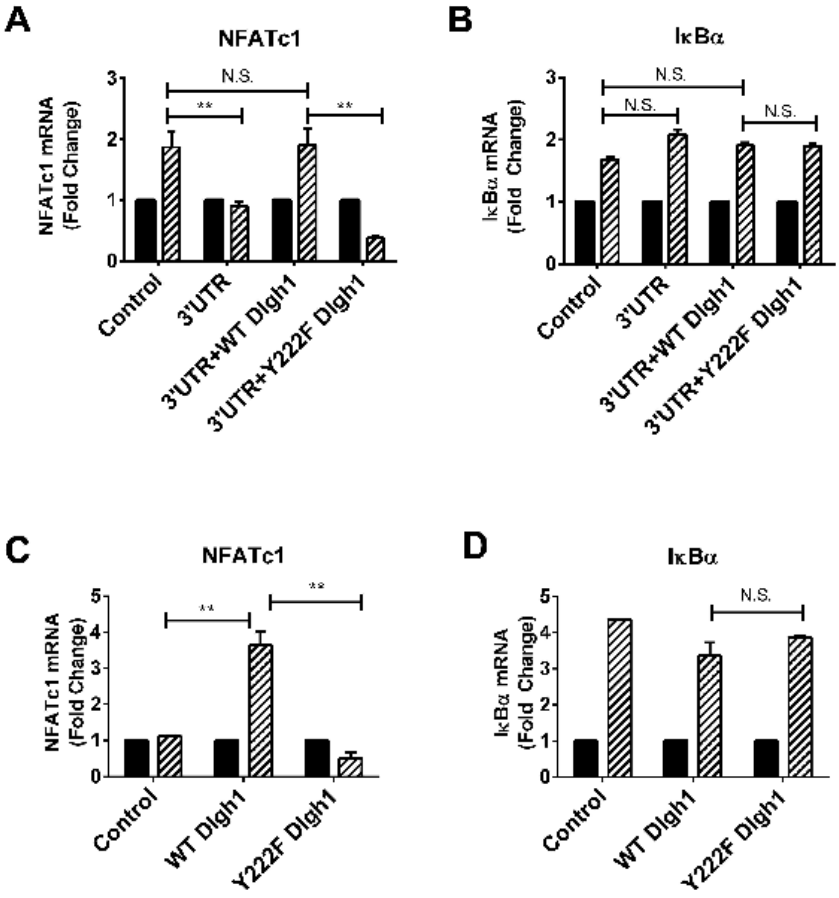
A
NFATc1
NFATc1 mRNA (Fold Change)
N.S.
**
**
Control
3'UTR
3'UTR+WT Dlgh1
3'UTR+Y222F Dlgh1
B
IκBα
IκBα mRNA (Fold Change)
N.S.
N.S.
N.S.
Control
3'UTR
3'UTR+WT Dlgh1
3'UTR+Y222F Dlgh1
C
NFATc1
NFATc1 mRNA (Fold Change)
**
**
Control
WT Dlgh1
Y222F Dlgh1
D
IκBα
IκBα mRNA (Fold Change)
N.S.
Control
WT Dlgh1
Y222F Dlgh1

Figure 3-7. Dlgh1 Tyr222 is required for p38-dependent production of TNFα and IFNγ, but not IL-2.

(A-F) Quantitative PCR analysis of (A,C) *Ifng,* (B,D) *Tnfa* or (C,F) *Il2* mRNA expression in (A-C) BI-141 T cell hybridomas where endogenous Dlgh1 has been knocked down using a mIR-based retroviral vector specific for the 3' untranslated region of Dlgh1 and wild-type (WT) or Y222F Dlgh1 has been re-expressed using an MSCV-based retroviral expression vector; or (D-F) Primary OT-1 T splenocytes stimulated for 2 days with plate-bound anti-CD3 and anti-CD28 and infected with MSCV-based retrovirus expressing either WT or Y222F Dlgh1; (A-F) 72hrs after infection cells were left unstimulated (solid bars) or re-stimulated with plate-bound 5ug/mL anti-CD3 and 5ug/mL anti-CD28 for 6hrs (hashed bars); *Ifng* (A,C), *Tnfa* (B,D) and (C,F) *Il2* were detected using gene-specific primers. **$p<0.05$; n=3 independent experiments.

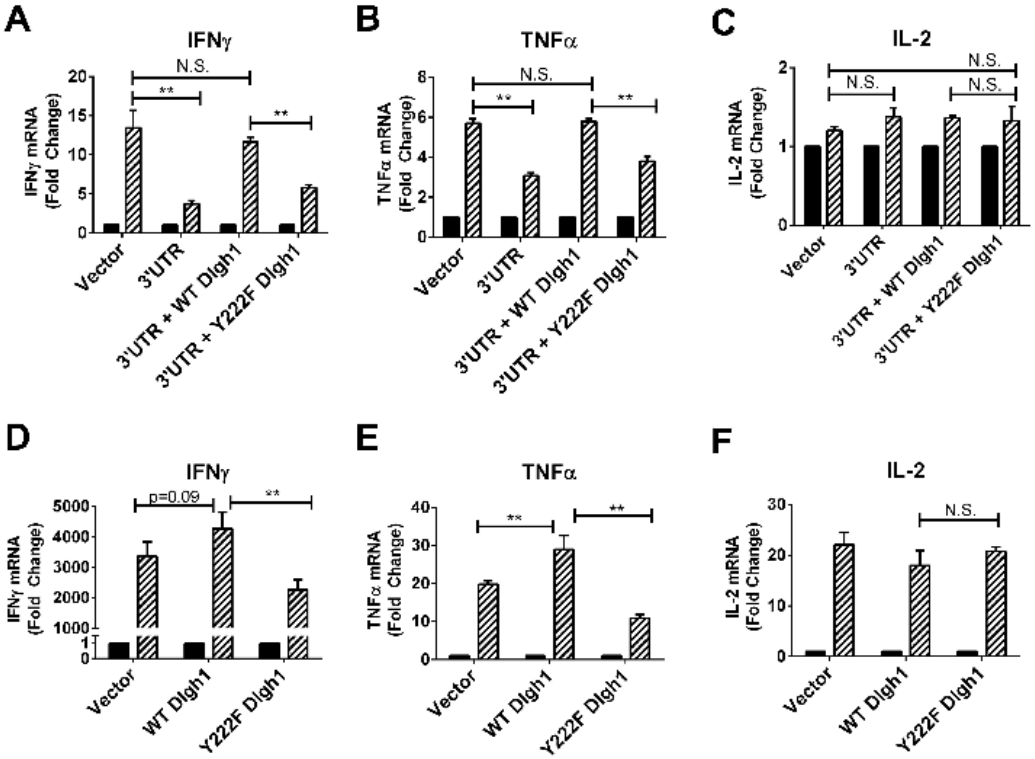
A
IFNγ
IFNγ mRNA (Fold Change)
N.S.
**
**
Vector
3'UTR
3'UTR + WT Dlgh1
3'UTR + Y222F Dlgh1
B
TNFα
TNFα mRNA (Fold Change)
N.S.
**
**
Vector
3'UTR
3'UTR + WT Dlgh1
3'UTR + Y222F Dlgh1
C
IL-2
IL-2 mRNA (Fold Change)
N.S.
N.S.
N.S.
Vector
3'UTR
3'UTR + WT Dlgh1
3'UTR + Y222F Dlgh1
D
IFNγ
IFNγ mRNA (Fold Change)
p=0.09
**
Vector
WT Dlgh1
Y222F Dlgh1
E
TNFα
TNFα mRNA (Fold Change)
**
**
Vector
WT Dlgh1
Y222F Dlgh1
F
IL-2
IL-2 mRNA (Fold Change)
N.S.
Vector
WT Dlgh1
Y222F Dlgh1

REFERENCES

1. Peng SL, Gerth AJ, Ranger AM, & Glimcher LH (2001) NFATc1 and NFATc2 together control both T and B cell activation and differentiation. *Immunity* 14(1):13-20.

2. Rutishauser RL & Kaech SM (2010) Generating diversity: transcriptional regulation of effector and memory CD8 T-cell differentiation. *Immunological reviews* 235(1):219-233.

3. Betts MR*, et al.* (2006) HIV nonprogressors preferentially maintain highly functional HIV-specific CD8+ T cells. *Blood* 107(12):4781-4789.

4. Newell EW, Sigal N, Bendall SC, Nolan GP, & Davis MM (2012) Cytometry by Time-of-Flight Shows Combinatorial Cytokine Expression and Virus-Specific Cell Niches within a Continuum of CD8(+) T Cell Phenotypes. *Immunity* 36(1):142-152.

5. Round JL*, et al.* (2005) Dlgh1 coordinates actin polymerization, synaptic T cell receptor and lipid raft aggregation, and effector function in T cells. *J Exp Med* 201(3):419-430.

6. Round JL*, et al.* (2007) Scaffold protein Dlgh1 coordinates alternative p38 kinase activation, directing T cell receptor signals toward NFAT but not NF-kappaB transcription factors. *Nat Immunol* 8(2):154-161.

7. Wang D*, et al.* (2002) A requirement for CARMA1 in TCR-induced NF-kappa B activation. *Nature immunology* 3(9):830-835.

8. Schlüter OM, Xu W, & Malenka RC (2006) Alternative N-terminal domains of PSD-95 and SAP97 govern activity-dependent regulation of synaptic AMPA receptor function. *Neuron* 51(1):99-111.

9. Lue RA, Marfatia SM, Branton D, & Chishti AH (1994) Cloning and characterization of hdlg: the human homologue of the Drosophila discs large tumor suppressor binds to protein 4.1. *Proc Natl Acad Sci USA* 91(21):9818-9822.

10. Hanada T, Takeuchi A, Sondarva G, & Chishti AH (2003) Protein 4.1-mediated membrane targeting of human discs large in epithelial cells. *J Biol Chem* 278(36):34445-34450.

11. Tully MD*, et al.* (2011) Conformational characterisation of SAP97 by NMR and SAXS shows both compact and elongated forms. *Biochemistry* 51(4):899-908.

12. Wu H*, et al.* (2000) Intramolecular interactions regulate SAP97 binding to GKAP. *EMBO J* 19(21):5740-5751.

13. Torres E & Rosen MK (2003) Contingent phosphorylation/dephosphorylation provides a mechanism of molecular memory in WASP. *Molecular cell* 11(5):1215-1227.

14. Sommer K, *et al.* (2005) Phosphorylation of the CARMA1 linker controls NF-kappaB activation. *Immunity* 23(6):561-574.

15. Brenner D, *et al.* (2009) Phosphorylation of CARMA1 by HPK1 is critical for NF-kappaB activation in T cells. *Proceedings of the National Academy of Sciences of the United States of America* 106(34):14508-14513.

16. Lasserre R, *et al.* (2010) Ezrin tunes T-cell activation by controlling Dlg1 and microtubule positioning at the immunological synapse. *EMBO J* 29(14):2301-2314.

17. Hanada T, Lin L, Tibaldi EV, Reinherz EL, & Chishti AH (2000) GAKIN, a novel kinesin-like protein associates with the human homologue of the Drosophila discs large tumor suppressor in T lymphocytes. *J Biol Chem* 275(37):28774-28784.

18. Xavier R, *et al.* (2004) Discs large (Dlg1) complexes in lymphocyte activation. *J Cell Biol* 166(2):173-178.

19. Salvador JM, *et al.* (2005) Alternative p38 activation pathway mediated by T cell receptor-proximal tyrosine kinases. *Nat Immunol* 6(4):390-395.

20. Ashwell JD (2006) The many paths to p38 mitogen-activated protein kinase activation in the immune system. *Nat Rev Immunol* 6(7):532-540.

21. Mittelstadt PR, Yamaguchi H, Appella E, & Ashwell JD (2009) T Cell Receptor-mediated Activation of p38 by Mono-phosphorylation of the Activation Loop Results in Altered Substrate Specificity. *Journal of Biological Chemistry* 284(23):15469-15474.

22. Diskin R, Lebendiker M, Engelberg D, & Livnah O (2007) Structures of p38alpha active mutants reveal conformational changes in L16 loop that induce autophosphorylation and activation. *J Mol Biol* 365(1):66-76.

23. Jirmanova L, Sarma DN, Jankovic D, Mittelstadt PR, & Ashwell JD (2009) Genetic disruption of p38alpha Tyr323 phosphorylation prevents T-cell receptor-mediated p38alpha activation and impairs interferon-gamma production. *Blood* 113(10):2229-2237.

24. Jirmanova L, Giardino Torchia ML, Sarma ND, Mittelstadt PR, & Ashwell JD (2011) Lack of the T cell-specific alternative p38 activation pathway reduces autoimmunity and inflammation. *Blood* 118(12):3280-3289.

25. Zanin-Zhorov A, *et al.* (2012) Scaffold protein Disc large homolog 1 is required for T-cell receptor-induced activation of regulatory T-cell function. *Proceedings of the National Academy of Sciences of the United States of America* 109(5):1625-1630.

26. Granum S, *et al.* (2008) Modulation of Lck function through multisite docking to T cell-specific adapter protein. *The Journal of biological chemistry* 283(32):21909-21919.

27. Isakov N, *et al.* (1995) ZAP-70 binding specificity to T cell receptor tyrosine-based activation motifs: the tandem SH2 domains of ZAP-70 bind distinct tyrosine-based activation motifs with varying affinity. *The Journal of experimental medicine* 181(1):375-380.

28. Rebeaud F, Hailfinger S, & Thome M (2007) Dlgh1 and Carma1 MAGUK proteins contribute to signal specificity downstream of TCR activation. *Trends Immunol* 28(5):196-200.

29. Kaminuma O, *et al.* (2008) Differential contribution of NFATc2 and NFATc1 to TNF-alpha gene expression in T cells. *J Immunol* 180(1):319-326.

30. Macian F (2005) NFAT proteins: key regulators of T-cell development and function. *Nat Rev Immunol* 5(6):472-484.

31. Hanada T, Lin L, Chandy KG, Oh SS, & Chishti AH (1997) Human homologue of the Drosophila discs large tumor suppressor binds to p56lck tyrosine kinase and Shaker type Kv1.3 potassium channel in T lymphocytes. *J Biol Chem* 272(43):26899-26904.

32. Matsumoto R, *et al.* (2005) Phosphorylation of CARMA1 plays a critical role in T Cell receptor-mediated NF-kappaB activation. *Immunity* 23(6):575-585.

33. Corse E, Gottschalk RA, & Allison JP (2011) Strength of TCR-Peptide/MHC Interactions and In Vivo T Cell Responses. *Journal of immunology (Baltimore, Md : 1950)* 186(9):5039-5045.

34. Olasz K, *et al.* (2012) T cell receptor (TCR) signal strength controls arthritis severity in proteoglycan-specific TCR transgenic mice. *Clinical and experimental immunology* 167(2):346-355.

35. López-Santalla M, *et al.* (2011) Tyr323-dependent p38 activation is associated with rheumatoid arthritis and correlates with disease activity. *Arthritis and rheumatism* 63(7):1833-1842.

CHAPTER FOUR

Characterization of *In Vivo* dlg1 deletion on T cell development and function

Humphries LA, Shaffer MH, Sacirbegovic F, Tomassian T, McMahon K-A, Humbert PO, Silva O, Round JL, Takamiya K, Huganir RL, Burkhardt JK, Russell SM, Miceli MC. (2012) Characterization of *In Vivo* Dlg1 Deletion on T Cell Development and Function. PLOS One 7(9): e45276, doi:10.1371/journal.pone.0045276

OPEN ACCESS Freely available online

PLOS ONE

Characterization of *In Vivo* Dlg1 Deletion on T Cell Development and Function

Lisa A. Humphries[1☯], Meredith H. Shaffer[2☯], Faruk Sacirbegovic[3,4☯], Tamar Tomassian[1,5], Kerrie-Ann McMahon[3,8], Patrick O. Humbert[4,6,7], Oscar Silva[1], June L. Round[1], Kogo Takamiya[9], Richard L. Huganir[10], Janis K. Burkhardt[2☯], Sarah M. Russell[3,4,7,8☯], M. Carrie Miceli[1,5*☯]

1 Department of Microbiology, Immunology, and Molecular Genetics, University of California Los Angeles, Los Angeles, California, United States of America, **2** Department of Pathology and Laboratory Medicine, Children's Hospital of Philadelphia and Perelman School of Medicine at the University of Pennsylvania, Philadelphia, Pennsylvania, United States of America, **3** Immune Signalling Laboratory, Peter MacCallum Cancer Centre, East Melbourne, Victoria, Australia, **4** Department of Pathology, University of Melbourne, Melbourne, Victoria, Australia, **5** Molecular Biology Institute, University of California Los Angeles, Los Angeles, California, United States of America, **6** Cell Cycle and Cancer Genetics Laboratory, Peter MacCallum Cancer Centre, East Melbourne, Victoria, Australia, **7** Sir Peter MacCallum Department of Oncology, University of Melbourne, Melbourne, Victoria, Australia, **8** Center for Micro-Photonics, Faculty of Engineering and Industrial Sciences, Swinburne University of Technology, Melbourne, Victoria, Australia, **9** Department of Neuroscience, Faculty of Medicine, University of Miyazaki, Miyazaki, Japan, **10** Department of Neuroscience, Howard Hughes Medical Institute and Brain Science Institute, The Johns Hopkins University School of Medicine, Baltimore, Maryland, United States of America

Abstract

Background: The polarized reorganization of the T cell membrane and intracellular signaling molecules in response to T cell receptor (TCR) engagement has been implicated in the modulation of T cell development and effector responses. In siRNA-based studies Dlg1, a MAGUK scaffold protein and member of the Scribble polarity complex, has been shown to play a role in T cell polarity and TCR signal specificity, however the role of Dlg1 in T cell development and function *in vivo* remains unclear.

Methodology/Principal Findings: Here we present the combined data from three independently-derived *dlg1*-knockout mouse models; two germline deficient knockouts and one conditional knockout. While defects were not observed in T cell development, TCR-induced early phospho-signaling, actin-mediated events, or proliferation in any of the models, the acute knockdown of Dlg1 in Jurkat T cells diminished accumulation of actin at the IS. Further, while Th1-type cytokine production appeared unaffected in T cells derived from mice with a *dlg1*germline-deficiency, altered production of TCR-dependent Th1 and Th2-type cytokines was observed in T cells derived from mice with a conditional loss of *dlg1* expression and T cells with acute Dlg1 suppression, suggesting a differential requirement for Dlg1 activity in signaling events leading to Th1 versus Th2 cytokine induction. The observed inconsistencies between these and other knockout models and siRNA strategies suggest that 1) compensatory upregulation of alternate gene(s) may be masking a role for *dlg1* in controlling TCR-mediated events in *dlg1* deficient mice and 2) the developmental stage during which *dlg1* ablation begins may control the degree to which compensatory events occur.

Conclusions/Significance: These findings provide a potential explanation for the discrepancies observed in various studies using different *dlg1*-deficient T cell models and underscore the importance of acute *dlg1* ablation to avoid the upregulation of compensatory mechanisms for future functional studies of the Dlg1 protein.

Citation: Humphries LA, Shaffer MH, Sacirbegovic F, Tomassian T, McMahon K-A, et al. (2012) Characterization of *In Vivo* Dlg1 Deletion on T Cell Development and Function. PLoS ONE 7(9): e45276. doi:10.1371/journal.pone.0045276

Editor: Derya Unutmaz, New York University, United States of America

Received May 15, 2012; **Accepted** August 15, 2012; **Published** September 18, 2012

Funding: Work by J.K.B. was supported by National Institutes of Health (http://www.nih.gov) grant P01 CA093615 and work by M.H.S. was supported by National Institutes of Health training grant T32-HD07516. Work by M.C.M. was supported by National Institutes of Health grant R01-AI067253-10 and by a UCLA (University of California, Los Angeles) dissertation year fellowship to J.L.R., a UCLA (University of California, Los Angeles) Microbial Pathogenesis Training Grant 2-T32-AI-07323 to T.T. and an Arthritis Foundation Postdoctoral Fellowship to L.A.H. Work by S.M.R. and P.O.H. was supported by the Australian National Health and Medical Research Council and the Australian Research Council. The funders had no role in study design, data collection, and analysis, decision to publish, or preparation of the manuscript.

Competing Interests: The authors have declared that no competing interests exist.

* E-mail: cmiceli@ucla.edu

☯ These authors contributed equally to this work.

Introduction

T cell development and effector function is dependent on the ability of T cells to dynamically polarize and selectively rearrange membrane and actin cytoskeletal components to mediate cell:cell interactions, trafficking to lymphoid compartments and sites of infection, and responses to antigen recognition [1–5]. Effective recognition of antigen by the T cell receptor (TCR) is an essential event for T cell activation in the context of an antigen-presenting cell (APC) and a critical control point for the development and regulation of adaptive immunity. Following TCR-mediated recognition of its cognate peptide, a T cell undergoes rapid and

dynamic cytoskeletal and membrane reorganization which facilitates the polarized recruitment and segregation of cellular components into specialized macromolecular assemblies: the immunological synapse (IS), located at the APC:T-cell interface, and the distal pole complex (DPC), formed opposite the [6,7].

The IS serves as a multi-tasking platform for coupling TCR proximal non-receptor tyrosine kinases, Lck and ZAP-70, to downstream transducer pathways. It has been suggested that recruitment of particular transducers at the synapse specifies distinct transcriptional activation profiles to selectively direct T cell functional outcome [8,9]. Furthermore, the IS directs reorientation of the microtubule-organizing center (MTOC) and the polarized trafficking of cytokines, cytolytic granules and fate determinants, to promote directional secretion, targeted cell killing and asymmetric cell division [1,10–12]. Distal to the APC:T cell contact site, DPC assembly may promote T cell activation by sequestering negative regulators away from the IS, or may orchestrate asymmetric cell division [7,13,14].

Formation of both the IS and DPC have been shown to correlate with the asymmetrical distribution of polarity proteins [3] providing a mechanism for diversifying signals for effector activity as well as to specify fate. The composition of the IS and DPC can vary in different T cell subsets and throughout activation [15–17] and these complexes have been shown to regulate T cell effector responses and fate decisions through the selective recruitment and juxtaposition of surface receptors, intracellular signal transducers, negative regulators, and cytoskeletal/membrane components into discrete functional domains [4,18,19]. It has been proposed that the polarization of activated T cells and resulting distribution of key signaling molecules and cellular machinery within the IS and DPC may also guide memory and effector fate decisions [20]. Indeed, asymmetric proteasome segregation to the DPC results in unequal partitioning of the transcription factor T-bet during T cell division and the generation of functionally distinct daughter populations [11]. Understanding the mechanisms that control and regulate T lymphocyte polarity may thus lend insight into methods by which T cell effector responses and memory development can be manipulated in a targeted fashion.

Lymphocyte cell polarity is orchestrated by evolutionarily conserved protein networks including the Scribble, PAR (partitioning-defective), and Crumbs complexes [3]. These ancestral polarity complexes are well characterized as master regulators of epithelial cell apico-basal polarity. The Scribble complex, composed of the Scribble, Lethal giant larvae (Lgl) and Discs large (Dlg) proteins, regulates epithelial polarity by recruiting surface receptors and signaling molecules through interaction with the cytoskeleton and other structural elements [21]. Similarly, Scribble complex proteins, including Dlg1, localize at the IS and DPC in an orchestrated manner and both Scribble and Dlg1 have been shown to regulate IS and DPC functions, including T cell morphology and migration [3,7,22,23].

Dlg1, (hDlg/Dlgh1, Synapse-associated protein 97/SAP97), is a founding member of the membrane associated guanylate kinase (MAGUK) family, a multi-domain scaffolding protein which associates with signaling and cytoskeletal effector molecules important for T cell signal transduction and polarity. Structurally, Dlg1 is composed of an N-terminal L27β oligomerization domain, a proline-rich domain (PRD), three PDZ (PSD-95, Dlg, and ZO-1) domains, an SH3 (Src Homology 3) domain and a catalytically-inactive GUK (GUanylate Kinase) domain. During antigen recognition, these modular domains allow Dlg1 to co-localize with synaptic actin, translocate into sphingolipid-rich microdomains within the IS and associate with Lck, ZAP-70, Vav, WASp, Ezrin and p38 [3,23–25], although the mode of regulation and functional significance of several of these interactions remain unclear. The association of Dlg1 with cytoskeletal regulators WASp and Ezrin is hypothesized to facilitate T cell polarity by coupling TCR engagement to actin polymerization, the clustering of synaptic TCRs, and MTOC polarization. Knockdown of Dlg1 expression attenuates TCR triggered F-actin polymerization and the polarized recruitment of lipid rafts, TCR and the MTOC to the IS [22], processes known to utilize WASp and Ezrin [2,26].

T cell functional outputs are regulated through integrating signal transduction pathways and cytoskeletal reorganization events initiated and maintained by TCR and co-receptor engagement to allow for proper magnitude, duration and type of effector response. TCR stimulation triggers the juxtaposition of Lck, ZAP-70 and p38 by Dlg1. This unique arrangement facilitates direct phosphorylation of p38 by ZAP-70, promoting p38 autophosphorylation [24,27] through a process referred to as alternative p38 activation. Dlg1-mediated alternative p38 activation selectively activates the nuclear factor of activated T cells (NFAT), but not nuclear factor κB (NFκB), due to the direct or indirect phosphorylation of the NFAT transactivation domain [24,26,28], affecting NFAT substrate specificity and directing its activity to a discrete set of downstream targets [29]. In line with these data, knockdown of Dlg1 expression in primary antigen-experienced CD8+ T cells disrupts TCR-induced cytokine production and contact-dependent cytolysis [22]. However, in one report, the overexpression of Dlg1in the presence of Vav in Jurkat T cells was found to impair NFAT activity [23], suggesting that Dlg1 activity may differ in particular T cell contexts or function as a dominant negative when expressed at high levels. While the mechanisms by which Dlg1 regulates these effector responses have not been completely elucidated, Dlg1 binding partners p38, WASp and Ezrin have all been implicated in processes that affect cytokine production and/or cytotoxicity [26,30–34].

While previous studies have implicated Dlg1 in regulating T cell signaling, polarity and effector responses, the majority of reports on Dlg1 in T cells have utilized siRNA-mediated knockdown strategies [22–24,26,28]. However, knockdown technology is limited, confining studies to activated T cells over a transient period of time and precluding the evaluation of T cell development. Moreover, since knockdown is often incomplete, it does not allow for analysis in a true null background. Thus, to build on and extend the current understanding of Dlg1 in T cell development, signaling, and actin-cytoskeletal events, three distinct *dlg1* deficient mouse strains were independently characterized by three groups. Here, we present the combined cellular and biochemical analyses of one conditional and two germline *dlg1* knockout mouse models from these groups. In total these data show that the ablation of *dlg1* expression in T cells in these independently-derived mouse models is largely unremarkable, with no, or minor, observable defects in T cell development, morphology, migration, signaling and/or proliferation. Nonetheless, the different knockout models do lead to subtle differences in T cell functionality, with the most significant effects observed in the model in which *dlg1* was knocked out conditionally during T cell development. These findings are consistent with suggestions that compensatory mechanisms may come into play at different stages of T cell development and mask Dlg1 function in T cell populations with long term Dlg1 ablation.

Results

Dlg1 is a Discs Large-family Member Expressed in T Cells

To examine which *dlg* genes are expressed in mouse T cells, specific primer sets were used to amplify a small region of four of

the seven *dlg* transcripts, *dlg1, dlg2 (PSD-93), dlg3 (NE-dlg),* and *dlg4* (PSD-95) from murine mRNA. The expression of the distantly related Dlg family members (*dlg5–dlg7*) was not determined. While mRNA from *dlg1, 2, 3 and 4* was detected in murine brain, only *dlg1* and *dlg4* were detected in murine T cells (Figure S1A). Previous studies have confirmed the presence of Dlg1 [3,22] and Dlg4 [3,35] in murine T cells by Western blotting. Therefore, while *dlg4* may play a role in T cells, our studies focused on *dlg1* which has been implicated in several key aspects of T cell function [3,7,22–24,26,28,36].

The Generation of *dlg1* Germline and Conditional Knockout Mice Using Three Independent Approaches

To address the role of Dlg1 in T cell development, three independent *dlg1* knockout mouse models were generated; two models contained a germline deletion in *dlg1* and one model was generated with a conditional loss of *dlg1* confined to the T cell compartment.

Since mice that are germline deficient for *dlg1* develop abnormally and exhibit perinatal lethality due to cleft palate and the inability to suckle [37], both mouse models containing a *dlg1* germline deletion were maintained and bred as heterozygotes. Resulting embryos were then used as donors for partial or full hematopoietic reconstitution of irradiated recipient mice, as indicated below, to evaluate *dlg1*-dependent T cell development and function. In one approach, mice were generated with a tissue-wide knockout of *dlg1* using RRN196 ES cells generated by the Bay Genomics (BG) Consortium, to yield BG-$dlg1^{-/-}$ mice (Miceli group). In this construct, the insertional mutation occurs in the fourth exon of *dlg1,* resulting in the first 150 amino acids of Dlg1 being fused to a β-galactosidase (β-Geo) insertion cassette (Figure S2A). While BG-$dlg1^{+/+}$, $^{+/-}$, and $^{-/-}$ pups were present at the expected Mendelian ratios, BG-$dlg1^{-/-}$ pups died shortly after birth, as expected, from severe birth defects. T cell development and function were therefore evaluated by adoptively transferring fetal liver cells from BG-$dlg1^{+/+}$and $^{-/-}$ donor littermates into sublethally irradiated Rag1 deficient mice ($rag1^{-/-}$) and will herein be referred to as $dlg1^{wt;BG}$ or $dlg1^{ko;BG}$ mice, respectively. Briefly, BG-*dlg1* heterozygote mice were bred and fetal livers harvested from embyros at embryonic day 14.5. Prior to injecting fetal liver cells into recipient mice, a FACS-based β-galactosidase assay was used as a preliminary screen to differentiate between wildtype, heterozygous, and homozygous BG-*dlg1* donors (Figure 1A). Donor genotypes were confirmed by PCR using primer sets spanning exon 4 and the β-Geo gene to determine the presence and/or absence of the β-Geo insertion cassette (Figure S2C). Western blotting of fetal tissue confirmed the absence of Dlg1 protein expression in BG-$dlg1^{-/-}$ donor pups (Figure 1B) as well as in lymphoid organs from $dlg1^{ko;BG}$ mice 8 weeks post-adoptive transfer (Figure 1C).

A second approach utilized a previously published *dlg1* germline deficient mouse generated via gene trap (GT) insertion (Russell group) [37]. In this construct, the first 549 amino acids were fused to a β-galactosidase insertion cassette, resulting in a tissue-wide loss of *dlg1* expression (Figure S2B). *dlg1*-deficientT cells were generated by hematopoietic reconstitution of lethally irradiated B6-Ptprca (Ly5.1) mice using fetal liver cells from GT-$dlg1^{-/-}$ gene trap mice or wild-type littermates and will herein be referred to as $dlg1^{ko;GT}$ or $dlg1^{wt;GT}$ mice, respectively.

In a third approach, the role of *dlg1* in T-lineage cell development was directly addressed by generating a conditional knock out mouse (Burkhardt group). Mice bearing a loxP-Dlg1 targeting allele, $dlg1^{flox/flox}$ [38], were crossed to CD4-Cre transgenic mice, in which Cre recombinase is driven by the CD4 promoter so that gene knockout is induced during the $CD4^+CD8^+$ double positive stage of T cell development. Resulting progeny with a targeted deletion of *dlg1* late in thymic development will herein be referred to as $dlg1^{flox/flox}$:$CD4^{cre}$. $dlg1^{flox/flox}$:$CD4^{cre}$ mice were viable and born in normal Mendelian ratios with no gross morphological defects (data not shown). While T cells from $dlg1^{flox/flox}$ mice had detectable levels of Dlg1 protein, following Cre-mediated deletion T cells from $dlg1^{flox/flox}$:$CD4^{cre}$ lacked detectable Dlg1 protein (Figure 1D, left panel). Importantly, the *dlg1* deletion was restricted to the T cell compartment, as T-depleted lymphocytes from $dlg1^{flox/flox}$:$CD4^{cre}$ transgenic mice maintained Dlg1 expression (Figure 1D, right panel). Mice with or without a conditional loss of *dlg1* in the T cell compartment will herein be referred to as $dlg1^{flox/flox}$:$CD4^{cre}$ and $dlg1^{flox/flox}$ mice, respectively.

Lymphocyte Development Appears Normal in *dlg1* Knock-out Mice

Previous studies have demonstrated a role for Dlg1 in regulating the activation of NFAT [1,23,24,26,28], a key transcription factor in T and B cell development and activation. To examine the role of *dlg1* ablation in the development of T cells and other lymphocyte populations, thymic and peripheral lymphocyte subsets were analyzed from $dlg1^{wt;BG}$ vs. $dlg1^{ko;BG}$, $dlg1^{wt;GT}$ vs. $dlg1^{ko;GT}$,and $dlg1^{flox/flox}$ vs $dlg1^{flox/flox}$:$CD4^{cre}$ mice. Examination of the lymphoid organs from all three *dlg1* knockout mice revealed no significant difference in total cellularity in the spleen, thymus, or lymph nodes compared to their respective wild-type littermates (Table S1 and data not shown). In addition, reconstitution was found to be equally efficient in $dlg1^{wt;GT}$ and $dlg1^{ko;GT}$ mice as measured by comparing CD45.1 with CD45.2 (data not shown) and by cell counts for various peripheral blood cell and bone marrow populations in both $dlg1^{ko;GT}$ and $dlg1^{ko;BG}$ mice (Figure S3 and data not shown). Analysis of developing T cell populations from the thymus revealed no developmental blocks in any of the three mouse models assessed (Figure 2A and B, upper panels, Table S1), and comparable B cell (IgM^+B220^+) and T cell populations, including naïve T cells ($CD62L^{high}CD44^{lo}$), were found in the periphery. $CD4^+$ vs $CD8^+$ ratios and $CD69^+$ T cell subsets also appeared normal (Figure 2A and B, Table S1, and data not shown). Notably, while ($CD4^+CD25^+$) regulatory T cell subsets appeared unremarkable in $dlg1^{flox/flox}$:$CD4^{cre}$ and $dlg1^{ko;GT}$ mice, $dlg1^{ko;BG}$ mice exhibited a trend towards a modest reduction in $CD4^+FoxP3^+$ splenic cells in 2 out of 3 experiments (2 experiments, WT n = 7, KO n = 6) both by percentage and cell number (Figure 2B, bottom panels and data not shown). These data suggest that although *dlg1* appears to be dispensable for T cell development in the context of these mouse models, it may contribute to the development of Treg populations.

TCR-induced Regulation of Early T Cell Activation Makers is Intact in *dlg1* Knockout Mice

To examine if T cells from *dlg1* knockout mice could properly modulate the expression levels of defined cell surface activation markers in response to TCR-mediated signals, naïve splenocytes from $dlg1^{ko;GT}$ and $CD4^+$ T cells from $dlg1^{flox/flox}$:$CD4^{cre}$ mice were stimulated with anti-CD3/CD28 or anti-CD3, respectively. T cells from both germline and conditional *dlg1* knockout mice were found to up-regulate early activation markers, including CD25 and CD69 (Figure 3A and B), and down-regulate CD62L (Figure 3A) or CD3 (Figure 3B) expression to a level comparable to that found on wild-type T cells. These data indicate that *dlg1* is not required for TCR-dependent regulation of early cell surface activation markers in these mouse models.

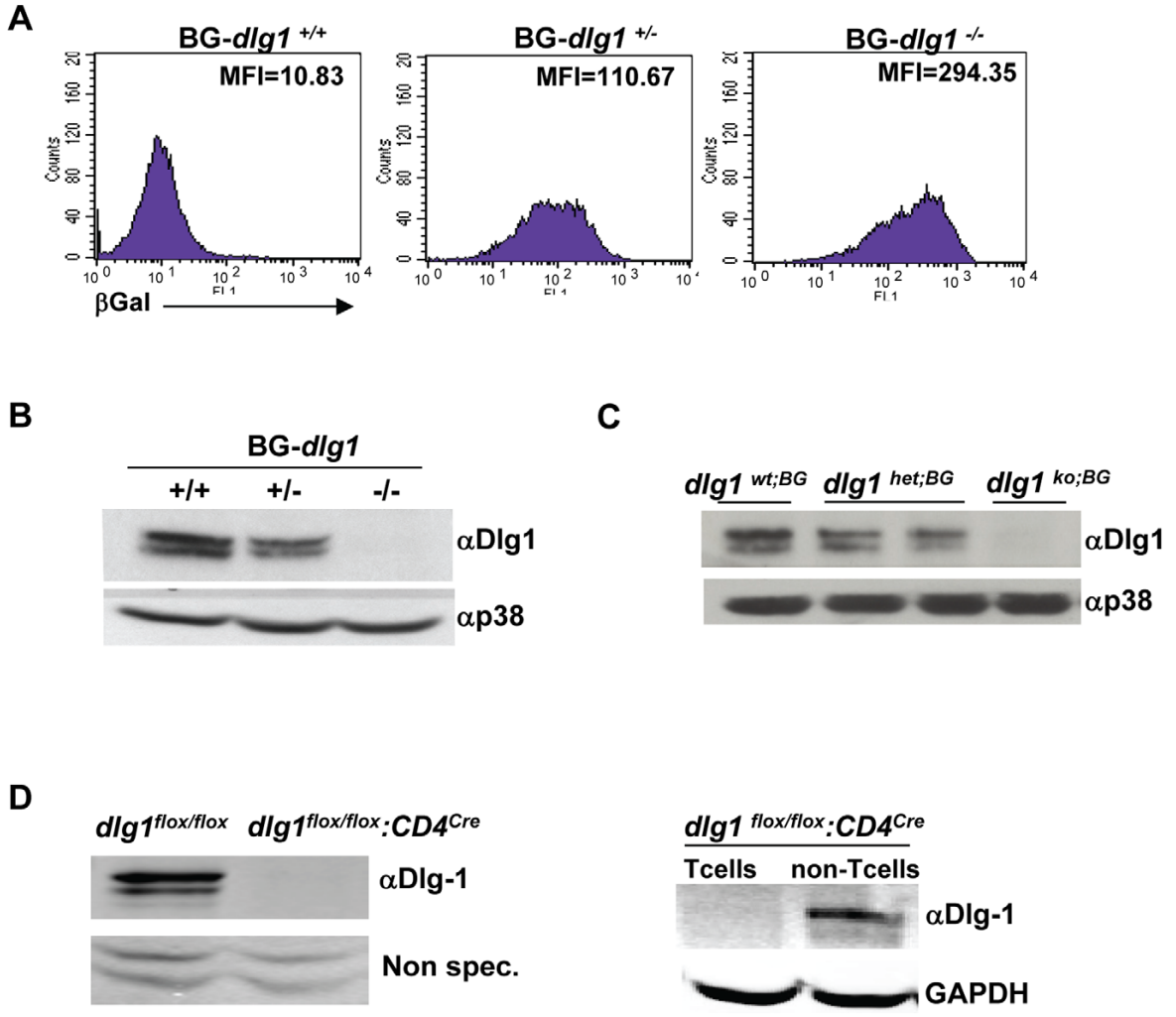

Figure 1. Dlg1 expression is ablated in the *dlg1*$^{ko;BG}$ and *dlg1*$^{flox/flox}$*:CD4*^{cre} mouse models. (A) Representative flow cytometry histograms show differential β-gal levels in fetal liver cells from BG *dlg1*$^{+/+}$ (*left*), *BG dlg1*$^{+/-}$ (*center*), or BG *dlg1*$^{-/-}$ (*right*) pups (n = 10 independent experiments). (B) Representative western blot of Dlg1 expression in whole cell lysates from BG *dlg1*$^{+/+}$, BG *dlg1*$^{+/-}$, or BG *dlg1*$^{-/-}$ fetal tissue using antibodies against Dlg1 or p38 (n = 6 independent experiments). (C) Western blot demonstrating Dlg1 expression in total splenocytes obtained from *dlg1*$^{wt;BG}$ and *dlg1*$^{ko;BG}$ mice 8 weeks post adoptive transfer. Data are representative of 3 independent experiments (D) *Left*, lymphocytes from Dlg1$^{flox/flox}$ or Dlg1$^{flox/flox}$:CD4^{cre} mice were enriched for T cells and whole cell lysates immunoblotted with antibodies against Dlg1. Non-specific bands (Non-spec.) from the same gel demonstrate equivalent loading in each lane. *Right*, splenocytes from Dlg1$^{flox/flox}$:CD4^{cre} mice were enriched or depleted for T cells, and lysates were immunoblotted with antibodies against Dlg1 or GAPDH, as indicated.
doi:10.1371/journal.pone.0045276.g001

TCR-dependent Pan Tyrosine- and Alternative p38-Phosphorylation are Unaffected in *dlg1* Knockout Derived T Cells

Dlg1 has been shown to orchestrate TCR proximal signaling by facilitating interactions between multiple kinases and effector proteins [22], however examination of TCR-induced total tyrosine phosphorylation revealed no gross changes in the pattern of phosphoproteins between *dlg1*$^{flox/flox}$ and *dlg1*$^{flox/flox}$*:CD4*^{cre} CD4^{+} T cells nor between T cells obtained from *dlg1*$^{wt;BG}$ and *dlg1*$^{ko;BG}$ mice (Figure 4A and data not shown). Strikingly, alternative p38 phosphorylation, as measured by specific dual-phosphorylation at residues T180 and Y182, also appeared unaffected in *dlg1*$^{ko;BG}$ T cells (Figure 4B). This is in contrast to previous studies utilizing acute knockdown, which demonstrated a pivotal role for Dlg1 in mediating alternative p38 phosphorylation and activation [24,26]. These data indicate that TCR-mediated proximal signaling events, including alternative p38 phosphorylation, are not affected in T cells from *dlg1*$^{flox/flox}$*:CD4*^{cre} and *dlg1*$^{ko;BG}$ mice.

TCR-induced Actin Polymerization is Defective in T Cells with Acute, but not Germline or Conditional, *dlg1* Ablation

WASp/WAVE family members function to mediate changes in the actin-cytoskeleton through the formation of F-actin [2,4].

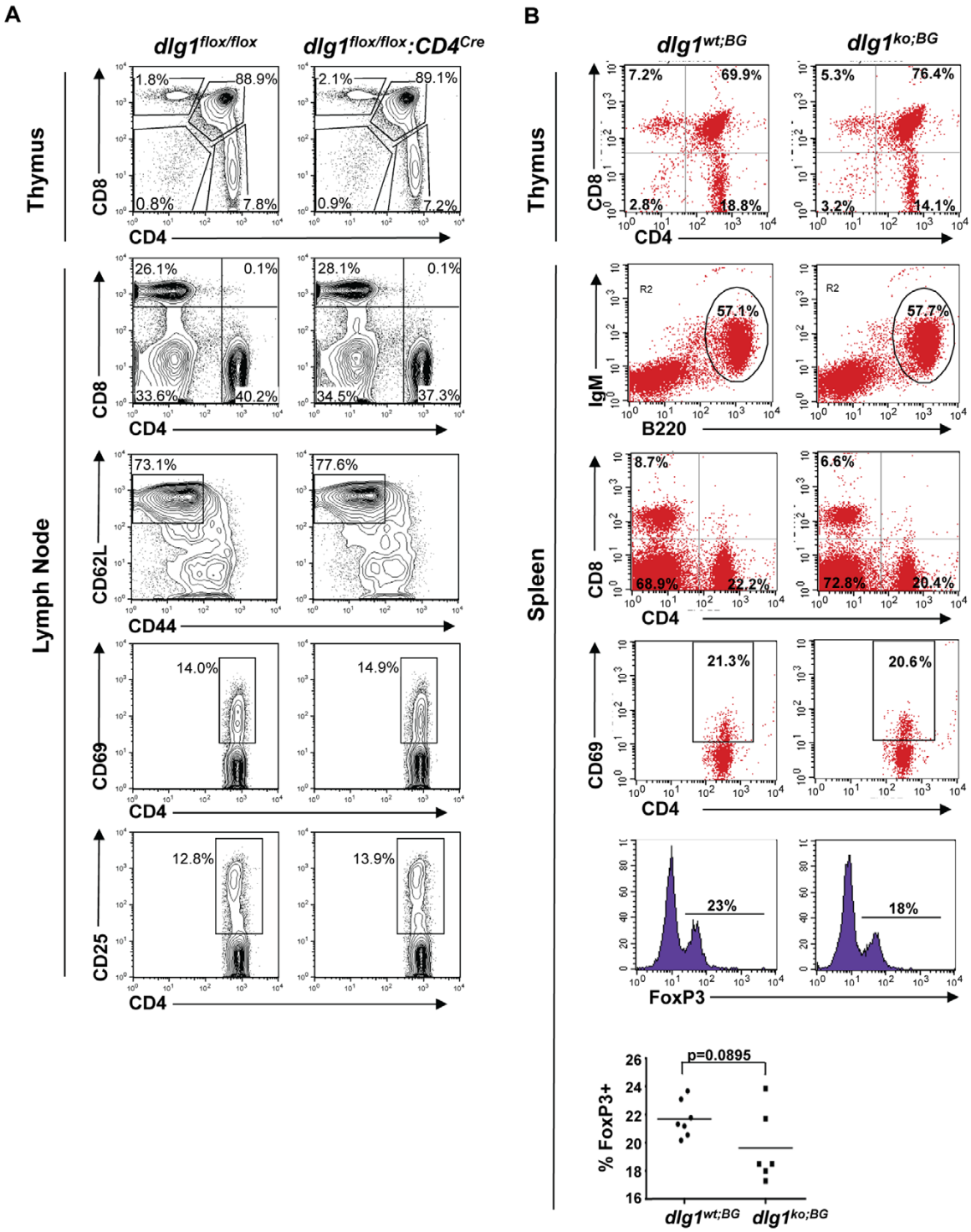

Figure 2. Lymphocyte development is not affected in *dlg1* knockout mice. (A) Flow cytometry profiles of thymocytes (Thymus) and lymph node cells (Lymph Node) from $dlg1^{flox/flox}$ or $dlg1^{flox/flox}$:$CD4^{cre}$ mice stained with the indicated antibodies. (B) Flow cytometry profiles of thymocytes (Thymus) and splenocytes (Spleen) from $dlg1^{wt;BG}$ or $dlg1^{ko;BG}$ mice stained with the indicated antibodies. Splenic Treg populations were determined by dual CD4+ surface and FoxP3 intracellular staining. Data are representative of 3 independent adoptive transfer experiments, where n≥6 for each genotype.

doi:10.1371/journal.pone.0045276.g002

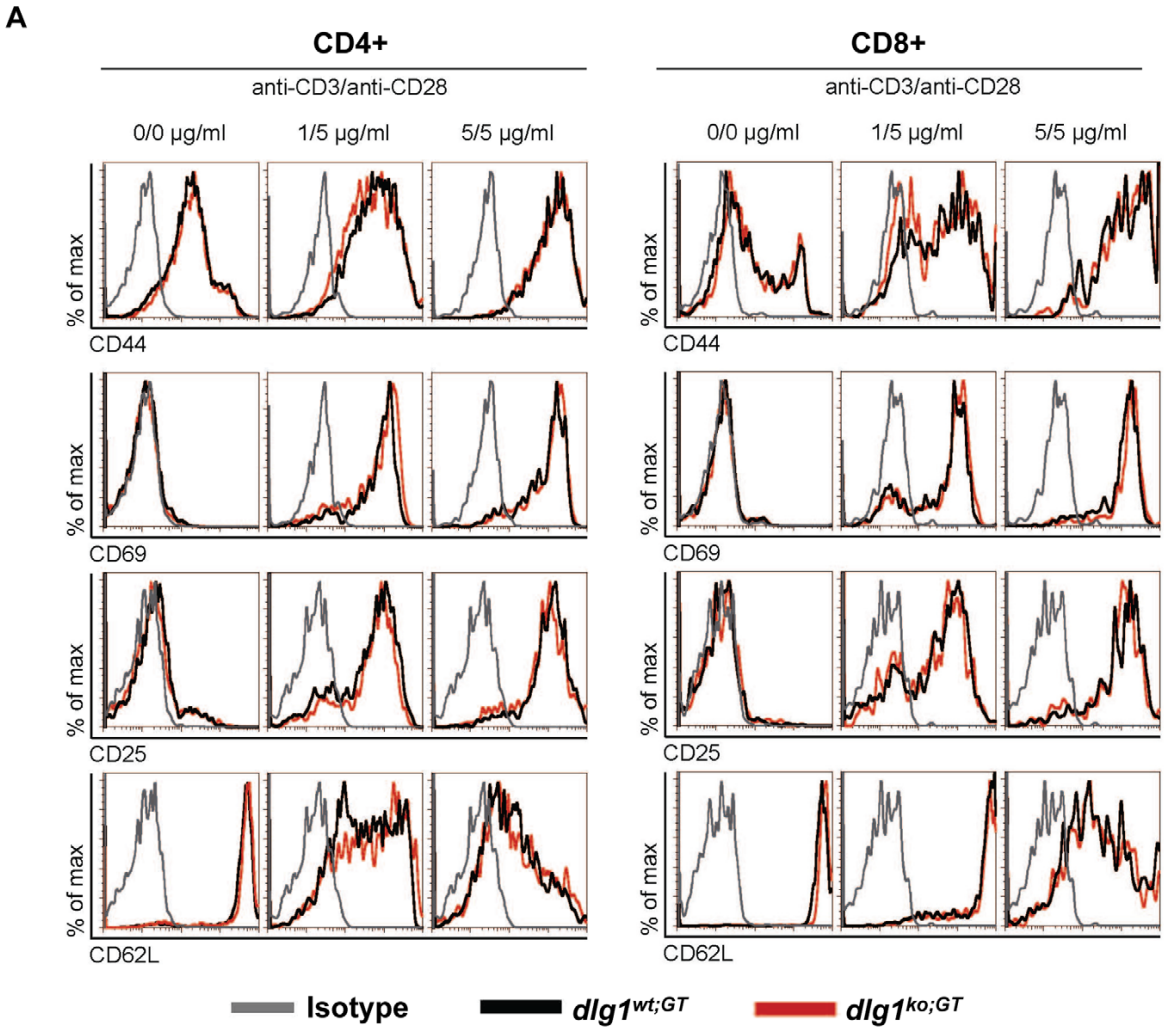
A
CD4+
anti-CD3/anti-CD28
0/0 µg/ml
1/5 µg/ml
5/5 µg/ml
CD8+
anti-CD3/anti-CD28
0/0 µg/ml
1/5 µg/ml
5/5 µg/ml
% of max
CD44
CD69
CD25
CD62L
Isotype
dlg1wt;GT
dlg1ko;GT
B
dlg1flox/flox
dlg1flox/flox:CD4Cre
CD3
CD69
CD25

Figure 3. The regulation of T cell surface activation markers is unaffected in *dlg1* knockout mice. (A) Splenocytes isolated from $dlg1^{wt;GT}$ (black) or $dlg1^{ko;GT}$ (red) mice were activated with indicated concentrations of plate bound anti-CD3 in the presence of anti-CD28 for 24 hours and assessed for the expression of activation markers. Histograms were gated on viable donor derived ($CD45.2^+$) $CD4^+$ or $CD8^+$ T cells and show one representative mouse per genotype ($n \geq 3$). (B) Flow cytometry profiles of selected surface markers on purified $CD4^+$ T cells from $dlg1^{flox/flox}$ (top *panel*) or $dlg1^{flox/flox}$:$CD4^{cre}$ (*bottom panel*) mice stimulated with T-depleted splenocytes with (unshaded) or without (shaded) anti-CD3 antibody for 24 hrs ($n \geq 3$).
doi:10.1371/journal.pone.0045276.g003

Previously Dlg1 had been shown to interact with WASp and to play a role in orchestrating TCR-induced actin polymerization and polarized synaptic raft clustering in the context of shRNA-mediated Dlg1 knockdown in CD8+ T cells [22,24]. To assess actin polymerization at the IS in the context of total *dlg1* ablation, $dlg1^{flox/flox;}$ and $dlg1^{flox/flox}$:$CD4^{cre}$ CD4+ T cells were allowed to conjugate with anti-TCR antibody-coated beads for 20 minutes and scored for actin localization to the T cell/bead interface (Figure 5A). In addition, $dlg1^{ko;BG}$ derived T cells were assessed for TCR-induced actin polymerization by flow cytometry at various time points (Figure 5B). In both experiments, no significant defects were observed in TCR-induced actin polymerization in T cells derived from either $dlg1^{flox/flox}$:$CD4^{cre}$ or $dlg1^{ko;BG}$ as compared with their wild-type counterparts suggesting *dlg1* is not required for TCR-induced actin polymerization in these mice.

This outcome contrasts with previous findings from the Miceli lab showing that Dlg1 knockdown impairs TCR actin polymerization in primary murine T cells [22]. We therefore tested actin polymerization in the context of acute Dlg1 deletion in an independent experimental system. Dlg1 suppressed Jurkat T cells were generated using an shRNA based vector. After optimization, Dlg1 expression in cells transfected with Dlg1 shRNA could typically be reduced to ~25% of control levels (vector alone), as judged by Western blot analysis (Figure 5C). Suppression to at least 25% of control was confirmed for all functional studies. Jurkat T cells transfected with control or Dlg1 shRNA were then conjugated to SEE-pulsed Raji B cells 72 hours post-transfection, and actin responses at the IS were analyzed by fluorescence microscopy. No gross changes were observed in the efficiency of SEE-induced conjugate formation as a result of Dlg1 suppression. Nonetheless, in contrast to T cells with a conditional or germline genomic deletion, T cells with acute Dlg1 suppression exhibited diminished F-actin accumulation with fewer Dlg1-deficient T cells accumulating F-actin at the IS (Figure 5D). These data are consistent with previous experiments performed in primary murine T cells [22]. We conclude that the effects on T cell actin responses differ in acute vs. long term models of *dlg1* deficiency, possibly because compensatory changes in the long-term knockout models mask the contribution of *dlg1*.

Polarization and Migration is not Affected in Activated T Cells from Dlg1 Knockout Mice

The formation of the IS results in the asymmetric distribution of select proteins to the IS and DPC [3,7]. Furthermore, the acute loss of Dlg1 and its functional partner Scribble in a T cell line has been shown to disrupt both random migration and uropod formation [3]. Therefore, activated T cells deficient in Dlg1 were assessed for morphology and polarization by examining the localization of specific surface and intracellular protein markers on in vitro cultured cells. $dlg1^{ko;GT}$ cells displayed normal uropod formation as well as normal polarization of the uropod markers CD43 and CD44 (Figure 6A).

Similarly, comparison of control and $dlg1^{flox/flox}$:$CD4^{cre}$ derived CD4+ T cells following conjugation with anti-TCR antibody-coated beads showed no significant differences in the localization of three well-defined marker proteins (Figure 6B). As reported previously, ezrin localizes to both the IS and the DPC [30], while

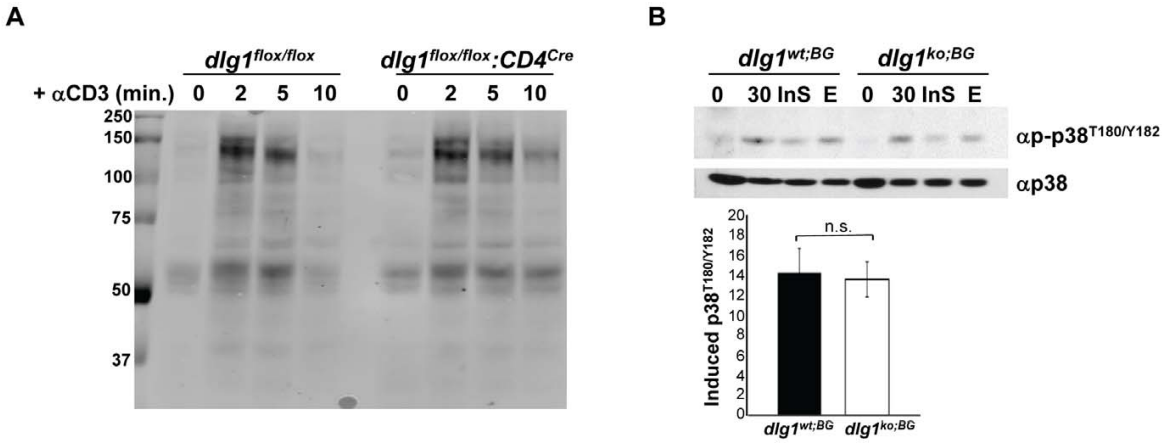

Figure 4. T cells from *dlg1* knockout mice show normal TCR-induced tyrosine- and alternative p38- phosphorylation. (A) Purified $CD4^+$ T cells from $dlg1^{flox/flox}$ or $dlg1^{flox/flox}$:$CD4^{cre}$ mice were stimulated with anti-CD3 antibody for the indicated times. Whole cell lysates were immunoblotted with anti-phosphotyrosine antibody. (B) *(Top panel)* Expanded T cells from $dlg1^{wt;BG}$ or $dlg1^{ko;BG}$ mice were restimulated with anti-CD3 and anti-CD28 antibodies for 30 minutes in the absence or presence of an Insolution p38 (InS) or U0126 Erk (E) inhibitor. Whole cell lysates were then immunoblotted with anti-phospho-p38 (T180/Y182) followed by anti-p38 to assess loading. *(Bottom panel)* Levels of induced p38 phosphorylation relative to corresponding unstimulated samples were determined by densitometry and normalized according to loading controls ($n = 3$ each for $dlg1^{wt;BG}$ and $dlg1^{ko;BG}$). Data represent mean +/− StDev. n.s. = not significant, ($p = 0.7236$).
doi:10.1371/journal.pone.0045276.g004

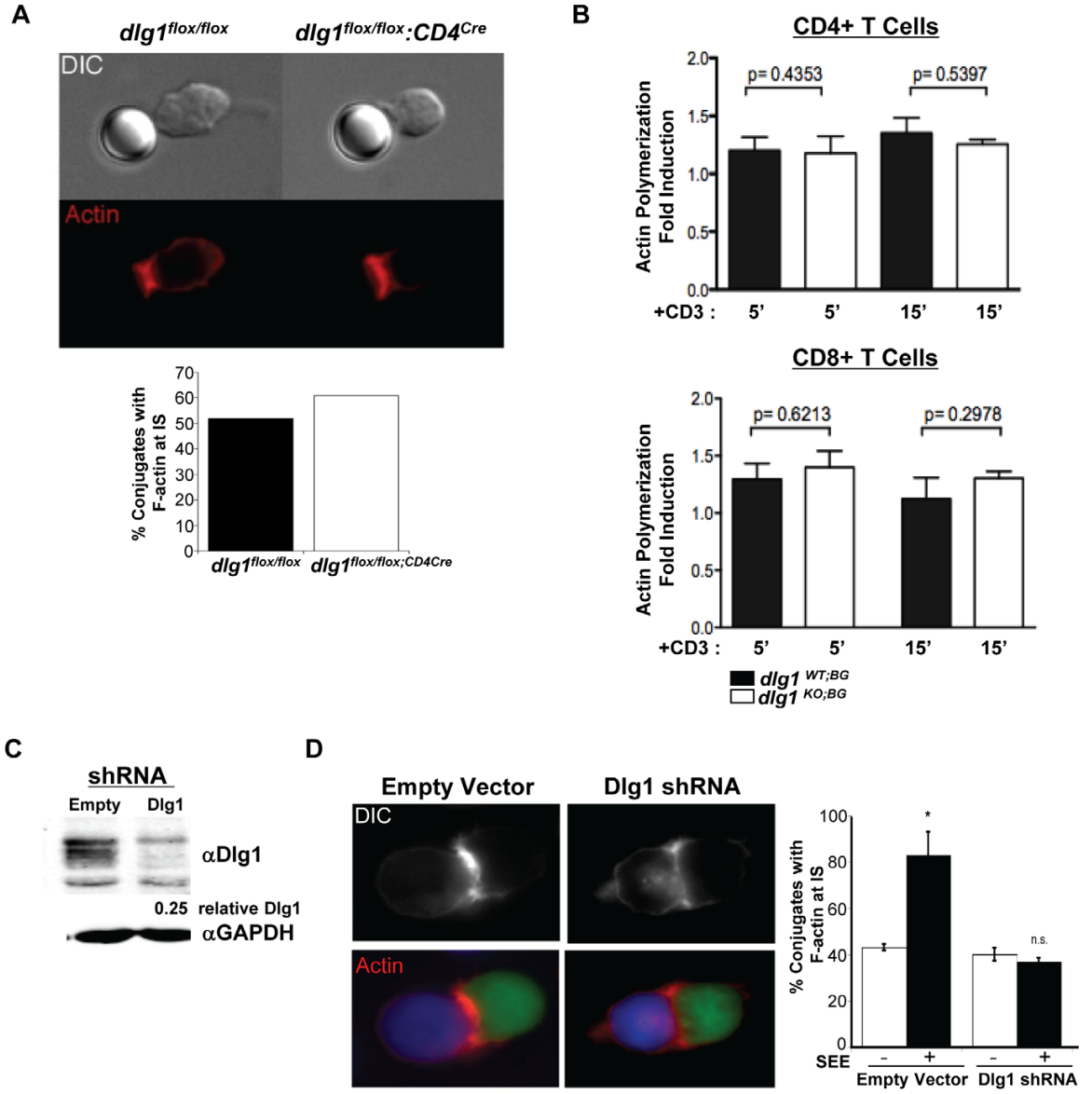

Figure 5. An acute, but not germline or conditional, loss of *dlg1* impairs receptor-mediated actin polymerization. (A) *dlg1*$^{flox/flox}$ or *dlg1*$^{flox/flox}$*:CD4*^{cre} CD4^{+} T cells were allowed to conjugate with anti-TCR antibody-coated beads for 20 minutes and stained for actin with rhodamine-phalloidin (*top panel*). At least 50 cells were scored for actin localization to the T cell/bead interface (*bottom panel*). (B) Expanded T cells from *dlg1*$^{wt;BG}$ or *dlg1*$^{ko;BG}$ mice were restimulated with plate-bound anti-CD3 and anti-CD28 antibodies for 5 or 15 minutes. Cells were stained with a combination of anti-CD4, anti-CD8, and FITC-phalloidin and assessed by FACS to determine the relative level of induced actin polymerization in CD4^{+} (*top panel*) and CD8^{+} (*bottom panel*) T cell populations. These data are representative of 2 independent experiments, n≥4 for WT and KO samples. (C) Whole cell lysates from Jurkat cells expressing empty vector (empty) or Dlg1 shRNA were immunoblotted with antibodies against Dlg1 or GAPDH, as indicated. (D) Jurkat T cells (green) were transfected with either pCMS3.eGFP.H1p empty vector or pCMS3.eGFP.H1p containing a shDlg1 target sequence. Cells were stimulated with SEE-pulsed (or untreated) Raji B cells (blue) and stained with rhodamine-phalloidin (red) (*left panel*). At least 50 conjugates were scored for F-actin localization to the T cell/APC interface in each of two independent experiments (*right panel*). Data represent mean +/− StDev. n.s., not statistically significant.
doi:10.1371/journal.pone.0045276.g005

moesin and CD43 localize to the DPC. PKCζ also polarized efficiently to the DPC in these cells (data not shown).

To examine the role of *dlg1* in random T cell migration, T cells which had been pre-activated with Concanavalin A for 5 days from *dlg1*$^{wt;GT}$ and *dlg1*$^{ko;GT}$ mice were compared for their ability to migrate using time-lapse microscopy. However no significant difference was observed in the distance traveled between *dlg1*$^{wt;GT}$ and *dlg1*$^{ko;GT}$ T cells (Figure 6C).

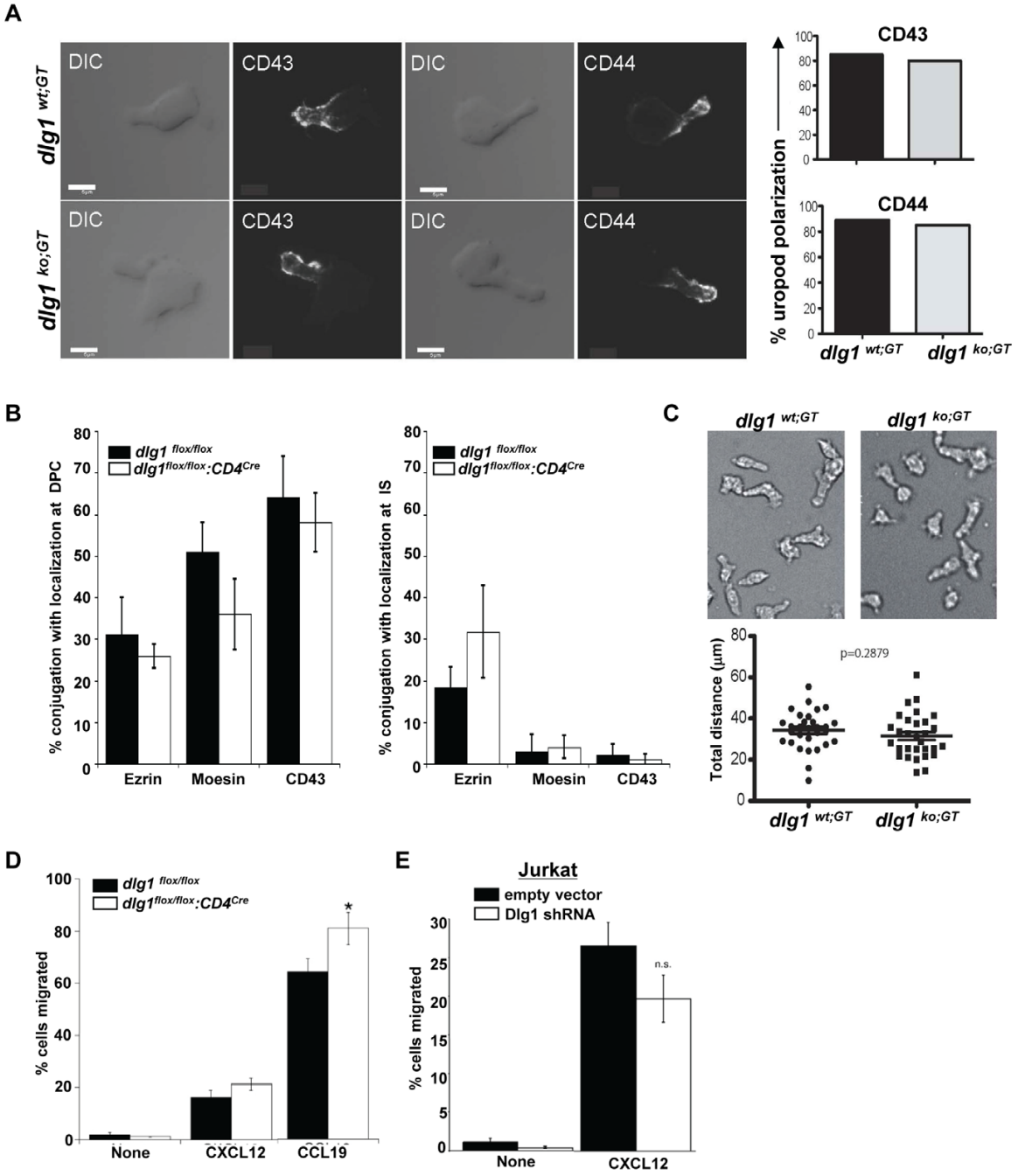

Figure 6. T cell polarization and migration are not hindered by the loss of *dlg1*. (A) $dlg1^{wt;GT}$ or $dlg1^{ko;GT}$ activated T lymphoblasts were stained with CD43 or CD44 and assessed for protein polarization (*left panel*). The percentage polarization of CD43 and CD44 to the T cell uropod was determined by scoring 45 cells in two independent experiments (*right panel, top and bottom*). (B) $dlg1^{flox/flox}$ *or* $dlg1^{flox/flox}$*:*$CD4^{cre}$ $CD4^{+}$ T cells were allowed to conjugate with anti-TCR antibody coated beads for 20 minutes, fixed and stained with the indicated antibodies. The indicated proteins were scored for localization to the DPC (*left panel*) or IS (*right panel*). 50–100 conjugates were scored for F-actin localization to the T cell/APC interface in each of 2–3 independent experiments (*right panel*). Data represent mean +/− StDev. Differences were not statistically significant for any sample pair. (C) $dlg1^{wt;GT}$ or $dlg1^{ko;GT}$ activated T lymphoblasts were subjected to time-lapse microscopy and assessed for random migration (*top panels*). Total distance was determined from DIC images acquired at 1 min intervals by tracking a total of 30 cells over a 30 min period (*bottom panels*). Data are representative of n = 2 experiments. (D) A modified Boyden chamber was used to assess the percent of $dlg1^{flox/flox}$ or $dlg1^{flox/flox}$*:*$CD4^{cre}$ T cells which migrated in response to no chemokine, CXCL12, or CCL19 over 2 hours and was calculated as the ratio of the total cells, to cells that migrated

* = p≤0.05. (E) The percentage of Jurkat cells transfected with either empty vector or shDlg1 which migrated in response to no chemokine or CXCL12 for 2 hours was calculated as: number of cells migrated/total number of cells. n.s. = no significiant difference.
doi:10.1371/journal.pone.0045276.g006

The role of *dlg1* in chemokine-directed migration was examined in both $dlg1^{flox/flox}$:$CD4^{cre}$ $CD4^+$ and Dlg1-suppressed Jurkat T cells. Despite the diminished actin polymerization observed in T cells expressing Dlg1 shRNA, no reduction was observed in the migration of control cells and $dlg1^{flox/flox}$:$CD4^{cre}$ $CD4^+$ T cells, or between Dlg1-suppressed and control Jurkat T cells in response to chemokines (Figure 6D and E). A modest, but statistically significant, increase was detected in the migration of $dlg1^{flox/flox}$:$CD4^{cre}$ $CD4^+$ T cells toward CCL19. The significance of this is unclear however, as no increase was observed in response to CXCL12. Nonetheless, these data suggest that *dlg1* may be dispensable for chemokine-induced actin-mediated motility.

TCR-induced Proliferation is not Affected in T Cells Derived from *dlg1* Germline Knockout Mice

The Drosophila ortholog of *dlg1* was originally identified as a tumor suppressor and attenuator of cell division [21]; thus alteration of its expression may affect cellular proliferation rates. Further, *dlg1* knockout has been reported to promote TCR-induced proliferation in naïve CD4+ and CD8+ T cells [36]. To address the role of *dlg1* in TCR-dependent proliferation in our models, naïve splenocytes or lymph node cells from $dlg1^{wt;BG}$ and $dlg1^{ko;BG}$ were labeled with CFSE and stimulated for 24, 48, or 72 hours with varying concentrations of anti-CD3 alone or in combination with anti-CD28 (Figure 7A and data not shown). In addition, naïve splenocytes from $dlg1^{wt;BG}$ and $dlg1^{ko;BG}$ were enriched for $CD8^+$ T cells and their proliferative response assessed by ^{3}H-Thymidine incorporation (data not shown). In both assays, the rates of TCR-mediated proliferation were indistinguishable between $dlg1^{wt;BG}$ and $dlg1^{ko;BG}$ derived T cells at all antibody concentrations and time points assessed. Similarly, no differences were observed in the proliferative responses between $dlg1^{wt;GT}$ and $dlg1^{ko;GT}$ derived CD4+ and CD8+ T cells in the presence of varying concentrations of anti-CD3 alone or in combination with anti-CD28 as measured by CFSE dilution (Figure 7B). These results were in contrast to previously published work by Stephenson et al. which indicated that *dlg1* knockout leads to hyper-proliferation of naïve CD4 and CD8 T cells in response to TCR/CD28 stimulation [36]. While our data suggest that *dlg1* does not function to regulate receptor-mediated proliferation in T lymphocytes in our mouse models, it remains possible that compensatory mechanisms may have masked a measurable phenotype.

Th1/Th2 Type Cytokine Production is Affected by the Acute or Conditional, but not Germline, Loss of *dlg1*

The differential reorganization of T cell membrane proteins and intracellular complexes during IS and DPC formation has been shown to modulate effector cytokine production [13,15]. To evaluate the effect of *dlg1* genomic ablation on TCR-induced effector cytokine production, $dlg1^{wt;BG}$ and $dlg1^{ko;BG}$ $CD8^+$ expanded T cells were assessed following 4 hours of stimulation with plate-bound anti-CD3. FACS analysis of intracellular protein levels revealed no significant differences in TCR-induced IFNγ or IL-2 production between CD8+ T cells from $dlg1^{wt;BG}$ and $dlg1^{ko;BG}$ mice (Figure 8A and data not shown). These results were in contrast to previous experiments in which CD8+ T cells with a transient Dlg1 deficiency via knock-down exhibited diminished IFNγ and IL-2 cytokine production in response to TCR engagement compared to wild-type cells [22,24]. Notably, purified, expanded $CD4^+$ T cells from $dlg1^{flox/flox}$ and $dlg1^{flox/flox}$:$CD4^{cre}$ mice that were re-stimulated with anti-CD3 demonstrated that $dlg1^{flox/flox}$:$CD4^{cre}$ $CD4^+$ T cells produced less IL-2 and Th1-associated cytokines IFNγ and TNFα, while levels of the Th2-associated cytokines IL-4 and IL-5 were significantly increased in comparison to wild-type littermates (Figure 8B).

To further examine the effect of acute Dlg1 diminution on Th-type cytokine production, Th1 and Th2 polarized cells from wild-type C57Bl/6 mice were transduced with either control- or Dlg1-miRNA expressing retroviruses resulting in an approximately 50% reduction of Dlg1 expression (Figure 8C, far right panels). Similar to $dlg1^{flox/flox;CD4cre}$CD4+ T cells, restimulation of Dlg1-suppressed Th1 cells resulted in significantly diminished levels of intracellular IFNγ and TNFα , whereas Dlg1 suppressed Th2 cells demonstrated significantly enhanced IL-4 production (Figure 8C, left panels). In combination, these data suggest that *dlg1* may play differential roles in the Th response; helping to promote Th1 responses, while suppressing Th2 responses.

Discussion

Polarity proteins have recently been implicated as key regulators of T cell migration, signaling, effector function, and fate [3,12,14]. Dlg1, a member of the ancestral Scribble polarity network, directly binds and regulates the activity of the proximal TCR-associated kinases and has been implicated in regulating TCR-mediated signal transduction and cell polarity in the context of IS formation and cell migration. Although studies using Dlg1 knockdown or over-expression technologies in primary T cells and transformed cell lines have demonstrated a role for Dlg1 in T cell signaling, activation, and the establishment of synaptic polarity during antigen recognition [22–24], its function in the context of T cell development, immune homeostasis or immune response *in vivo* remains unclear. This is due in part to seemingly conflicting reports which have alternatively suggested that Dlg1 is a negative regulator [23,36], or a positive regulator [22,24,26,28,30] of T cell function.

In this study, three independent *dlg1*-deficient mouse models were generated and examined in an effort to unravel the functional significance of Dlg1 in T cell development and effector function in a null background. In general, we found that germline and conditional *dlg1* knockout mice had no apparent defects in CD4+ or CD8+ T cell polarization-dependent events such as development, migration, activation, signaling or proliferation. These data were surprising considering previous reports demonstrating a role for Dlg1 in regulating TCR-mediated actin polymerization, signal specificity and function, in the context of acute knockdown or over-expression in mature T cells. While we observed diminished cytoskeletal reorganization in primary mouse CD8+ [24] and human Jurkat T cells (Figure 5D) with acute Dlg1 knockdown, we did not observe defects in mature T cells from conditional or germline *dlg1* knockout mouse models (Figure 5A and B). These data suggest that the timing and/or duration of *dlg1* ablation may greatly affect the phenotype of Dlg1-deficient cells and impact the ability to examine the role Dlg1 on T cell function. This hypothesis is supported by studies of Th1 and Th2-type cytokine secretion, which demonstrated differential cytokine secretion in T cells with an acute or conditional loss of Dlg1, but not a germline loss of *dlg1* (Figure 8). Because the conditional

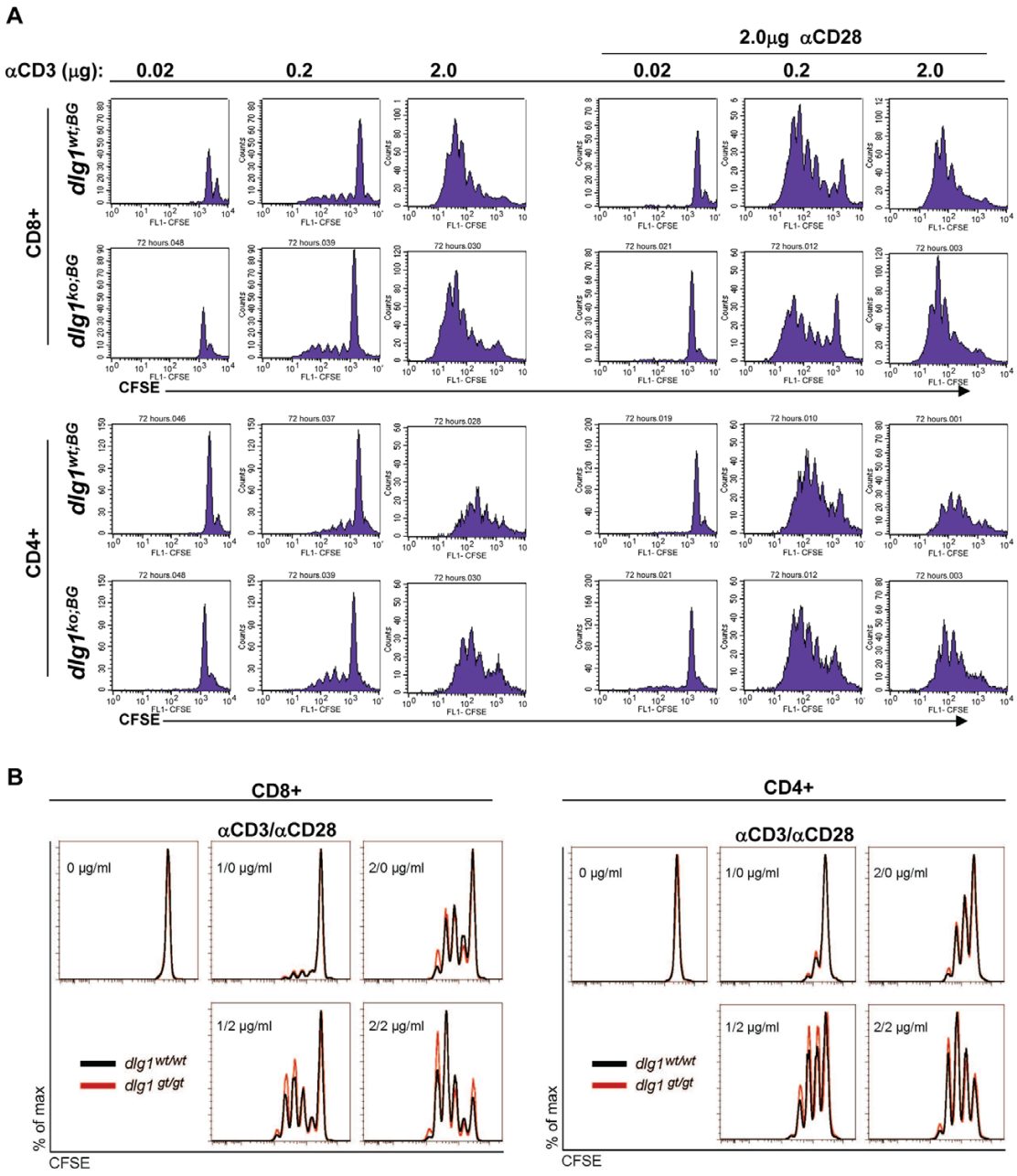

Figure 7. T cells from *dlg1* germline knockout mice proliferate comparably to wildtype T cells. (A) $dlg1^{wt;BG}$ or $dlg1^{ko;BG}$ derived splenocytes were stained with CFSE and stimulated with various concentrations of anti-CD3 alone or anti-CD3 and anti-CD28 antibodies for 72 hours. Cells were subsequently surface stained with anti-CD8 or anti-CD4 antibodies and T cell populations analyzed by flow cytometry. (B) Naive splenic T lymphocytes isolated from $dlg1^{wt;GT}$ (black) or $dlg1^{ko;GT}$ (red) were labeled with CFSE and activated with the indicated concentrations of plate bound anti-CD3 in the presence or absence of anti-CD28. CFSE profiles at 62 hours were gated on $CD8^+$ or $CD4^+$ T cells and are representative of 2 independent experiments.
doi:10.1371/journal.pone.0045276.g007

dlg1 knockout leads to Dlg1 ablation later in T cell development, we hypothesize that a shorter developmental window was available for selection of cells that have compensated for Dlg1 loss. Indeed, while all three models demonstrated modest, if any, defects, it is noteworthy that the most significant defects observed (i.e. in Th1 and Th2 development) occurred under the conditions where *dlg1* was ablated later in development or in experiments using acute knockdown strategies.

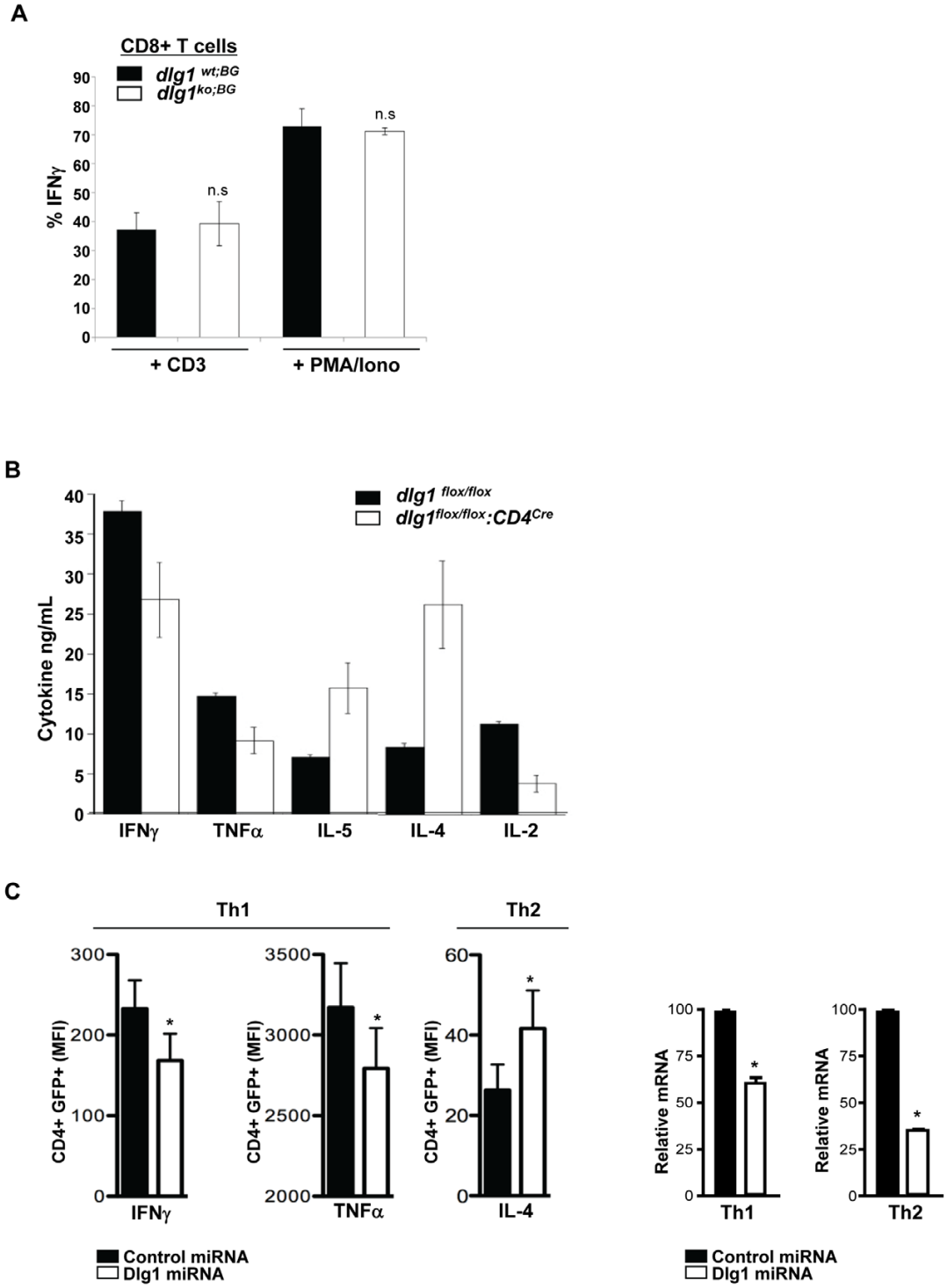

Figure 8. The acute or conditional loss of *dlg1* results in differential Th1/Th2-type cytokine production. (A) Expanded splenocytes from *dlg1*$^{wt;BG}$ or *dlg1*$^{ko;BG}$ mice were restimulated with plate-bound anti-CD3 and anti-CD28 antibodies or PMA/Ionomycin for 4 hours. Cells were stained with anti-CD8, permeabilized, and subsequently stained with anti-IFN-γ to determine intracellular cytokine levels (n≥3 each for *dlg1*$^{wt;BG}$ and *dlg1*$^{ko;BG}$ mice). Data represent mean +/− StDev. n.s. = no significance where p>0.05. (B) Expanded CD4^{+} T cells from *dlg1*$^{flox/flox}$ or *dlg1*$^{flox/flox}$*:CD4*^{cre} mice were

restimulated with plate-bound anti-CD3 and anti-CD28 antibodies for 24 hours. Cell supernatants were collected and cytokine production analyzed by ELISA. Standard deviations were calculated from triplicate stimulations and statistical significance determined using a paired Student's t test. *$p<0.05$. (C) Th1 or Th2 polarized T cells from C57Bl/6 mice were transduced with either control- or Dlg1-miRNA retrovirus (*right panel*) and subsequently stimulated with plate-bound anti-CD3/CD28 for 6 hours. Cells were then surface stained with anti-CD4 followed by intracellular staining with antibodies against either IFNγ or TNFα (Th1 cells) or IL-4 (Th2 cells). Cells were analyzed by FACS and gated on CD4+ and GFP+ (miRNA vector) cells to determine the relative level of cytokine production (MFI) in control and knockdown populations (*left panel*) (IFNγ, TNFα n = 4; IL-4 n = 3). Data represent means from ≥3 experiments ± SEM. *$p<0.05$.
doi:10.1371/journal.pone.0045276.g008

The phenomenon of compensatory factors that mask the effects of Dlg1 deficiency is not unprecedented. In neuronal cells, evidence suggests a key role for Dlg1 in regulating synaptic AMPA receptor trafficking. However neurons from mouse embryos in which the *dlg1* gene has been ablated develop normally and form synapses with normal levels of AMPA receptors and no detectable abnormalities [39]. Investigators have hypothesized that the lack of a phenotype in Dlg1-mutant cells could be caused by the compensation of other Dlg-family members (Dlg2, Dlg3, Dlg4) or other adaptive processes during neuronal development and synapse maturation that could compensate for the normal function of Dlg1 [40]. Based on the results of our collaborative study, we hypothesize that similar event(s) could be occurring in developing T lymphocytes, making it difficult to appreciate the functional role of Dlg1 in developing and peripheral lymphocyte populations. Further support for this working hypothesis comes not only from comparative investigation within this study, but also from comparison of previously published works demonstrating a critical role for Dlg1 in cytoskeletal organization [24,26], alternative p38 activation [24,26,28], NFAT activation [24,26,28] and effector function [24,28], in the context of acute knockdown in T cells (Figures 5 and 6). An important area for future investigation will be to identify the changes in Dlg family protein expression and/or the regulation of other proteins that may compensate for the loss of Dlg1; this will lay the groundwork to more fully assess the significance of this pathway for T cell development and function.

Notably, our studies also uncovered novel contextual roles for Dlg1 as both a positive and negative regulator of T cell function, as Dlg1 ablation was found to inhibit Th1, while enhancing Th2, cytokine production in CD4+ T cells. Initial studies of Dlg1 by Xavier et al. found that the overexpression of Dlg1 in conjunction with Vav1, attenuated Vav1-induced NFAT activity in Jurkat T cells. These studies also found that the long term diminution of Dlg1 in Jurkat T cells via stable siRNA-based knockdown resulted in impaired NFAT reporter activation [23]. In a follow-up study, Stephenson et al provided data indicating that Dlg1 may negatively regulate T cell proliferation utilizing mouse *dlg1*-deficient T cells generated by recombination-activating gene 2 (*rag2*)-deficient complementation [36]. Both reports supported a role for Dlg1 as a negative regulator of T cell activation and function by suppressing NFAT-mediated transcription and cycle entry, respectively. However, two studies by Round et al., utilizing acute siRNA-based knockdown in mouse TCR transgenic CD8+ T cells found that Dlg1 knockdown attenuated NFAT-mediated transcription of endogenously regulated NFAT genes (NFATc1 and IFNγ), while complementary studies of Dlg1 overexpression resulted in a tightly regulated, dose-dependent enhancement of NFAT-mediated transcription. Moreover, Round et al provided clear biochemical evidence for a direct interaction between the MAP kinase p38 and Dlg1, which allows for nucleation of a signaling complex that results in alternative p38 activation and downstream NFAT phosphorylation [22,24].

Collectively, these results may appear conflicting and contradictory, regarding a role for Dlg1 as a positive or negative regulator of T cell activation and function. However, our data supports a view where Dlg1 may specify TCR signals that enhance or attenuate particular T cell responses in a context dependent manner. Indeed, the differential assembly of membrane microdomains, signaling molecules, and co-polarization of cytokine receptors at the IS has been implicated in controlling memory versus effector cell development [20], as well as Th1/Th2 lineage commitment and effector function [15,41,42]. In this study, both conditional knockout and acute knockdown approaches demonstrated that Dlg1 positively regulates Th1 cytokine production, while negatively regulating Th2 cytokine production. Specifically, acute siRNA-mediated knockdown of Dlg1in differentiated Th1 and Th2 cells inhibited IFNγ and TNFα production in Th1 cells, while enhancing IL-4 production in Th2 cells (Fig. 8). While similar results were observed in the conditional knockout system, we did not observe differences in cytokine production in T cells derived from *dlg1* germline knockout mice.

More recently, two groups have shown experimental data which support a model in which Dlg1 couples p38 to NFAT activation and T cell function in primary human T cells to promote distinct signaling pathways in distinct T cell subsets [28,30]. Work by Zanin-Zhorov et al. has demonstrated that in primary human CD4+CD25+ FoxP3+ T regulatory (Treg) cells, Dlg1 accumulation at the IS is significantly higher than in effector CD4+CD25− T cells. In addition, diminution of Dlg1 expression impaired Treg cell suppression activity, caused a reduction in the amount of Foxp3 per cell, and led to diminished alternative p38 phosphorylation and NFATc1 activation, while enhancing Akt phosphorylation in response to TCR stimulation. These data support our working hypothesis by demonstrating that in human Treg cells, Dlg1 functions as both a positive and negative regulator of discrete signal transduction pathways; promoting alternative p38 activation, while inhibiting Akt activation. Similarly, opposing effects of Dlg1 activity have been observed between TCR-induced p38 and ERK activation [26]. Zanin-Zhorov et al. also elucidate a relationship between Dlg1, NFAT, and Foxp3, which may be of significance since both Foxp3 and NFAT are critical for Treg cell function, commitment, and maintenance [43,44]. In this study our data, although subtle, hints at a possible relationship between Foxp3 and Dlg1 in Treg cell commitment or maintenance; we observed a trend towards a decreased percentage of CD4+Foxp3+ cells in $dlg1^{ko;BG}$ germline deficient mice (Fig. 2B). It is interesting to speculate that while compensatory mechanisms may have allowed for T cell development in the mouse models investigated here, Dlg1 may be indispensable for the maintenance as well as function of Treg cell populations. Zanin-Zhorov et al. indicated that Dlg1 recruitment to the IS was diminished in patients with rheumatoid arthritis, suggesting that Dlg1 function and the regulation of the alternative p38 pathway may contribute to dysregulated Treg cell function in rheumatoid arthritis or human autoimmune conditions [28].

While addressing the entire list of discrepancies observed among all the groups investigating the role of Dlg1 in T lymphocytes is beyond the scope of this paper, it seems clear from our and others' results reported to date that Dlg1 can facilitate or attenuate discrete TCR signals and that its role in regulating T cell functionality can vary within T cell subsets or at particular stages of T cell development [23,24,26,28,30,36].

If there are compensatory mechanisms in play, then many of our studies of the role of Dlg1 in T cell function, including surface receptor regulation during primary activation, uropod formation and localization of DPC and IS constituents, and proliferation should be revisited in experimental systems where Dlg1 is acutely knocked out rather than stably deleted during T cell development. Because these data preclude further analysis of Dlg1 using long-term genetic approaches, future efforts to characterize the role of *dlg1* in T cell development and function should make use of genetic systems that allow one to acutely delete *dlg1*. For example, an estrogen-receptor Cre-recombinase (ER-Cre) system where "floxed" alleles can be induced to recombine following exposure to tamoxifen permits targeted and controlled acute Dlg1 ablation might work well. Until the ideal model systems are developed and validated, however, acute knock-down of Dlg1 remains a potent strategy by which to continue exploring the functional significance of Dlg1.

Materials and Methods

Ethics Statement

Bay Genomics (BG)- *dlg1* knockout mice. All mice were bred and housed at the University of California Division of Laboratory Animal Medicine facility and all experiments were performed in strict accordance with a protocol reviewed and approved by the University of California Animal Research Committee (ARC approval #1996-155-51).

Gene Trap (GT)- *dlg1* knockout mice. All mice were bred and housed at the Peter MacCallum Cancer Centre animal facility and all experiments were performed in accordance with the Animal Experimentation Ethics Committee of the Peter MacCallum Cancer Centre (Approval #E349).

$CD4^{Cre}$ conditional *dlg1* knockout mice. All studies involving these animals were carried out according to guidelines put forth by the NIH Guide for the Care and Use of Laboratory Animals, as approved under protocol #2008-10-667 by the Children's Hospital of Philadelphia Institutional Animal Care and Use Committee.

Mice

Bay Genomics (BG)- *dlg1* knockout mice. Mice with a *dlg1* null allele were generated through the Bay Genomics consortium using the gene trap vector pGToLxf. pGToLxf contains a splice acceptor sequence upstream of a β-Geo reporter gene, a fusion of β-galactosidase and neomycin phosphotransferase II. Insertion of the β-Geo cassette disrupts translation of the *dlg1* gene via insertional mutation. The BG-RRN196 ES clone generated by gene trap contains an insertional mutation in the fourth intron of *dlg1* resulting in the production of a fusion transcript consisting of exons 1–4, encoding the first 150 amino acids of Dlg1. Chimeric pups with germline transmission were bred with C57BL/6J to generate a BG-*dlg1* founder line. BG-$dlg1^{+/-}$ founder mice on a mixed 129/C57BL/6J background were crossed with C57BL/6J mice (Jackson Labs) 3+ generations before beginning experiments and maintained as BG-*dlg1* heterozygotes by additional crosses to C57BL/6J mice.

Gene Trap (GT)- *dlg1* knockout mice. Mice containing the gene trap insertion allele *dlg1* have been described [37]. GT-*dlg1* mice were crossed with C57BL/6-CD45.2 mice (Walter and Eliza Hall Institute) for at least 10 generations before beginning experiments and maintained as GT-*dlg1* heterozygotes by additional crosses to C57BL/6 mice.

$CD4^{Cre}$ conditional *dlg1* knockout mice. Mice homozygous for a floxed *dlg1* gene [38] (generously provided by Dr. R. Huganir, Johns Hopkins University), were crossed with $CD4^{Cre}$ transgenic mice on the C57Bl/6 background (Taconic Farms) to generate mice with deletion of *dlg1* late in T cell development($dlg1^{flox/flox}$:$CD4^{Cre}$). Wild-type littermates ($dlg1^{flox/flox}$) were used as controls.

Genotyping

BG- *dlg1* knockout mice. BG- $dlg1^{+/+}$ and BG- $dlg1^{+/-}$ mice were genotyped by the absence or presence, respectively, of the β-Geo reporter gene cassette within genomic DNA using a mixture of primers for β-Geo and Tcrd (a control for the presence of genomic DNA): β-Geo forward 5′- CAA ATg gCg ATT ACC gTT gA-3′; β-Geo reverse 5′- TgC CCA gTC ATA gCC gAA TA - 3′; Tcrd forward 5′-CAA ATg TTg CTT gTC Tgg Tg -3′; Tcrd reverse 5′-gTC AgT CgA gTg CAC AgT TT-3′. PCR conditions for 30 cycles were: 94°C for 60 sec; 60°C for 45 sec; 72°C for 60 sec. All successful PCR reactions result in a Tcrd product of 581 base pairs. The presence of β-Geo in BG-$dlg1^{+/-}$, $dlg1^{BG;+/-}$ or $dlg1^{BG;-/-}$ samples results in an additional 200 base pair product.

To evaluate β-gal expression levels in donor fetal liver samples and assign a wild-type, heterozygous, or knockout status to the BG-*dlg1* donor pup, 1×10^6 fetal liver cells were stained using a FluoReporter lacZ Flow Cytometry kit (F1930; Invitrogen/Molecular Probes), according to the manufacturer's directions. The corresponding heads and bodies of the fetal pups were collected to generate DNA (genomic and cDNA) for further examination by PCR and to extract protein to assess Dlg1 expression by Western blotting, respectively.

"Junctional" primer sets, which span the junction between *dlg1* and the β-Geo insert in cDNA, were also used to differentiate between BG-$dlg1^{+/+}$, BG-$dlg1^{+/-}$, or BG-$dlg1^{-/-}$, donor pups and to confirm genotypes in the lymphoid organs of recipients following adoptive transfer: *dlg1* Forward 5′- gAg Cgg gTT ATT AAC ATA TTT CAg - 3′; *dlg1* PDZ Reverse 5′- CCg CTC gAg CCC TTC TCC ATC TTC ACC TCC -3′; β-Geo Reverse 5′- ATT CAg gCT gCg CAA ATg TTg gg -3′. PCR conditions for 30 cycles were: 94°C for 60 sec; 60°C for 45 sec; 72°C for 60 sec. BG-$dlg1^{+/+}$ and $dlg1^{BG;wt}$ yield a single product of 1525 bp, BG-$dlg1^{-/-}$ and $dlg1^{BG;ko}$ yield a single product of 537 bp, and BG-$dlg1^{+/-}$ and $dlg1^{BG;+/-}$ yield 537 base pairs and 1525 base pair products.

GT- *dlg1* knockout mice. For GT- *dlg1*or $dlg1^{GT}$ mice, the genotype of wild-type, heterozygous or homozygous mutant animals was determined using genomic DNA and primers for the Dlg1 and LacZ reporter gene. Dlg1 forward5′ -GAGTTACC-TAAGCCTGGC -3′; Dlg1 reverse 5′- CTGGAATGGGAAA-CATATAC -3′; LacZ forward 5′-TTGGCGTAAGTGAAGC-GAC -3′; LacZ reverse 5′- AGCGGCTGATGTTGAACTG -3′. PCR conditions for 32 cycles were: 94°C 60 sec; 56°C 90 sec; 72°C 90 sec.

Adoptive Transfer Experiments

BG- *dlg1* donor and $dlg1^{BG}$ HSC recipient mice. Fetal livers from embryonic day 14.5 pups were harvested from BG-$dlg1^{+/-}$ females crossed to BG-$dlg1^{+/-}$ males and assigned donor genotypes. 9–14 week old $rag1^{-/-}$ recipients (B6.129S7-$RAG1^{tm1-Mom/J}$; Jackson Labs) were sublethally irradiated (400 rads) one day prior to intravenous injection of 0.5×10^6 donor fetal liver cells. $rag1^{-/-}$ recipient mice ($dlg1^{BG}$) were analyzed 8–12 weeks post-transfer at which time the bone marrow, thymus, spleen, and lymph nodes were collected. A total of six adoptive transfers were completed with 35 recipient mice examined experimentally ($dlg1^{BG;wt}$ = 11, $dlg1^{BG;+/-}$ = 12, and $dlg1^{BG;ko}$ = 12).

GT- *dlg1* donor and *dlg1*^{GT} recipient mice. B6-Ptprca recipients (C57BL/6-CD45.1; Walter and Eliza Hall Institute of Medical Research) 8–12 week old were lethally irradiated (550 rads) twice 3 hours apart and injected with 1×10^6 *dlg1*$^{GT;wt}$ and *dlg1*$^{GT;ko}$ fetal liver cells.

Cell Culture

***dlg1*^{BG} cells and *dlg1*^{GT} cells.** All primary cells were cultured in complete RPMI media composed of RPMI 1640 supplemented with 10% FBS, sodium pyruvate, GlutaMAX, β-Mercaptoethanol, penicillin, and streptomycin. Total T cells were generated from murine splenocytes +/− lymph nodes, as indicated and red blood cells were removed from single cell suspensions by hypotonic lysis. 293T cells were cultured in DMEM, 10% FBS, non-essential amino acids, sodium pyruvate, penicillin, streptomycin, and glutamate. T lymphoblasts were produced by stimulating spleen cells in complete RPMI 1640 media with 2 μg/ml concanavalin A (Sigma-Aldrich) and 50 U/ml IL-2 (Chiron Corp., USA) for 3 days, and then with 50 U/ml IL-2 for an additional 2 days.

dlg1$^{flox/flox}$:CD4^{cre} and jurkat cells. All tissue culture reagents were from Invitrogen. Murine CD4$^+$ lymph node T cells were isolated by negative selection using a mixture of anti-MHC class II (M5/114.15.2) and anti-CD8 (2.43) followed by magnetic bead-conjugated goat anti-rat Ig (Qiagen). Labeled cells were removed using magnetic separation. To generate T-depleted splenocytes, red cells were removed from single cell suspensions by hypotonic lysis. Cells were washed and subjected to complement-mediated lysis using α-Thy1.1 (AT83.A) hybridoma supernatant. Dead cells were removed by centrifugation over Histopaque (Sigma). Cells were maintained using DMEM supplemented with 5% FBS, non-essential amino acids, penicillin, streptomycin, HEPES and β-Mercaptoethanol (Sigma). The human T cell line Jurkat E6.1 was maintained in RPMI supplemented with 5% FBS, 5% newborn calf serum, penicillin, streptomycin and GlutaMAX.

T Cell Expansion

Cells isolated from the spleen and lymph nodes of individual mice were pooled together to expand CD4$^+$ and CD8$^+$ T-cell populations. Approximately 10×10^6 cells were stimulated with 5 ug anti-CD3 and 20 ug anti-CD28 in one well of a 6-well plate for 72 hours. Cells were then harvested and re-plated at a concentration of approximately 15×10^6 cells per well in a 12-well plate in fresh media containing 200 U/ml IL-2 for an additional 48 hrs. Expanded T cell populations were used to assess intracellular cytokine production, phospho-38 phosphorylation, and actin polymerization.

Reverse Transcription and Quantitative PCR

Total RNA was isolated from purified murine T cells, brain, or Th1 and Th2 cells using Trizol according to the manufacturer's instructions in order to synthesize cDNA by RTPCR. Resulting cDNA was used to amplify Dlg transcripts with the following primer sets: Dlg1 Forward 5′-CAg AgC AAC CTC TTT CAg gCT T-3′ and Dlg1 Reverse 5′-Tgg ACA TTC TCA ATC TCT gAC A-3′; Dlg2 Forward,5′ CTA CTg TCT ggC AAC AAT ggC A-3′ and Dlg2 Reverse, 5′-TgC AgT ACT gTg CTg AgA ATg A-3′; Dlg3 Forward, 5′-TCg gAC TCg TgA CAg CTg TCT A-3′ and Dlg3 Reverse, 5′-CTC CAT AAT AAT CgT CAC TTA AC-3′; Dlg4 Forward, 5′-TAC CgC TAC CAA gAT gAA gAC AC-3′ and Dlg4 Reverse, 5′-ACT TCA TTG ACA AAC Agg ATg C-3′; Dlg5 Forward, 5′-Tgg CCA Agg AgC Agg ACC ACT T-3′ and Dlg5 Reverse, 5′-gCC TCT CAT AAT CAg gAT TCA gg-3′. PCR products were resolved on a 1% agarose gel, stained with EtBr and visualized with an UV light. An Alpha Imager was used to capture pictures.

Similarly, total RNA from murine CD4+ T cells following Th skewing conditions and transduction with retrovirus expressing control or Dlg1 miRNA was isolated using Trizol according to the manufacturer's instructions in order to synthesize cDNA by RTPCR. Dlg1 expression and cytokine production was determined by quantitative PCR using 2 ug of total cDNA with the following primer sets: Dlg1 Forward 5′-AgA TCg CAT CAT ATC ggT gAA-3′and Reverse 5′- TCA AAA CgA CTg TAC TCT TCg g-3; IFNγ Forward 5′- gTC AAC AAC CCA CAg gTC CAg -3′and IFNγ Reverse 5′- CCT TTT CCg CTT CCT gAg g -3′; IL4 Forward 5′-ACA ggA gAA ggg ACg CCAT-3′ and IL4 Reverse 5′-gAA gCC CTA CAg ACg AgC T-3′; TNFα Forward 5′- AAT ggC CTC CCT CTC ATC AgT -3′ and TNFα Reverse 5′- gCT ACA ggC TTg TCA CTC gAA TT -3′. A BioRad MyiQ qPCR machine and BioRad iQ5 software was used to generate and quantify data. All samples were normalized to L32 levels (L32 Forward 5′- AAg Cga AAC Tgg Cgg AAA C- 3′and L32 Reverse 5′ –TAA CCg ATg TTg ggC ATC Ag- 3′ in order to determine relative expression levels.

Cellular Analysis of Cell Populations by Flow Cytometry

Single cell suspensions of 1.5×10^6 cells were generated from the spleen, lymph nodes, or thymus and surface stained for 20 minutes at 4°C with combinations of following fluorescently-conjugated antibodies at a concentration of 1 ug/ul: CD3, CD4, CD8, CD25, CD44, CD62L, CD69, CD62L, CD44, B220, IgM, and IgD. Intracellular staining for FoxP3 was performed using a FITC anti-mouse FoxP3 staining set according to manufacturer's directions (eBioscience). Samples were acquired using LSRII or FACSCalibur (BD Biosciences) and analyzed with FlowJo (Treestar) or CellQuest software (BD Biosciences) Dead cells were excluded based on forward versus side scatter analysis.

The hematopoietic composition in peripheral blood was determined by running aliquots of freshly obtained blood samples harvested from the orbital plexus of live mice 8 weeks post-transplantation using sodium heparin-coated capillary tubes (Vitrex Medical AS) on a BAYER ADVIA 120 hematology analyzer (GMI Inc.).

Cellular Analysis of T Cell Activation

To assay for the modulation of early activation markers on the cell surface, naïve splenocytes (5×10^5) were stimulated with varying concentrations of plate-bound anti-CD3 and anti-CD28, cultured for 24 hours and labeled with anti-CD8, anti-CD4, anti-CD45.2, anti-CD44, anti-CD69, anti-CD25 and anti-CD62L antibodies for analysis by flow cytometry (FACSDiva) using FlowJo software. Cells were gated for CD4$^+$ or CD8$^+$. Alternatively, 2×10^5 enriched CD4$^+$ T cells were stimulated with 1 ug/mL each plate-bound anti-CD3 and anti-CD28 for 3 days. Cells were cultured for an additional 2 days and restimulated with plate-bound anti-CD3 and anti-CD28 for 24 hours. Cells were harvested at 24 hours, washed and labeled with anti-CD69, anti-CD25, and anti-CD3 antibodies for analysis by flow cytometry. Dead cells were excluded from analysis based upon forward versus side scatter, and cells were gated in CD4$^+$ events.

Biochemical Analysis of T Cell Activation

General tyrosine phosphorylation. For TCR crosslinking, purified *dlg1*$^{flox/flox}$ or *dlg1*$^{flox/flox}$*:CD4*^{cre} CD4$^+$ T cells were resuspended in RPMI containing 1% FBS, rested on ice in the presence of 10 μg/ml biotinylated anti-CD3 antibody (Biolegend). Stimulation was initiated by the addition of strepavidin (20 μg/

ml). Cells were incubated at 37°C, removed at indicated times, and lysed using TTX lysis Buffer (1% Triton X-100, 50 mM TrisHCl, pH 8.0, 50 mM NaCl, 5 mM EDTA, 50 mM NaF, protease inhibitors, 1 mM $NaVO_4$). Insoluble material was pelleted at 13,000 rpm for 20 minutes. Protein concentrations were determined using a BCA assay (Pierce). Cell lysates were boiled in sample buffer and separation was performed using SDS-PAGE electrophoresis on Tris-glycine gels with 10% acrylamide. Proteins were transferred to nitrocellulose and blocked in 3% BSA in PBS. Blots were probed with anti-phosphotyrosine (4G10) in 3% BSA in TBST. Blots were probed with Alexa-Fluor680 donkey anti-mouse Ig (Invitrogen), and visualized using the Odyssey Imager (Licor).

Alternative p38 phosphorylation. 3×10^6 expanded T cells from $dlg1^{wt;BG}$ or $dlg^{ko;BG}$ mice were rested for 4 hrs at 37°C, and subsequently pretreated with either 10 uM of "InSolution" p38 inhibitor (506148; Calbiochem), 10 uM of ERK inhibitor U0126 (662005; Calbiochem), or DMSO (control) in the presence of complete RPMI media for 30′ minutes at 37°C. Cells were then restimulated with platebound antibody (5 ug anti-CD3 and 20 ug anti-CD28) for 30 minutes at 37°C followed by lysis in TNE buffer (50 mM Tris, 1% Nonidet P-40, 2 mM EDTA, pH 8.0) plus protease (leupeptin and aprotinin 10 ug/ml each, 1 mM PMSF) and phosphatase (1 mM $NaVO_4$) inhibitors for 20 minutes on ice. Cellular debris was spun down at 12,000 RPM for 20 minutes at 4°C and cleared lysates were used to assess protein phosphorylation by separation on a 10% SDS-PAGE. Immunoblots were performed with anti-phospho-p38 (Thr180/Tyr182) (3D7) rabbit monoclonal antibody (9215;Cell Signaling), after which the blots were stripped and reprobed with anti-p38α α (C20) rabbit polyclonal antibody (sc-535;Santa Cruz Biotechnologies) to assess loading. Secondary antibodies to detect primary antibodies were donkey anti-rabbit HRP from (sc-2305; Santa Cruz Biotechnology). The induction of p38 phosphorylation was determined by performing densitometry (ImageJ) on immunblots and calculating the relative fold change between an individual unstimulated and stimulated sample.

RNA-Interference

shRNA-Dlg1. For studies in Jurkat T cells, knockdown oligos were synthesized and cloned as a short hairpin into pCMS3.eGFP.H1p. The following targeting sequences were used: Dlg1-Miceli: 5′-TAC ggg AgC AgA TgA TgA A-3′ (adapted from [2]); Dlg1-Harvard: 5′-CCC AAA TCC ATg gAA AAT A-3′ (adapted from [45]). shRNA-containing plasmids (40 μg) were transfected into Jurkat cells growing at log phase using a square wave electroporator (BioRad) as described [46]. Cells were cultured in antibiotic-free media and assayed at 72 hours after transfection. Analysis of GFP^+ cells by flow cytometry showed >95% transfection efficiency (data not shown). To directly assess protein knockdown, cell lysates were prepared using TTX lysis Buffer as described under methods for "Biochemical analysis of T cell activation", and separated SDS-PAGE electrophoresis on Tris-glycine gels with 10% acrylamide. Immunoblots were probed with primary antibodies specific for Dlg1 (Santa Cruz) or GAPDH in 3% BSA in TBST, followed by secondary IR800 goat anti-rabbit Ig, (Rockland) or AlexaFluor680 donkey anti-mouse Ig (Invitrogen), and visualized using the Odyssey Imager (Licor).

miR-Dlg1. For T helper cell studies, knockdown oligos were synthesized and cloned into the MSCV-based retroviral vector, MGP, where GFP is located downstream of the 5′-LTR. Downstream of the GFP stop codon, the mouse miR-155 expression cassette containing the miR-155 loop sequence and flanking regions was inserted. Anti-sense sequences targeting Dlg1 were designed using the Invitrogen Block-iT polII miR RNAi strategy and cloned into the miR-155 expression cassette, to generate a miR-Dlg1 retroviral construct. The following target sequence was used for MGP-Dlg1:5′- AgC TTA gAg ACA CCA ACT TAT -3′. A scramble sequence that does not target any known mouse transcript was also cloned into the MGP construct generating a miR-control: 5′-gCg CAg TAC ATT T-3′. To generate retrovirus 293T cells were transfected with pCL-Eco and either miR-control or miR-Dlg1 constructs. Transfection was performed with TransIT 293 (Mirus) as per manufacturer's instructions. After 48 and 72 hours, viral supernatant was harvested, filtered through a 0.45 um syringe filter and used to spin-infect T helper cells for 90 minutes, at 1250 RPM at 20°C in the presence of 8 ug/ml polybrene (Millipore). After each transduction, retrovirus was removed and cells were cultured in complete RPMI supplemented with 40 U/ml IL-2 for 24 hrs. Analysis of GFP^+ cells by flow cytometry showed >70% transfection efficiency (data not shown).

Actin Polymerization

Immunofluorescence microscopy –based assay. Analysis of actin polarization was carried out essentially as previously described [47]. Briefly, for Figure 5A, $dlg1^{flox/flox}$ or $dlg1^{flox/flox}$:$CD4^{cre}$ $CD4^+$ T cells were allowed to conjugate with anti-TCR antibody coated sulfate latex beads in a 2:1 ratio (beads:cells) for 20 minutes at 37°C, plated on poly-L-lysine coated coverslips, fixed with 3% paraformaldehyde in PBS, permeabilized with 0.3% TX-100, and stained for actin with rhodamine-phalloidin. Cells were then scored for actin localization to the T cell/bead interface by an individual blinded to experimental conditions. For Figure 5D, Jurkat T cells were transfected with either pCMS3.eGFP.H1p empty vector or pCMS3.eGFP.H1p containing a shDlg1 target sequence, and stimulated with SEE-treated or untreated Raji B cells that had been labeled blue with CMAC cell tracker blue. Conjugates were then allowed to settle on poly-L-lysine coated coverslips, fixed, and stained with rhodamine phalloidin as described above. Cell conjugates were then scored for actin localization to the T cell/APC interface by an individual blinded to experimental conditions. Images were collected using a Coolsnap FX-HQ camera (Roper Scientific), and deconvolution and 3-D rendering was performed using Slidebook v4.0 software (3I). 3D images of maximum intensity projections of Z sections spanning the entire cells were compressed and processed using Photoshop CS software (Adobe Systems Inc., USA) to adjust greyscale levels.

FACS-based assay. 2×10^6 expanded T cells from $dlg1^{wt;BG}$ or $dlg1^{ko;BG}$ mice were stimulated with 5 ug anti-CD3 and 20 ug anti-CD28 of plate-bound antibody in one well of a 6–well dish for 5 or 15 minutes. Cells were harvested and fixed and permeabilized in 200 ul Cytofix/Cytoperm (51–2090KZ; BD Biosciences) overnight at 4°C. Cells were washed in FACS buffer (1× PBS, 3% FCS, and 0.1% sodium azide) and stained for 1 hour at room-temperature with a cocktail of 5 ug/ml FITC-conjugated phalloidin (p-5282; Sigma-Aldrich), anti-CD8b PE and anti-CD4 APC. Cells were then washed twice with FACS buffer and analyzed by flow cytometry (FACSCalibur) using CellQuest software.

T Cell Polarization Assays

For immunofluorescent imaging, T lymphoblasts were allowed to adhere overnight to Lab-Tec® II chamber slides (Nunc, USA). Cells were washed, fixed in 3.7% paraformaldehyde in PBS, processed with anti-CD43 or anti-CD44 (BD Pharmingen)

antibodies to label T cell uropod markers and scored for polarization.

Alternatively, $CD4^+$ T cells from $dlg1^{flox/flox}$ or $dlg1^{flox/flox}$:$CD4^{cre}$ mice were incubated with anti-TCR antibody-coated beads for 20 minutes, fixed and stained with one of the following antibodies: Ezrin (Cell Signaling), Moesin (Q480; Cell Signaling), CD43 (BD Pharmingen), or PKCζ (Santa Cruz). T cell/bead conjugates were then scored for localization to the DPC or IS interface as above. Quantitation was performed by randomly selecting conjugates containing a T cell contacting a latex bead or blue-dyed B cell. Localization to the IS was defined by the presence of a distinct band at the cell-cell contact site. Localization to the DPC was defined as exclusion of the protein of interest from the cell-cell contact or as capping at the T cell pole opposite the site of TCR engagement. Wherever possible, analysis was performed by an individual blinded to experimental conditions. At least 50 conjugates were scored in each of three experiments. Data represent average +/− standard deviation.

T Cell Migration Assays

Random migration analysis. To assess random migration using time-lapse microscopy, T lymphoblasts cultured overnight in Ibidi chamber slides (Integrated BioDiagnostics, Germany) were followed over 3 hours on a Leica TCS SP5 (Leica Microsystems GmBH, Germany) live-cell microscope equipped with a motorized stage and 37°C heated chamber supplied with CO_2. Differential interference contrast (DIC) images were captured at 1 min intervals using a Nikon 40X 0.85 N.A. objective. Movement, presented as distance (distances between successive points of each cell from frame to frame), was quantified by individual cell tracking using MetaMorph® 6.3 software.

Chemokine-mediated migration assay. $dlg1^{flox/flox}$ or $dlg1^{flox/flox}$:$CD4^{cre}$ derived T cell blasts or Jurkat T cells were collected were collected, washed, and resuspended at 20×10^6 cells/mL in RPMI containing 1% FBS, 25 mM HEPES, 5 mM glutamax and penicillin/streptomycin. Media with or without CCL19 (250 nM) or CXCL12 (10 nM) was plated in bottom wells of 96 well, 3 or 5 um pore ChemoTx® disposable chemotaxis system (NeuroProbe) for T cell blasts or Jurkat T cells, respectively. For some experiments, one side of the chemotaxis chamber membrane was coated with either 20 ug/mL fibronectin or 6 ug/mL rmICAM-1 for two hours, washed, dried, and repeated on the other side. 25 uL of cells were plated on top of the membrane, and plates were incubated at 37°C for 2 hours. Migrated cells were counted by hemocytometer and percent migrated was calculated by dividing by the input cell number. Data represent the average of at least three duplicates +/− standard deviation; statistical significance was calculated using a paired Student's *t*-test. Data shown is representative of at least 3 independent experiments. *$p \leq 0.05$.

CFSE Proliferation Assay

Total splenocytes from $dlg1^{wt;BG}$ or $dlg1^{ko;BG}$ mice were labeled with a final concentration of 1.5 uM CFSE (Invitrogen) and stimulated in 6-well plates coated with varying concentrations of anti-CD3 and anti-CD28 antibodies for 24, 48, or 72 hours. Cells were stained with anti-CD8 antibody (BD Pharmingen) and analyzed by flow cytometry (FACSCalibur) using CellQuest software (BD Biosciences).

Similarly, naïve splenic T lymphocytes isolated by negative bead selection using pan-T cell isolation kits (Miltenyi Biotec) from $dlg1^{wt;GT}$ or $dlg1^{ko;GT}$ mice were labeled with 5 μM final concentration of CFSE (Invitrogen), and stimulated with varying concentrations of anti-CD3 antibody in the presence or absence of anti-CD28 and cultured for 62 hours. Cells were washed and labeled with anti-CD8 and anti-CD4 antibodies and analyzed by flow cytometry (LSRII, BD Biosciences) using FlowJo software.

Intracellular Cytokine Staining

Expanded T cells from $dlg1^{wt;BG}$ or $dlg^{ko;BG}$ mice and retrovirally transduced Th1 and Th2 cells were restimulated with plate-bound anti-mouse CD3ε (2 ug/ml) and anti-mouse CD28 (5 ug/ml), or PMA/Ionomycin for 4 or 6 hours, respectively in the presence of GolgiStop (BD Pharmingen). Cells were harvested and surface stained with anti-CD8 or anti-CD4 antibodies as indicated, fixed and permeabilized with Cytofix/Cytoperm (BD Pharmingen) overnight, and subsequently stained with either anti-TNFα (clone MP6-XT22), anti-IFNγ (clone XMG1.2) or anti-IL-4 (clone 11B11) (all BD Pharmingen). Cells were analyzed on a FACSCaliber (BD).

ELISA

Cytokines were measured by ELISA per antibody manufacturer recommendations (eBioscience).

Differentiation of T Helper cells

CD4+ T cells were purified from the spleen and lymph nodes of C57Bl/6 mice using anti-CD4 magnetic microbeads (Miltenyi Biotec 130-049-201) according to the manufacturer instructions. Purified CD4+ T cells were stimulated with plate-bound anti-mouse CD3ε (Clone 145-2C11 from BD) at 2 ug/mL and anti-mouse CD28 (Clone 37.51 from BD) at 5 ug/mL under Th1-differentiating conditions (10 ng/mL IL-12, 10 ug/mL anti-IL-4, 40 U/mL IL-2) or Th2-differentiating conditions (20 ng/mL IL-4, 20 ug/mL anti-IFNγ, 20 U/mL IL-2). All antibodies used for Th1/Th2 polarization were from eBiosciences, including neutralizing rat mAb for murine IL-4 (clone 11B11) and IFNγ (clone R4-6A2). Recombinant IL-2, IL-4, and IL-12 were from R and D systems. One week after primary stimulation, cultures were transduced with miR-Dlg1 or miR-control retroviral supernatants, restimulated, and analyzed for cytokine production as described. Data represent average +/− standard error mean and statistical significance was calculated using a paired Student's *t*-test.

Supporting Information

Figure S1 Characterization of *dlg* gene expression in wild-type T cells. (A) cDNA from primary mouse T cells and mouse brain was analyzed by PCR using primer pairs specific for 4 distinct *dlg* genes (*dlg* 1–4).
(TIF)

Figure S2 Schematic for the deletion of *dlg1* in the germline deficient mouse models. (A) The RRN196 Dlg1 knockout mouse (BG-$dlg1^{-/-}$) contains a β-galactosidase insertion cassette at the 3′ end of exon 4 expected to result in a truncated 105 amino acid Dlg1-β-Geo fusion protein. (B) The GT-*dlg1* knockout mouse contains a β-galactosidase insertion cassette between the Dlg1 PDZ3 and SH3 domain expected to result in a truncated 549 amino acid Dlg1-β-Geo fusion protein. (C) *Top*, Diagram of primers sets for junctional PCR to differentiate between BG-$dlg1^{+/+}$, BG-$dlg1^{+/-}$, or BG-$dlg1^{-/-}$ donor pups. Expected PCR products are as follows: BG-$dlg1^{+/+}$ = 1525 bp;BG-$dlg1^{-/-}$ = 525 bp. *Bottom*, Representative agarose gel showing differential products of junctional PCR from BG-$dlg1^{+/+}$, BG-$dlg1^{+/-}$, or BG-$dlg1^{-/-}$ fetal pups (n = 6 independent experiments).
(TIF)

Figure S3 Hematopoiesis is not altered in $dlg1^{ko;GT}$ mice. Eight weeks following reconstitution, peripheral blood from $dlg1^{wt;GT}$ or $dlg1^{ko;GT}$ mice was collected and analyzed for total blood composition using BAYER ADVIA 120 hematology analyzer. Data are expressed as mean ± SD. (n = 10 mice per genotype).
(TIF)

Table S1 Thymic and splenic cellularity and composition are not altered in in $dlg1^{ko;GT}$ mice. Total thymocyte and splenocyte cellularity (1×10^6) and percentage of cellular subsets was determined by cell counts on a hemocytometer and flow cytometric analysis of indicated cell surface markers. Shown are averages ± standard deviations of 12 $dlg1^{wt;GT}$ and $dlg1^{ko;GT}$ mice.
(TIF)

References

1. Stinchcombe JC, Majorovits E, Bossi G, Fuller S, Griffiths GM (2006) Centrosome polarization delivers secretory granules to the immunological synapse. Nature 443: 462–465.
2. Thrasher AJ, Burns SO (2010) WASP: a key immunological multitasker. Nat Rev Immunol 10: 182–192.
3. Ludford-Menting MJ, Oliaro J, Sacirbegovic F, Cheah ET, Pedersen N, et al. (2005) A network of PDZ-containing proteins regulates T cell polarity and morphology during migration and immunological synapse formation. Immunity 22: 737–748.
4. Burkhardt JK, Carrizosa E, Shaffer MH (2008) The actin cytoskeleton in T cell activation. Annu Rev Immunol 26: 233–259.
5. Krummel MF, Macara I (2006) Maintenance and modulation of T cell polarity. Nat Immunol 7: 1143–1149.
6. Grakoui A (1999) The Immunological Synapse: A Molecular Machine Controlling T Cell Activation. Science 285: 221–227.
7. Cullinan P, Sperling AI, Burkhardt JK (2002) The distal pole complex: a novel membrane domain distal to the immunological synapse. Immunol Rev 189: 111–122.
8. Fooksman DR, Vardhana S, Vasiliver-Shamis G, Liese J, Blair DA, et al. (2010) Functional anatomy of T cell activation and synapse formation. Annu Rev Immunol 28: 79–105.
9. Friedl P, den Boer AT, Gunzer M (2005) Tuning immune responses: diversity and adaptation of the immunological synapse. Nat Rev Immunol 5: 532–545.
10. Huse M, Quann EJ, Davis MM (2008) Shouts, whispers and the kiss of death: directional secretion in T cells. Nat Immunol 9(10): 1105–1111.
11. Chang JT, Ciocca ML, Kinjyo I, Palanivel VR, McClurkin CE, et al. (2011) Asymmetric proteasome segregation as a mechanism for unequal partitioning of the transcription factor T-bet during T lymphocyte division. Immunity 34: 492–504.
12. Chang JT, Palanivel VR, Kinjyo I, Schambach F, Intlekofer AM, et al. (2007) Asymmetric T lymphocyte division in the initiation of adaptive immune responses. Science 315: 1687–1691.
13. Allenspach EJ, Cullinan P, Tong J, Tang Q, Tesciuba AG, et al. (2001) ERM-dependent movement of CD43 defines a novel protein complex distal to the immunological synapse. Immunity 15: 739–750.
14. Oliaro J, Van Ham V, Sacirbegovic F, Pasam A, Bomzon Z, et al. (2010) Asymmetric cell division of T cells upon antigen presentation uses multiple conserved mechanisms. J Immunol 185: 367–375.
15. Maldonado RA, Irvine DJ, Schreiber R, Glimcher LH (2004) A role for the immunological synapse in lineage commitment of CD4 lymphocytes. Nature 431: 527–532.
16. Dustin ML, Chan AC (2000) Signaling takes shape in the immune system. Cell 103: 283–294.
17. Yeh JH, Sidhu SS, Chan AC (2008) Regulation of a late phase of T cell polarity and effector functions by Crtam. Cell 132: 846–859.
18. Miceli MC, Moran M, Chung CD, Patel VP, Low T, et al. (2001) Co-stimulation and counter-stimulation: lipid raft clustering controls TCR signaling and functional outcomes. Semin Immunol 13: 115–128.
19. Russell S (2008) How polarity shapes the destiny of T cells. J Cell Sci 121: 131–136.
20. Teixeiro E, Daniels MA, Hamilton SE, Schrum AG, Bragado R, et al. (2009) Different T cell receptor signals determine CD8+ memory versus effector development. Science 323: 502–505.
21. Humbert P, Russell S, Richardson H (2003) Dlg, Scribble and Lgl in cell polarity, cell proliferation and cancer. Bioessays 25: 542–553.
22. Round JL, Tomassian T, Zhang M, Patel V, Schoenberger SP, et al. (2005) Dlgh1 coordinates actin polymerization, synaptic T cell receptor and lipid raft aggregation, and effector function in T cells. J Exp Med 201: 419–430.
23. Xavier R, Rabizadeh S, Ishiguro K, Andre N, Ortiz JB, et al. (2004) Discs large (Dlg1) complexes in lymphocyte activation. J Cell Biol 166: 173–178.
24. Round JL, Humphries LA, Tomassian T, Mittelstadt P, Zhang M, et al. (2007) Scaffold protein Dlgh1 coordinates alternative p38 kinase activation, directing T cell receptor signals toward NFAT but not NF-kappaB transcription factors. Nat Immunol 8: 154–161.
25. Lue RA, Brandin E, Chan EP, Branton D (1996) Two independent domains of hDlg are sufficient for subcellular targeting: the PDZ1–2 conformational unit and an alternatively spliced domain. J Cell Biol 135: 1125–1137.
26. Lasserre R, Charrin S, Cuche C, Danckaert A, Thoulouze MI, et al. (2010) Ezrin tunes T-cell activation by controlling Dlg1 and microtubule positioning at the immunological synapse. Embo J 29: 2301–2314.
27. Salvador JM, Mittelstadt PR, Guszczynski T, Copeland TD, Yamaguchi H, et al. (2005) Alternative p38 activation pathway mediated by T cell receptor-proximal tyrosine kinases. Nat Immunol 6: 390–395.
28. Zanin-Zhorov A, Lin J, Scher J, Kumari S, Blair D, et al. (2012) Scaffold protein Disc large homolog 1 is required for T-cell receptor-induced activation of regulatory T-cell function. Proc Natl Acad Sci USA 109: 1625–1630.
29. Mittelstadt PR, Yamaguchi H, Appella E, Ashwell JD (2009) T cell receptor-mediated activation of p38{alpha} by mono-phosphorylation of the activation loop results in altered substrate specificity. J Biol Chem 284: 15469–15474.
30. Adachi K, Davis MM (2011) T-cell receptor ligation induces distinct signaling pathways in naive vs. antigen-experienced T cells. Proc Natl Acad Sci USA 108: 1549–1554.
31. Jirmanova L, Sarma DN, Jankovic D, Mittelstadt PR, Ashwell JD (2009) Genetic disruption of p38alpha Tyr323 phosphorylation prevents T-cell receptor-mediated p38alpha activation and impairs interferon-gamma production. Blood 113: 2229–2237.
32. Morales-Tirado V, Johannson S, Hanson E, Howell A, Zhang J, et al. (2004) Cutting Edge: Selective Requirement for the Wiscott-Aldrich protein in cytokine, but not chemokine, secretion by CD4+ T cells. J Immunol 173(2): 726–730.
33. Shaffer MH, Dupree RS, Zhu P, Saotome I, Schmidt RF, et al. (2009) Ezrin and moesin function together to promote T cell activation. J Immunol 182: 1021–1032.
34. Cannon JL, Burkhardt JK (2004) Differential roles for Wiskott-Aldrich syndrome protein in immune synapse formation and IL-2 production. J Immunol 173: 1658–1662.
35. Affaticati P, Mignen O, Jambou F, Potier MC, Klingel-Schmitt I, et al. (2011) Sustained calcium signalling and caspase-3 activation involve NMDA receptors in thymocytes in contact with dendritic cells. Cell Death Differ 18: 99–108.
36. Stephenson LM, Sammut B, Graham DB, Chan-Wang J, Brim KL, et al. (2007) DLGH1 is a negative regulator of T-lymphocyte proliferation. Mol Cell Biol 27: 7574–7581.
37. Caruana G, Bernstein A (2001) Craniofacial dysmorphogenesis including cleft palate in mice with an insertional mutation in the discs large gene. Mol Cell Biol 21(5): 1475–1483.
38. Zhou W, Zhang L, Guoxiang X, Mojsilovic-Petrovic J, Takamaya K, et al. (2008) GluR1 controls dendrite growth through its binding partner, SAP97. J Neurosci 28: 10220–10233.
39. Klocker N, Bunn RC, Schnell E, Caruana G, Bernstein A, et al. (2002) Synaptic glutamate receptor clustering in mice lacking the SH3 and GK domains of SAP97. Eur J Neurosci 16: 1517–1522.
40. Schlüter OM, Xu W, Malenka RC (2006) Alternative N-terminal domains of PSD-95 and SAP97 govern activity-dependent regulation of synaptic AMPA receptor function. Neuron 51: 99–111.
41. Balamuth F, Leitenberg D, Unternaehrer J, Mellman I, Bottomly K (2001) Distinct patterns of membrane microdomain partitioning in Th1 and th2 cells. Immunity 15: 729–738.
42. Madrenas J (2003) A SLAT in the Th2 signalosome. Immunity 18: 459–461.
43. Josefowicz SZ, Rudensky A (2009) Control of regulatory T cell lineage commitment and maintenance. Immunity 30: 616–625.

Acknowledgments

The Burkhardt lab would like to thank Renell Dupree and Alan Hsu for excellent technical assistance The Miceli lab would like to thank Jillian Crocetti for critical reading.

The Russell lab would like to thank Georgina Caruana for providing the Dlg^{GT} mice, and Jane Oliaro, Mandy Ludford-Menting and Edwin Hawkins for advice.

Author Contributions

Conceived and designed the experiments: LAH MHS FS TT KAM OS JLR JKB SMR MCM. Performed the experiments: LAH MHS FS TT KAM OS JLR KT. Analyzed the data: LAH MHS FS TT KAM OS JLR JKB SMR MCM. Contributed reagents/materials/analysis tools: POH RLH JKB SMR MCM. Wrote the paper: LAH MHS FS TT OS JKB SMR MCM. Oversaw and coordinated the projects: JKB SMR MCM.

44. Wu Y, Borde M, Heissmeyer V, Feuerer M, Lapan AD, et al. (2006) FOXP3 controls regulatory T cell function through cooperation with NFAT. Cell 126: 375–387.
45. Nakagawa T, Futai K, Lashuel HA, Lo I, Okamoto K, et al. (2004) Quaternary structure, protein dynamics, and synaptic function of SAP97 controlled by L27 domain interactions. Neuron 44: 453–467.
46. Carrizosa E, Gomez TS, Labno CM, Klos Dehring DA, Liu X, et al. (2009) Hematopoietic lineage cell-specific protein 1 is recruited to the immunological synapse by IL-2-inducible T cell kinase and regulates phospholipase Cgamma1 microcluster dynamics during T cell spreading. J Immunol 183: 7352–7361.
47. Cannon JL, Labno CM, Bosco G, Seth A, McGavin MH, et al. (2001) Wasp recruitment to the T cell:APC contact site occurs independently of Cdc42 activation. Immunity 15: 249–259.

CHAPTER FIVE

Acute Dlgh1 knockout prevents optimal T cell activation and proinflammatory cytokine production

ABSTRACT

Dlgh1 knockout mouse models have not substantiated numerous studies utilizing siRNA-mediated knockdown demonstrating that Dlgh1 serves as a molecular scaffold in T lymphocytes to promote T cell signaling and effector function. Here we report that acute deletion of Dlgh1 *in vitro* and *in vivo* prevented optimal T cell activation and proinflammatory cytokine production. Utilizing mice containing loxP sites flanking *dlgh1* (Dlgh1$^{fllox/flox}$) and mice also expressing a fusion protein of a modified estrogen-receptor and Cre recombinase (ER-Cre Dlgh1$^{fllox/flox}$) we find that Dlgh1 can be acutely deleted *in vitro* and *in vivo* to produce Dlgh1-deficient (Dlgh1^{KO}) T cells. Dlgh1^{KO} T cells generated *in vitro* showed impaired TCR-induced p38 phosphorylation and a selective defect in p38-dependent gene expression, which could be rescued by re-expression of the Dlgh1 alternative splice variant Dlgh1 AB, but not Dlgh1 B. Moreover, Dlgh1^{KO} T cells generated *in vivo* were defective in TCR-induced upregulation of CD25, CD44 and CD69, and had a selective impairment in the production of IFNγ and TNFα, but not IL-2. These findings demonstrate that Dlgh1 is a critical molecular scaffold involved in a subset of T cell responses and that acute methods of Dlgh1 deletion should be utilized in future studies assessing the role of Dlgh1 in T lymphocytes.

INTRODUCTION

The adaptive immune response depends on proper T cell activation. Essential to that process is the recognition of antigenic peptides in major histocompatibility complex (MHC) molecules expressed on antigen presenting cells (APCs). T cell receptor (TCR) engagement of antigenic peptide-MHC induces the activation of proximal non-receptor tyrosine kinases, which in turn trigger a dynamic cellular process of actin-mediated reorganization. Following TCR engagement, T cell receptors, intracellular signaling molecules and cytoskeletal components are recruited and positioned into a polarized macromolecular structure facing the APC (1). This molecular platform, often referred to as the immunological synapse (IS), provides an area for the concentration and selective assembly of signaling complexes coupling the tyrosine kinases Lck and ZAP70 to the activation of specific mitogen-activated protein kinases (MAPKs) and transcription factors, such as nuclear factor of activated T cells (NFAT) or nuclear factor-κB (NFκB) (2). The selective activation of these signaling pathways has distinct effects on TCR-induced outcomes, including surface marker upregulation, cytokine production, proliferation and differentiation (3-6). How proximal TCR signals are coupled to specific downstream pathways and discrete cellular functions is just beginning to be elucidated (7, 8).

Scaffolding proteins have emerged as key molecular intermediates coupling extracellular receptors to intracellular signaling pathways, thus having the potential to govern T cell activation and manipulate functional outcomes of TCR engagement. Discs large homolog 1 (Dlgh1), a membrane associated guanylate kinase (MAGUK) family member is recognized as a key molecular scaffold that localizes to the IS during antigen recognition and associates with Lck and ZAP70 (9). At the IS, Dlgh1 juxtaposes Lck, ZAP70 and the MAPK p38, facilitating the activation of the alternative p38 pathway. The

binding of Lck and ZAP70 to Dlgh1 allows for the direct phosphorylation of p38 by ZAP70, permitting p38 autophosphorylation and enabling p38 to modify discrete downstream targets. Indeed, Dlgh1-mediated alternative p38 activation selectively affects NFAT, but not NFκB, via the direct or indirect phosphorylation of the transactivating domain of NFAT (8). In addition to binding p38, Dlgh1 also associates with the cytoskeletal regulators WASp and Ezrin, and controls antigen-induced F-actin polymerization, TCR and lipid raft clustering, and MTOC focusing at the IS (9, 10).

Given the involvement of Dlgh1 in regulating T cell transcriptional activation and cytoskeletal reorganization, we and others have proposed that Dlgh1 could play a critical role in T cell activation, development, effector functions and fate determination. Indeed, utilizing siRNA-mediated knockdown methodologies groups have found a role for Dlgh1 in regulating T cell signaling in human antigen-experienced T cells and suppressor function in human regulatory T cells (11, 12). We have also recently discovered that Dlgh1 mediates p38-independent lytic factor degranulation in murine CD8+ CTLs, in addition to p38-dependent transcriptional activation of proinflammatory cytokines (Chapter 2). Despite growing evidence to support a role for Dlgh1 in T lymphocyte signaling and function, recent attempts to extend the current understanding of Dlgh1 utilizing Dlgh1 knockout mouse models has been largely unavailing. One group has observed hyperproliferation of T cells from Dlgh1 knockout mice (13). However, we and others reported the combined cellular and biochemical analyses of one conditional and two germline *dlgh1* knockout mouse models and found no, or minor, observable defects in T cell development, morphology, migration, signaling, activation and/or proliferation (14). We proposed that compensatory mechanisms may be responsible for the lack of functional defects, and that acute knockout of Dlgh1 may allow for a more accurate assessment of the functional role of Dlgh1 in T lymphocytes.

Here we report that acute knockout of Dlgh1 *in vitro* and *in vivo* prevents optimal T cell activation and effector function. Utilizing mice containing loxP sites flanking the *dlgh1* exon encoding a portion of PDZ1 and PDZ2 (Dlgh1$^{fllox/flox}$) or mice also expressing a fusion protein of a modified estrogen-receptor and Cre recombinase (ER-Cre Dlgh1$^{fllox/flox}$) we found that Dlgh1 could be acutely deleted *in vitro* and *in vivo* to produce Dlgh1-deficient (Dlgh1^{KO}) T cells. Dlgh1^{KO} T cells generated *in vitro* were defective in activating the alternative p38 dependent pathway, as Dlgh1^{KO} CD8+ T cells failed to optimally phosphorylated p38 in response to TCR stimulation. Furthermore, Dlgh1^{KO} CD8+ T cells had a selective defect in the TCR-induced upregulation of a subset of NFAT-dependent genes, which could be rescued by re-expression of the Dlgh1 alternative splice variant Dlgh1 AB, but not Dlgh1 B. Finally, Dlgh1^{KO} T cells generated *in vivo* failed to upregulate early activation markers and demonstrated a selective impairment in the production of proinflammatory cytokines. These findings suggest that Dlgh1 is indeed a critical molecular scaffold involved in T cell responses and that future experiments assessing the role of Dlgh1 in T lymphocytes or other hematopoietic cells should be done in experimental systems where Dlgh1 can be acutely deleted.

MATERIALS AND METHODS

Mice

The generation of Dlgh1$^{flox/flox}$ mice has been previously described (15). These mice have loxP sites flanking the *dlgh1* exon encoding a portion of PDZ1 and PDZ2. Dlgh1$^{flox/flox}$ mice were crossed with ER-Cre transgenic mice (Jackson Lab) and offspring (ER-Cre Dlgh1$^{flox/+}$) were crossed with Dlgh1$^{flox/flox}$ mice to generate ER-Cre Dlgh1$^{flox/flox}$ mice. All mice were maintained and used in accordance with the University of California Los Angeles Chancellor's Animal Research Committee.

Reagents and Antibodies

For T cell stimulations and re-stimulations anti-CD3, clone 145-2C11 (BD 553057) and anti-CD28, clone 37.51 (BD 553295) were used. For immunoblotting Mouse anti-Dlg1 (BD 610875), Rabbit anti-p38, clone C20 (Santa Cruz Biotechnology sc-535), Mouse anti-Lck, clone 3A5 (Santa Cruz Biotechnology sc-433), Donkey Anti-Mouse IgG-HRP (Jackson ImmunoResearch 715-035-150), and Donkey-Anti-Rabbit IgG-HRP (Santa Cruz Biotechnology sc-2305) were used. For flow cytometry, Rat anti-CD8b-PE, clone H35-17.2 (BD 550798), Alexa Fluor647 Mouse anti-p38 MAPK (pT180/pY182), clone 36 (BD 612595), anti-Mouse CD25 eFluor660, clone 7D4 (eBioscience 50-0252), anti-Human/Mouse CD44-APC, clone IM7 (eBioscience 17-0441), anti-Mouse CD69-APC, clone H1.2F3 (eBioscience 17-0691), Rat anti-IFNγ-APC, clone XMG1.2 (BD 554413), Rat anti-TNFα-APC, clone MPX-XT22 (BD 554420), Rat anti-IL-2-APC, clone JES6-5H4 (BD 554429), Mouse anti-Dlg1 (BD 610875), and Alexa Fluor647 AffiniPure F(ab)$_2$ Donkey Anti-Mouse IgG (Jackson ImmunoResearch 715-606-150) were used. For in vitro *dlgh1* recombination, 4-hydroxytamoxifen (Sigma H7904) was dissolved in sterile ethanol (Sigma E7023) to make stock 2mM solutions. For in vivo *dlgh1* recombination,

tamoxifen (Sigma T5648) was dissolved in sterile ethanol and diluted in sterile sunflower seed oil (Sigma S5007) to make 5mg/mL solutions. These solutions were sonicated for 15 mins prior to injection.

DNA Constructs

pMSCV-IRES-GFP (MIG)-Empty and MIG-Cre have been previously described (16). MIG-Dlgh1 AB (Dlgh1-L27β-i1Ai1B-i3i5), MIG-Dlgh1 B (Dlgh1-L27β-i1B-i3i5) and the packaging construct pCL-Eco have also been previously described (Chapter 2).

Retroviral Production

293T cells were transfected with pCL-Eco and MIG constructs. Transfection was performed with TransIT 293 (Mirus 2705) per manufacturer's instructions. After 48 hrs, viral supernatant was harvested, 0.45μm filtered and supplemented with polybrene (8μg/mL) prior to infection of T cells.

In Vitro Dlgh1 Knockout and Reexpression

For retroviral Cre-mediated *dlgh1* knockout experiments, splenocytes from 8-16 week old Dlgh1$^{flox/flox}$ mice were isolated. CD8+ cells were sorted using CD8a (Ly-2) microbeads (Miltenyi 130-049-401) or a CD8+ T cell isolation kit (Miltenyi 130-090-859). Sorted CD8+ T cells were stimulated with plate-bound anti-CD3 (2μg/mL) and anti-CD28 (2μg/mL) for 48-72 hrs in complete media composed of RPMI 1640 medium with 10% FCS, sodium pyruvate, 50nM β-mercaptoethanol, penicillin, streptomycin and glutamine. After stimulation, cells were infected with MIG-Empty or MIG-Cre retroviral supernatant by spin inoculation at 1250*g* for 90 mins at room temperature. After centrifugation, virus-containing medium was removed and cells were cultured in fresh

complete media supplemented with rIL-2 (100U/mL). Two spin-infections were performed on cells 24hrs apart. Infected primary T cells were used 24-48 hrs after the last spin-infection. For retroviral Dlgh1 re-expression experiments, splenocytes from 8-16 weeks old ER-Cre Dlgh1$^{flox/flox}$ mice were isolated. CD8+ cells were sorted using CD8a (Ly-2) microbeads. Sorted CD8+ T cells were stimulated with plate-bound anti-CD3/anti-CD28 for 48-72 hrs in complete media. After stimulation, cells were infected with MIG-Empty, MIG-Dlgh1 AB, or MIG-Dlgh1 B retroviral supernatant by spin inoculation at 1250*g* for 90 mins at room temperature. After centrifugation, virus-containing medium was removed and cells cultured in fresh complete media supplemented with rIL-2 (100U/mL) and 4-hydroxytamoxifen (200nM). Two spin-infections were performed on cells 24 hrs apart. Infected T cells were used 24-48 hrs after the last spin-infection.

In Vivo Dlgh1 Knockout

For in vivo Dlgh1 knockout experiments, 8-16 weeks old ER-Cre Dlgh1$^{flox/flox}$ and Dlgh1$^{flox/flox}$ mice were injected with 200µL of 5mg/mL tamoxifen (1mg) or mock solution (10% ethanol in sunflower seed oil) for five consecutive days. Ten days after the last injection, total splenocytes were isolated and stimulated with platebound anti-CD3/anti-CD28 for 24-48 hrs in complete media.

gDNA Isolation and PCR

gDNA was isolated from total splenocytes or sorted CD8+ T cells using the QIAGEN DNeasy Blood & Tissue kit (69506). gDNA was eluted in 50µL of AE buffer and 2.0µL of eluted gDNA was used as a template for *dlgh1* recombination analysis via PCR. In 25µL reactions the following components were added: 1X PCR Buffer without MgCl

(Invitrogen), 2mM MgCl (Invitrogen), 0.4mM dNTPs (Invitrogen), 0.4 μM gF1, 0.4 μM gR1, 2.0μL gDNA and DEPC-H_2O. The PCR program used was 95°C for 3 mins (1X), 95°C for 30 seconds, 60°C for 45 seconds, 72°C for 2 minutes (40X), and 72°C for 5 minutes (1X). Primers used were gF1: 5-TAGATAGACACTTGTCAGGCTAAG-3 and gR1: 5-AGGTAGAACATCAGGCTTTAAAATGTG-3

Protein Isolation and Immunoblotting

Splenocytes or sorted T cells were lysed on ice with TNE buffer (50mM Tris pH 6.8, 1% NP-40, and 20mM EDTA) containing 1X protease inhibitor cocktail (Pierce 87786) and cleared by centrifugation. Proteins were separated by SDS-PAGE and transferred to nitrocellulose. Membranes, blocked with TBS plus 5% milk and 0.1% Tween-20, were incubated with primary antibodies (1:1000) overnight at 4°C, followed by incubation with HRP-conjugated secondary antibodies (1:5000) for either 4 hrs (Dlgh1 blots) or 1 hr (all others) at room temperature. Signals were detected by enhanced chemiluminescence reagents (Western Lightening *Plus*-ECL; Pierce NEL104001EA).

RNA Isolation and qPCR

T cells were re-stimulated with platebound anti-CD3 (2μg/mL) and anti-CD28 (2μg/mL) antibodies or left unstimulated. RNA was isolated using TRIZOL reagent. RNA (2.0 μg) was reverse-transcribed using Superscript III (Invitrogen) according to the manufacture's instructions with oligo(dT) primer in 20μL reactions. cDNA was diluted 1:5 with DEPC-H20 and used for subsequent qPCR analysis. Sybrgreen-based quantitative PCR analysis was performed on the iCycler BioRad instrument according to the manufacturer's instructions (Bio-Rad). Amplification conditions were: 95°C for 3 mins, followed by 40 cycles of 95°C for 30 s and 60°C for 30 s. For all experiments,

mRNA was normalized to L32. Primers used were L32 (forward: 5-AAGCGAAACTGGCGGAAAC-3, reverse: 5-TAACCGATGTTGGGCATCAG-3) Dlgh1 (forward: 5-AGATCGCATCATATCGGTGAA-3, reverse: 5-TCAAAACGACTGTACTCTTCGG-3), NFATc1 (forward: 5-GCCTCGTATCAGTGGGCGAAG-3, reverse: 5- CGAAGCTCGTATGGACCA-3), IκBα (forward: 5- CTGCAGGCCACCAACTACAA-3, reverse: 5-CAGCACCCAAAGTCACCAAGT-3), TNFα (forward: 5- AATGGCCTCCCTCTCATCAGT-3, reverse: 5- GCTACAGGCTTGTCACTCGAATT-3) and IL-2 (forward: 5-CCTGAGCAGGATGGAGAATTACA-3, reverse: 5- TCCAGAACATGCCGCAGAG-3)

Intracellular Phospho-p38

For intracellular phospho-p38 analysis, T cells were stimulated with plate-bound anti-CD3 (1µg/mL) and anti-CD28 (1µg/mL) by quickly spin-contacting the cells to plates. After the stimulation, cells were immediately fixed in 4% paraformaldehyde for 15 minutes on ice. Cells were then harvested, washed with FACS buffer (PBS + 3% FBS + 0.1% sodium azide), and permeabilized with ice cold methanol overnight at 4°C. Cells were then stained with Alexa Fluor647 Mouse anti-p38 MAPK (pT180/pY182) for 30 mins at room temperature, washed and immediately analyzed using a BD FACS-Calibur.

Intracellular Dlgh1 Analysis

For intracellular Dlgh1 analysis, cells were first surface stained with CD8b-PE (1:200) in FACS wash buffer (PBS + 3% FCS + 0.1% sodium azide) prior to fixation and permeabilization with the Foxp3 Fixation/Permeabilization buffer set (eBioscience 00-5523-00). Cell were washed and stained for 30 mins at 4°C with anti-Dlgh1 (1:1000). Cells were washed, stained for 30 mins at 4°C with Alexa Fluor647 AffiniPure $F(ab)_2$

Donkey Anti-Mouse IgG (1:5000). Cells were then washed, resuspended in 2% paraformaldehyde and analyzed with a BD FACS-Caliber.

Surface Activation Marker Analysis

For surface activation marker analysis, cells were surface stained with CD8b-PE (1:200) and anti-CD25, anti-CD44 or anti-CD69 (each at 1:200) in FACS wash buffer for 30 mins at 4°C. Cells were then washed, fixed in 2% PFA and analyzed with a BD FACS-Caliber. For experiments concurrently assessing surface activation markers and intracellular Dlgh1, after surface staining cells were fixed and permeabilized with the Foxp3 Fixation/Permeabilization buffer set. Cell were washed and stained for 30 mins at 4°C with anti-Dlgh1 (1:1000). Cells were washed, stained for 30 mins at 4°C with Alexa Fluor647 AffiniPure $F(ab)_2$ Donkey Anti-Mouse IgG (1:5000). Cells were then washed, resuspended in 2% PFA and then analyzed with a BD FACS-Caliber.

Intracellular Cytokine Analysis

For intracellular cytokine analysis, cells were surface stained with CD8b-PE (1:200) in FACS wash buffer prior to fixation and permeabilization with Foxp3 Fixation/Permeabilization buffer set at 4°C. Cells were then washed, stained for 30 mins with anti-IFNγ, anti-TNFα or anti-IL-2, washed and data collected using a BD FACS-Calibur. For experiments where intracellular cytokines and Dlgh1 were concurrently assessed, after fixation and permeabilization with Foxp3 buffer, cells were stained for 30 mins at 4°C with anti-Dlgh1 (1:1000). Cells were washed, stained for 30 mins at 4°C with Alexa Fluor647 AffiniPure $F(ab)_2$ Donkey Anti-Mouse IgG (1:5000) and anti-IFNγ, anti-TNFα or anti-IL-2. Cells were then washed, resuspended in 2% PFA and analyzed with a BD FACS-Caliber.

Statistical Significance

Standard deviation was calculated using Numbers (Apple). Statistical significance was determined by performing a student's t test. p values < 0.05 were considered significant

RESULTS

In Vitro Dlgh1 Knockout Selectively Diminishes NFAT-mediated Transcriptional Activation and p38 Phosphorylation in CD8+ T Cells

To clarify the functional relevance of Dlgh1 in primary T cells, we first decided to acutely delete *dlgh1* in peripheral CD8+ T cells from mice in which *dlgh1* was flanked by loxP sites (Dlgh1$^{flox/flox}$). Infection with a GFP-expressing Cre retrovirus efficiently induced *dlgh1* recombination and diminished Dlgh1 protein levels (Figure 5-1). Similar results were also obtained utilizing a non-viral mediated methodology to delete *dlgh1*, were Dlgh1$^{flox/flox}$ mice were crossed with transgenic mice expressing Cre from an estrogen receptor-dependent cassette (*Tg(CAG-cre/Esr1)5Amc*; called '*ER*-Cre' here). CD8+ T cells from these ER-Cre Dlgh1$^{flox/flox}$ mice treated with 4-hydroxytamoxifen induced a significant reduction in *dlgh1* mRNA (Figure 5-2A). Furthermore in agreement with previous reports, these Dlgh1-deficient T cells (referred to as Dlgh1^{KO} T cells) had a selective defect in TCR-induced NFATc1, but not IκBα gene expression (Figure 5-2B) (8). Because Dlgh1 serves as a molecular conduit for Lck and ZAP70 to induce NFAT-mediated transcription via the alternative p38 pathway, we decided to assess intracellular p38 phosphorylation (T180/Y182) in these Dlgh1-deficient cells. Dlgh1^{KO} T cells had decreased intracellular phospho-p38 levels in response to anti-CD3/anti-CD28 stimulation compared to Dlgh1^{WT} T cells (Figure 5-2C), indicating that Dlgh1 indeed couples TCR signals to p38 activation and NFAT-mediated transcriptional activation in peripheral CD8+ effector T cells.

Dlgh1 AB, but not Dlgh1 B Re-Expression Rescues Transcriptional Activation in Dlgh1^{KO} CD8+ T Cells

Recent evidence suggests that Dlgh1 alternative splice variants differentially regulate the alternative p38 pathway and hence NFAT-mediated transcription (Chapter 2). To test this working model, we decided to reintroduce the two Dlgh1 splice variants expressed in CD8+ T lymphocytes, Dlgh1-L27β-i1Ai1B-i3i5 (Dlgh1 AB) and Dlgh1-L27β-i1B-i3i5 (Dlgh1 B), in Dlgh1^{KO} CD8+ T cells. Re-expression of Dlgh1 AB, but not Dlgh1 B rescued TCR-induced gene expression of NFATc1 and TNFα (Figure 5-3). In line with our previous findings utilizing Dlgh1 knockdown, Dlgh1 knockout had no major appreciable affects on TCR-induced IκBα or IL-2 gene expression. Furthermore, re-expression of Dlgh1 AB or Dlgh1 B had no effect on IκBα or IL-2 gene expression, indicating that rescue of Dlgh1 protein levels with Dlgh1 AB did not globally affect TCR-induced transcriptional activation but rather there was a selective rescue of genes diminished with Dlgh1 knockout (Figure 5-3). Collectively, these results provide evidence to support a working model by which Dlgh1 splice variants differentially regulate TCR-induced upregulation of a select subset of NFAT-dependent genes.

In Vivo Dlgh1 Knockout in Peripheral CD8+ T Cells Prevents Optimal T Cell Activation

Germline and conditional knockout Dlgh1 mice have been demonstrated to have minimal effects on peripheral T cell activation and function, despite numerous studies utilizing acute siRNA mediated knockdown methodologies in murine and human T cells demonstrating a significant role for Dlgh1 in T cell signaling, cytoskeletal reorganization and effector functions (10, 11, 13, 14). We have previously proposed that compensatory mechanisms may be responsible for the lack of functional defects seen in germline and conditional Dlgh1 knockout mice, and that acute knockout of Dlgh1 may allow for a more

accurate assessment of the functional role of Dlgh1 in T lymphocytes (14). To determine if ER-Cre Dlgh1$^{flox/flox}$ mice could be used as a model to induce *dlgh1* deletion *in vivo*, ER-Cre Dlgh1$^{flox/flox}$ mice were treated with tamoxifen or mock solution (sunflower seed oil) for five consecutive days and splenocytes isolated ten days afterward. Mice treated with tamoxifen induced *dlgh1* recombination and diminished Dlgh1 protein levels in total splenocytes and CD8+ T cells (Figure 5-4). To begin to assess the role of Dlgh1 in these *in vivo* deleted Dlgh1^{KO} cells we first assessed their basal expression of activation markers. CD8+ T cells isolated from Dlgh1^{KO} mice did not show aberrant basal T cell activation compared to Dlgh1^{WT} T cells. Furthermore, the majority of T cells seemed to have low levels of activation marker expression indicating that they were in a "resting," and possibly naïve state. Next, to assess the functional capacity of these resting (naïve) Dlgh1^{KO} T cells, their ability to become activated after TCR stimulation was assessed. Dlgh1^{KO} T cells failed to properly upregulate CD25, CD44 and CD69 in response to anti-CD3/anti-CD28 stimulation (Figure 5-5). This defect was not due to tamoxifen administration as Dlgh1$^{flox/flox}$ mice treated with tamoxifen had a similar percentage of CD8+ T cells upregulate CD25, CD44 and CD69 compared to mock treated mice (Figure 5-5). Being aware that residual Dlgh1 protein may still be expressed in Dlgh1^{KO} T cells due to slow Dlgh1 protein turnover and/or Dlgh1 mRNA stability, we decided to assess intracellular Dlgh1 protein levels concurrently with TCR-induced surface activation markers. In some ER-Cre Dlgh1$^{flox/flox}$ mice treated with tamoxifen, two populations of Dlgh1 could be appreciated in CD8+ cells: Dlgh1-hi and Dlgh1-lo (Figure 5-7A). When gated on CD8+Dlgh1-hi and CD8+Dlgh1-lo a more apparent effect on TCR-induced surface activation marker upregulation was observed, with CD8+Dlgh-lo cells showing only slight upregulation of CD25, CD44 and CD69 compared to CD8+Dlgh-hi cells (Figure 5-7B).

Dlgh1 Controls Proinflammatory Cytokine Production in CD8+ T Cells

Proper T cell activation is required for the development of T cell effector functions, particularly the *de novo* synthesis of cytokines (4). Because we previously demonstrated that Dlgh1 is responsible for the selective transcriptional activation of proinflammatory cytokines IFNγ and TNFα but not other cytokines such as IL-2 in CD8+ effector T cells (Chapter 2), we decided to assess the functional capacity of resting (naïve) CD8+ T cells from $Dlgh1^{KO}$ mice to generate cytokines. We found that knockout of Dlgh1 significantly impaired the ability of CD8+ T cells to produce intracellular IFNγ and TNFα, but not IL-2 (Figure 5-6). This defect was not due to tamoxifen administration as $Dlgh1^{flox/flox}$ mice treated with tamoxifen had a similar capacity to produce all three cytokines compared to mock treated mice (Figure 5-6). Gating on CD8+Dlgh1-hi and CD8+Dlgh1-lo cells in ER-Cre $Dlgh1^{flox/flox}$ mice treated with tamoxifen demonstrated a more appreciable effect on TCR-induced proinflammatory cytokine production (Figure 5-7C). Collectively, these results demonstrate that Dlgh1 is required for optimal T cells activation and the selective synthesis of proinflammatory cytokines. Moreover, acute Dlgh1 knockout in peripheral resting (naïve) T cells reveals functional defects not observed with previous approaches used for Dlgh1 ablation.

DISCUSSION

Previous reports of Dlgh1 knockout mice have not substantiated the numerous studies utilizing siRNA-mediated knockdown demonstrating that Dlgh1 serves as a molecular scaffold for the proximal kinases Lck and ZAP70 to promote T cell signaling and effector function (8-12, 14). Here we demonstrated that acute deletion of Dlgh1 validates previous results demonstrating that Dlgh1 couples TCR engagement to p38 phosphorylation, the transcriptional upregulation of a subset of NFAT-dependent genes and the selective synthesis of proinflammatory cytokines in restimulated (antigen-experienced) CD8+ T cells (8) (Chapter 2). In addition, acute deletion of Dlgh1 in peripheral resting (naïve) CD8+ T cells uncovered the requirement for Dlgh1 in surface activation marker expression, as $Dlgh1^{KO}$ CD8+ T cells failed to properly upregulate CD25, CD44 and CD69 following TCR stimulation. Collectively, these data demonstrate that Dlgh1 couples TCR engagement to T cell signaling, activation and effector function. Furthermore, these data suggest that acute methods of Dlgh1 deletion should be utilized in future studies assessing the role of Dlgh1 in T lymphocytes, and possibly other hematopoietic cells.

Proper upregulation of surface activation markers relies on cytoskeletal reorganization of the immunological synapse and the formation of signaling complexes that activate downstream transcription factors required for the transcriptional activation of these genes (17, 18). Because Dlgh1 controls actin polymerization and immune synapse formation, in addition to the activation of the transcription factor NFAT, Dlgh1 may promote upregulation of surface activation markers by at least two distinct mechanisms. Cytoskeletally, Dlgh1 may control T cell activation by promoting WASp activation, as WASp directly associates with the SH3 domain of Dlgh1 and is required for p38-independent Dlgh1-mediated CTL effector function (Chapter 2). WASp is required

for TCR-induced actin polymerization, lipid raft clustering and upregulation of surface activation markers. In particular, WASp -/- T cells are defective in upregulating CD69 in response to anti-CD3/anti-CD28 (17). Thus, Dlgh1 may promote p38-independent activation of WASp leading to upregulation of surface activation markers. Alternatively, Dlgh1 may regulate the transcriptional activation of surface activation marker gene expression via the alternative p38 pathway. One known downstream target of the alternative p38 pathway is the transcription factor NFAT, which binds *cis*-regulatory elements in the gene encoding CD25 and regulates CD25 gene expression (18). Despite the precise molecular mechanism by which Dlgh1 controls TCR-induced upregulation of surface activation markers, it is clear that Dlgh1 couples TCR engagement to T cell activation.

Improper T cell activation can lead to defects in CD8+ T cell differentiation into cytotoxic T lymphocyte (CTL) effectors (19). In this study, deletion of Dlgh1 in resting CD8+ T cells prevented optimal upregulation of CD25, CD44 and CD69, and production of IFNγ and TNFα, suggesting that Dlgh1 may play a role in CD8+ T cell differentiation. Recently, Dlgh1-mediated alternative p38 phosphorylation has been demonstrated to control CD4+ T cell differentiation and autoimmunity. Specifically, CD4+ T cells from p38 knockin mice in which Y323, the critical tyrosine residue phosphorylated by Dlgh1-associated ZAP70 in the alternative p38 pathway, is replaced with phenylalanine failed to properly polarize into T helper 1 (Th1) and T helper 17 (Th17) cells. Moreover, p38 Y323F CD4+ T cell skewed under Th1-conditions showed defective expression of T-bet, a NFAT-dependent T-box transcription factor critical for guiding T cell differentiation in CD4+ T cells (4). Our preliminary investigation assessing CTL differentiation have demonstrated that Dlgh1^{KO} CD8+ T cells also fail to properly express T-bet (data not shown), suggesting that Dlgh1 may regulate CD8+ differentiation through a p38/NFAT-dependent

mechanism. In addition, Dlgh1 may regulate CD8+ T cell effector differentiation through NFAT-dependent expression of CD25. Surface expression levels of CD25 and IL-2 signaling differentially guide effector and memory T cell generation. Specifically, CD8+CD25^{hi} T cells differentiate into terminal effectors expressing higher levels of granzyme B, IFNγ, and BLIMP1 compared to CD8+CD25^{low} T cells which have more of a memory cell phenotype (20). Because Dlgh1 is required for the generation of CD25^{high} cells (Fig 6 and Fig S2C), Dlgh1 could guide T cells toward an effector phenotype by allowing for enhanced IL-2 signaling. Indeed, a recent study by Swat looking at CD4+ T cell memory development found that Dlgh1 regulates the generation of CD4+ effector memory T cells after antigenic challenge (21). A third possible mechanism by which Dlgh1 may regulate T cell differentiation is through asymmetric cell division. Asymmetric cell division of naïve T cells has been proposed as a mechanism to generate distinct daughter cells that are destined to be effector (proximal daughter) or memory (distal daughter) cells. Polarity proteins are critical regulators of this process by promoting asymmetric proteasome segregation leading to the unequal partitioning of the transcription factor T-bet during cell division (22). Dlgh1, a member of the ancient Scribble polarity network, regulates the polarized recruitment of T cell receptors, lipids rafts and the MTOC during antigen recognition, suggesting that Dlgh1 could contribute to the polarization of signaling molecules or cellular machinery required for guiding memory and effector fate decisions. Collectively these data suggest that Dlgh1 may be a critical player in fating of T cells into either terminal effectors or effector memory T cells.

In summary, we have uncovered that acute deletion of Dlgh1 in peripheral T cells reveals previously masked defects in T cell signaling, activation and effector function. These results suggest that the timing and/or duration of Dlgh1 deletion may greatly affect the phenotype of Dlgh1-deficient cells. Thus, we recommend that future studies

assessing the role of Dlgh1 in T lymphocytes, and possibly other hematopoietic cells utilize acute methods of Dlgh1 deletion. It will be interesting and necessary to reassess previously studied T cells function in the context of acute Dlgh1 knockout, in particular T cell proliferation, migration, and uropod formation. Furthermore, this acute Dlgh1 knockout model will allow us to assess the functional role of Dlgh1 in T lymphocytes, and possible other hematopoietic cells, in models of infection and autoimmunity.

Figure 5-1. Cre-mediated *dlgh1* knockout in Dlgh1$^{flox/flox}$ T cells

(A) Schematic representation of *dlgh1* exon flanked by loxP sites in Dlgh1$^{flox/flox}$ mice (Dlgh1^{WT}) and resulting genomic *dlgh1* allele after Cre-mediated recombination (Dlgh1^{KO}). Primers used to assess *dlgh1* recombination are also shown.

(B-C) Dlgh1$^{flox/flox}$ CD8+ T cells were infected with MIG-Empty (-CRE) or MIG-Cre (+CRE).

(B) gDNA was isolated from cells and assessed for *dlgh1* recombination via PCR.

(C) Sorted CD8+GFP+ cells were analyzed for Dlgh1 protein expression via immunobloting; p38 was used as a loading control. Data are representative of at least three independent experiments.

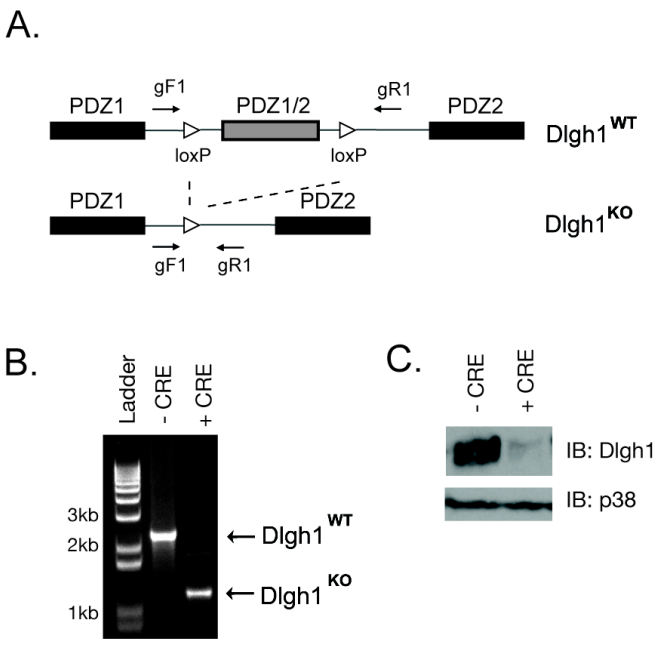
A.
gF1
gR1
PDZ1
PDZ1/2
PDZ2
loxP
loxP
Dlgh1WT
PDZ1
PDZ2
Dlgh1KO
gF1
gR1
B.
Ladder
- CRE
+ CRE
3kb
2kb
1kb
Dlgh1WT
Dlgh1KO
C.
- CRE
+ CRE
IB: Dlgh1
IB: p38

Figure 5-2. ER-Cre-mediated *dlgh1* knockout in effector CD8+ T cells impairs NFAT-dependent transcription and p38 phosphorylation

(A-C) ER-Cre Dlgh1$^{flox/flox}$ CD8+ T cells were stimulated with anti-CD3/anti-CD28 for 48 hours followed by expansion in rIL-2 (100U/mL) and 4-hydroxytamoxifen (200nM) for an additional 3 days.

(A-B) Cells were with anti-CD3 (2ug/mL) and anti-CD28 (2ug/mL) for 2 hrs or left unstimulated.. RNA was isolated for qPCR. mRNA was normalized to L32 and fold-increase in mRNA expression vs. unstimulated samples is shown. Error bars represent SD of samples analyzed in triplicate. Data are representative of three independent experiments.

(C) Cells were restimulated with platebound anti-CD3/anti-CD28 for 15 mins or left unstimulated, and analyzed for intracellular phospho-p38 (T180/Y182). The fold change in geometric mean fluorescent intensity (gMFI) relative to control was quantified as, gMFI (fold change) = gMFI stimulated – gMFI unstimulated for each condition, and where control is set to 1.0.

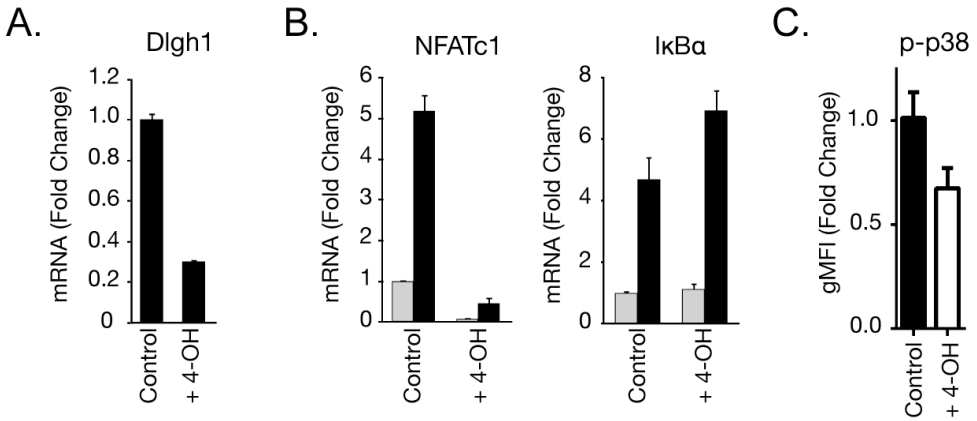
A.
Dlgh1
mRNA (Fold Change)
1.2
1.0
0.8
0.6
0.4
0.2
0
Control
+ 4-OH
B.
NFATc1
mRNA (Fold Change)
6
5
4
3
2
1
0
Control
+ 4-OH
IκBα
mRNA (Fold Change)
8
6
4
2
0
Control
+ 4-OH
C.
p-p38
gMFI (Fold Change)
1.0
0.5
0.0
Control
+ 4-OH

Figure 5-3. Re-expression of Dlgh1 AB, but not Dlgh1 B selectively rescues alternative p38-dependent transcriptional activation in ER-Cre-mediated *dlgh1* knockout CD8+ T cells

(A-F) ER-Cre Dlgh1$^{flox/flox}$ CD8+ T cells were stimulated with anti-CD3/anti-CD28 for 48 hrs, infected with the indicated MIG viruses and expanded in rIL-2 (100U/mL) and 4-hydroxytamoxifen (200nM) for an additional 3 days.

(A) Cells were analyzed for Dlgh1 protein levels via immunoblotting; p38 was used as a loading control.

(B) Cells were isolated for RNA and analyzed for Dlgh1 mRNA levels via qPCR.

(C-F) Cells were restimulated with anti-CD3/anti-CD28 for 2 hrs or left unstimulated. RNA was isolated for qPCR. mRNA was normalized to L32 and fold-increase in mRNA expression vs. unstimulated samples is shown. Error bars represent SD of samples analyzed in triplicate.

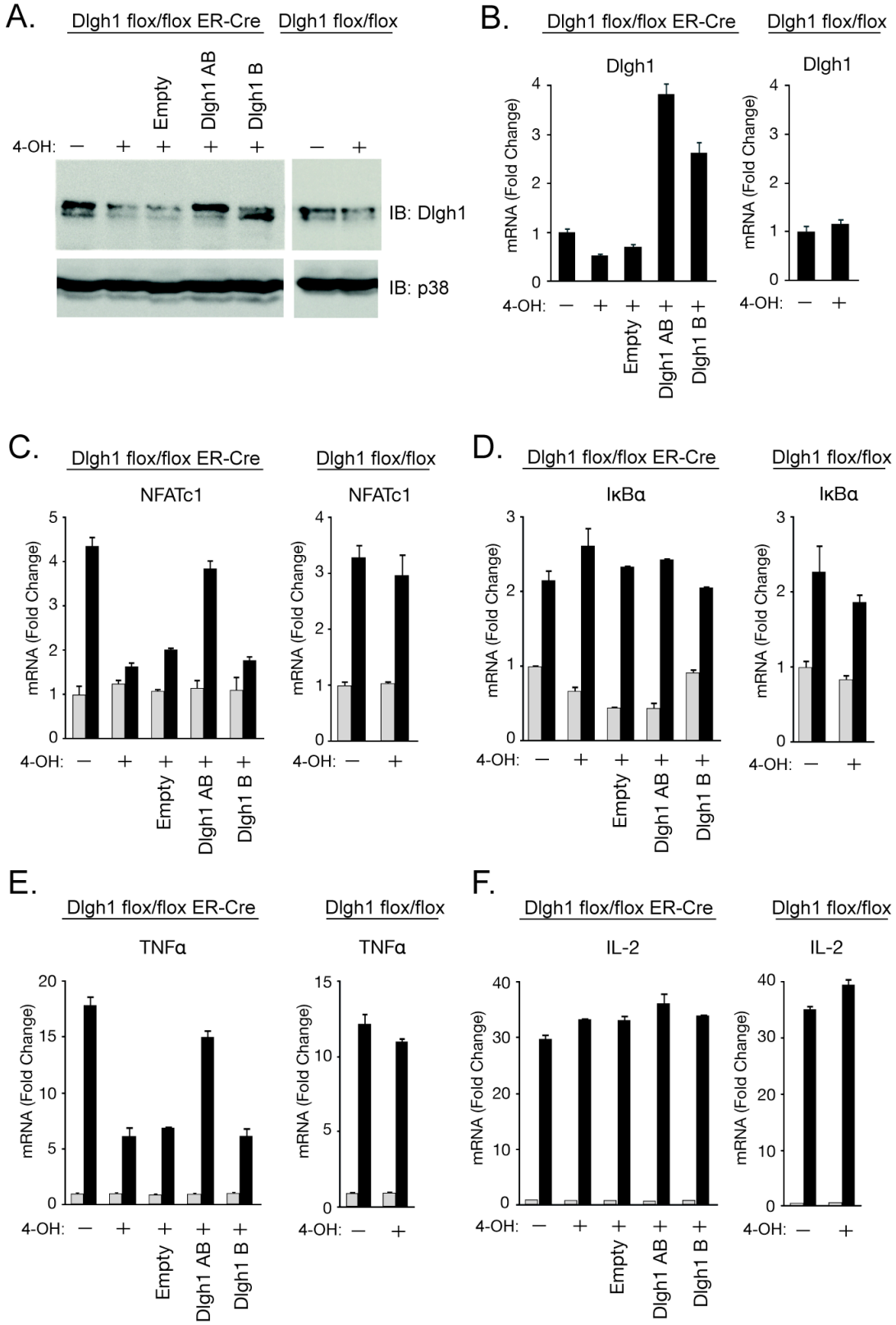
A.
Dlgh1 flox/flox ER-Cre
Dlgh1 flox/flox
Empty
Dlgh1 AB
Dlgh1 B
4-OH:
IB: Dlgh1
IB: p38
B.
Dlgh1
mRNA (Fold Change)
C.
NFATc1
D.
IκBα
E.
TNFα
F.
IL-2

Figure 5-4. *In Vivo* Dlgh1 knockout in ER-Cre Dlgh1$^{flox/flox}$ mice

(A-C) ER-Cre Dlgh1$^{flox/flox}$ mice were injected with tamoxifen (1mg) or mock solution (10% ethanol in sunflower seed oil) for five consecutive days. Ten days after the last injection splenocytes were isolated.

(A) gDNA was isolated from splenocytes and assessed for *dlgh1* recombination via PCR.

(B) Protein lysate was isolated from total splenocytes and assessed for Dlgh1 levels via immunoblotting; Lck was used as a loading control.

(C) A representative histogram of intracellular Dlgh1 protein levels from CD8+ cells is shown. Data are representative of at least three independent experiments.

A.

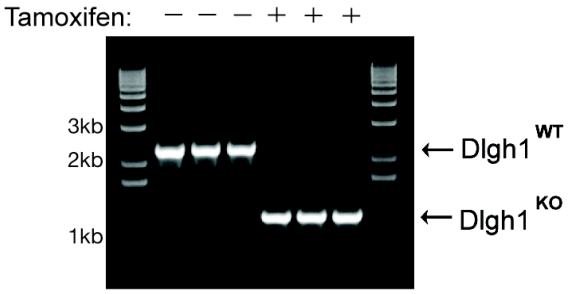
Tamoxifen: – – – + + +
3kb
2kb
1kb
← Dlgh1 WT
← Dlgh1 KO

B.

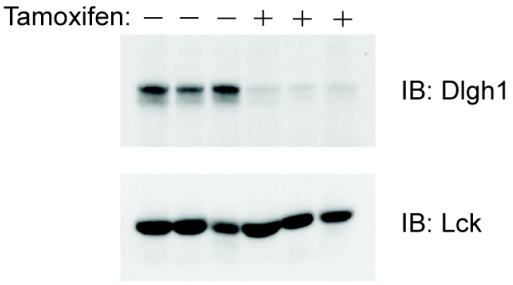
Tamoxifen: – – – + + +
IB: Dlgh1
IB: Lck

C.

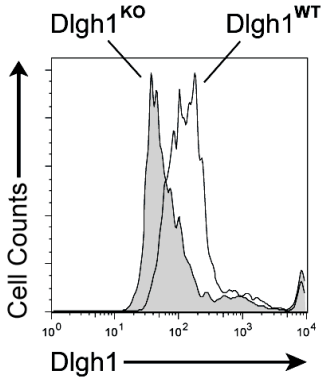
Dlgh1 KO
Dlgh1 WT
Cell Counts
10^0
10^1
10^2
10^3
10^4
Dlgh1

Figure 5-5. *In Vivo* Dlgh1 knockout prevents optimal CD8+ T cell activation

(A-F) ER-Cre Dlgh1$^{flox/flox}$ and Dlgh1$^{flox/flox}$ mice were injected with 1mg tamoxifen (+TAM) or mock solution (-TAM) for five consecutive days. Ten days after the last injection splenocytes were isolated and stimulated with anti-CD3/anti-CD28 for 24 hrs. (A,C,E) ER-Cre Dlgh1$^{flox/flox}$ CD8+ T cells were assessed for basal (0h) and TCR-induced (24h) surface activation marker expression. Representative histograms are shown. (B,D,E) The percentage of ER-Cre Dlgh1$^{flox/flox}$ and Dlgh1$^{flox/flox}$ CD8+ activation marker-positive cells is graphed. Error bars represent SD of means from individual mice. Data are representative of two independent experiments with at least three Dlgh1^{WT} and three Dlgh1^{KO} mice analyzed in each experiment.

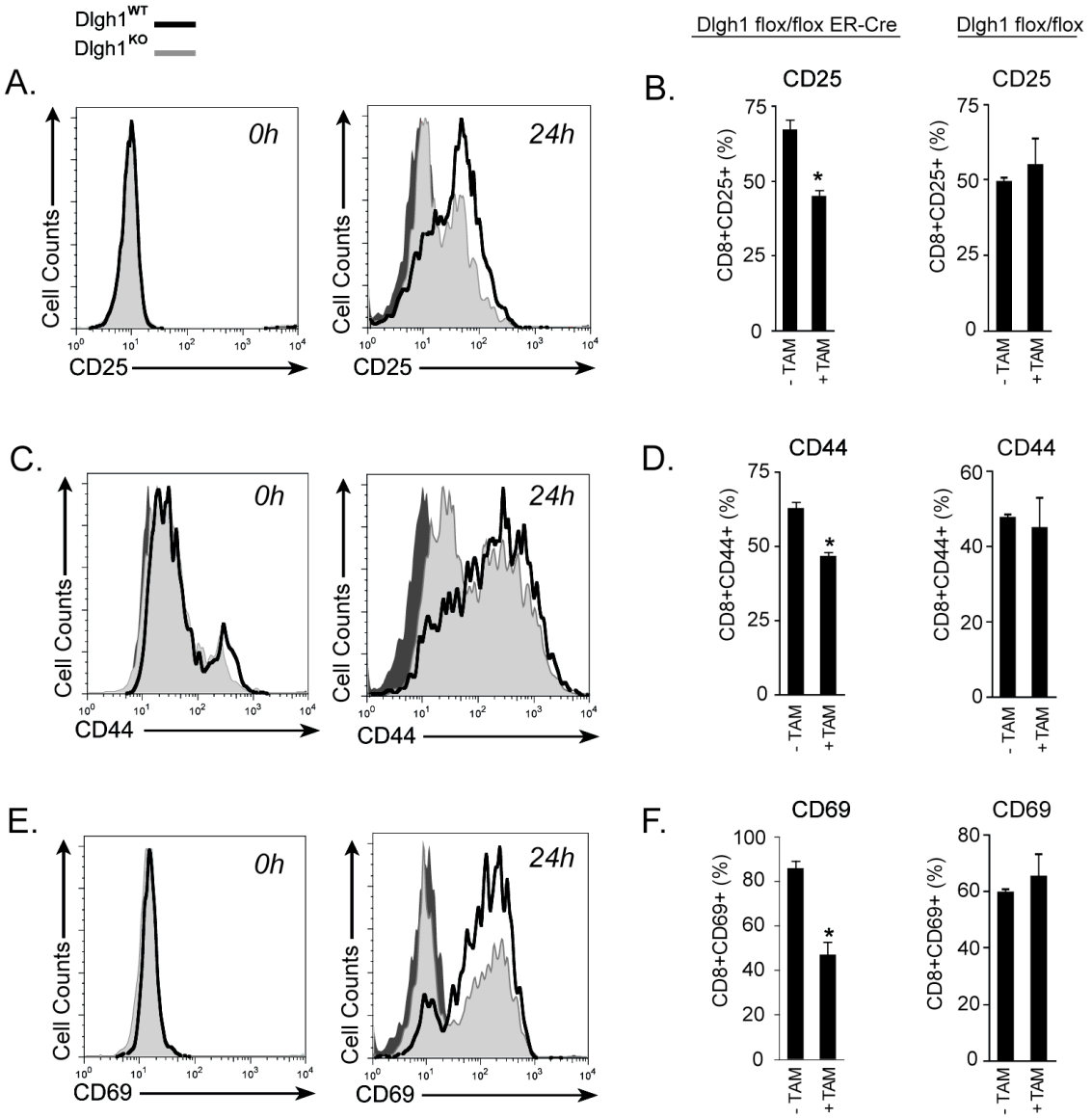
Dlgh1WT
Dlgh1KO
A.
0h
24h
Cell Counts
CD25
B.
Dlgh1 flox/flox ER-Cre
Dlgh1 flox/flox
CD25
CD8+CD25+ (%)
- TAM
+ TAM
C.
CD44
D.
CD8+CD44+ (%)
E.
CD69
F.
CD8+CD69+ (%)

Figure 5-6. *In Vivo* Dlgh1 knockout selectively impairs IFNγ and TNFα, but not IL-2 production in CD8+ T Cells

(A-F) ER-Cre Dlgh1$^{flox/flox}$ and Dlgh1$^{flox/flox}$ mice were injected with 1mg tamoxifen (+TAM) or mock solution (-TAM) for five consecutive days. Ten days after the last injection splenocytes were isolated and stimulated with anti-CD3/anti-CD28 for 24 or 48 hours.

(A,C,E) ER-Cre Dlgh1$^{flox/flox}$ CD8+ T cells were assessed for intracellular IFNγ (A), TNFα (C), and IL-2 (E) at both 24 and 48 hrs. Representative histograms are shown.

(B,D,F) The average intracellular cytokine geometric mean fluorescent intensity (gMFI) for ER-Cre Dlgh1$^{flox/flox}$ and Dlgh1$^{flox/flox}$ CD8+ cells is graphed. Error bars represent SD of means from individual mice. Data are representative of two independent experiments with at least three Dlgh1^{WT} and three Dlgh1^{KO} mice analyzed in each experiment.

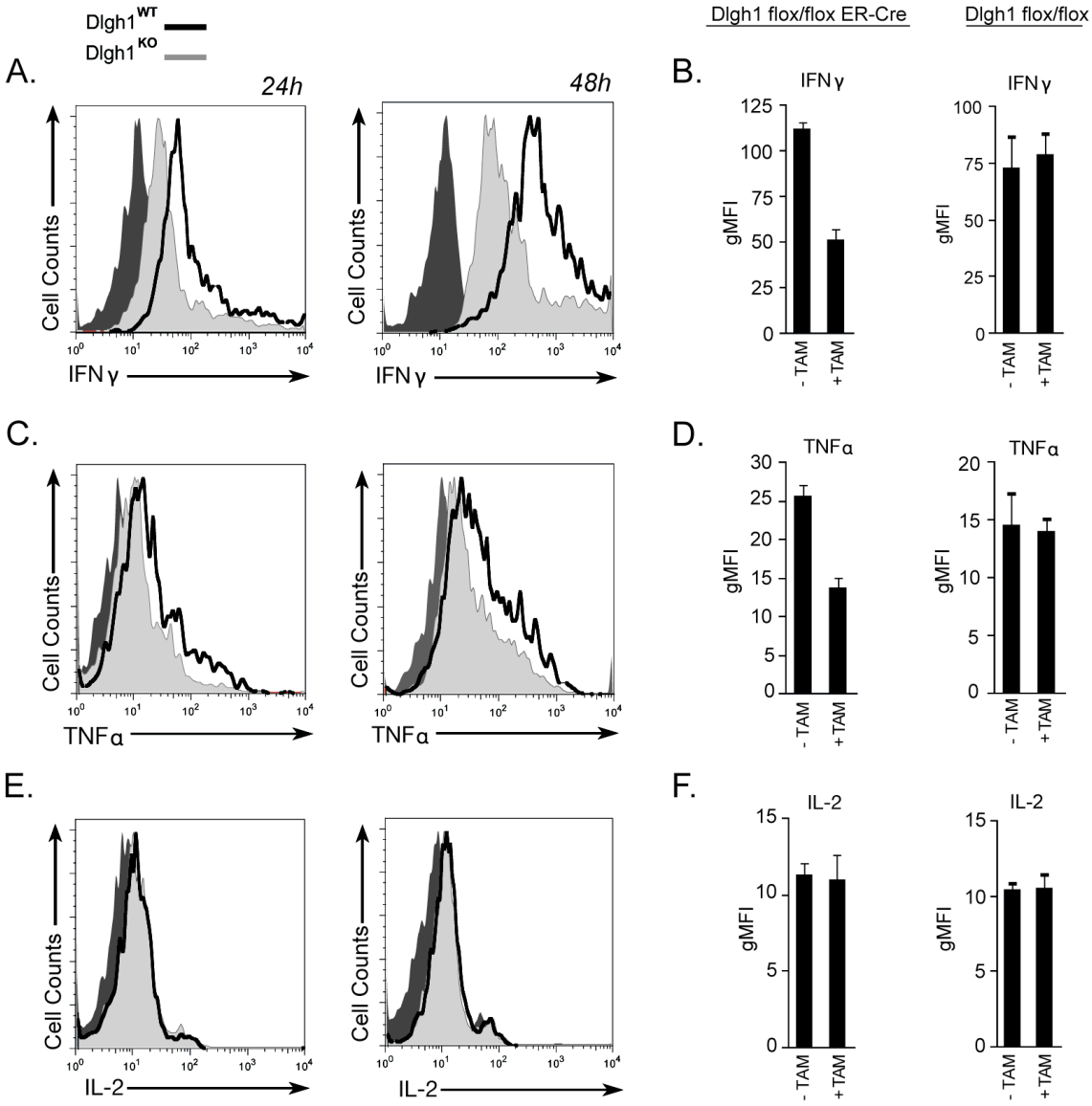
Dlgh1 WT
Dlgh1 KO
A.
24h
48h
Cell Counts
IFN γ
B.
Dlgh1 flox/flox ER-Cre
Dlgh1 flox/flox
IFN γ
gMFI
- TAM
+ TAM
C.
TNFα
D.
E.
IL-2
F.

Figure 5-7. Dlgh1 hi versus Dlgh1 lo cells in Dlgh1^{KO} CD8+ T cells delineates activation and functional phenotypes

(A-C) ER-Cre Dlgh1$^{flox/flox}$ mice were injected with tamoxifen (1mg) for five consecutive days. Ten days after the last injection splenocytes were isolated and stimulated with anti-CD3/anti-CD28 for 24 or 48 hrs and assessed for surface activation marker upregulation or intracellular cytokine production.

(A) Histrogram of intracellular Dlgh1 levels in Dlgh1^{KO} CD8+ T cell demonstrating incomplete Dlgh1 knockout. Two populations of Dlgh1 are present: *Dlgh1 hi and Dlgh1 lo*.

(B) Gated CD8+ Dlgh1 *hi* and CD8+ Dlgh1 *lo* were assessed for surface activation marker upregulation. Representative histograms are shown. The percentage of CD8+ activation marker-positive cells is graphed. Error bars represent SD of means from individual mice. Data are representative of two independent experiments.

(C) Gated CD8+ Dlgh *hi* and CD8+ Dlgh1 *lo* were assessed for intracellular IFNγ at 24 hrs (*left*) and 48 hrs (*right*). Representative histograms are shown. The average MFI is graphed. Error bars represent SD of means from individual mice. Data are representative of two independent experiments.

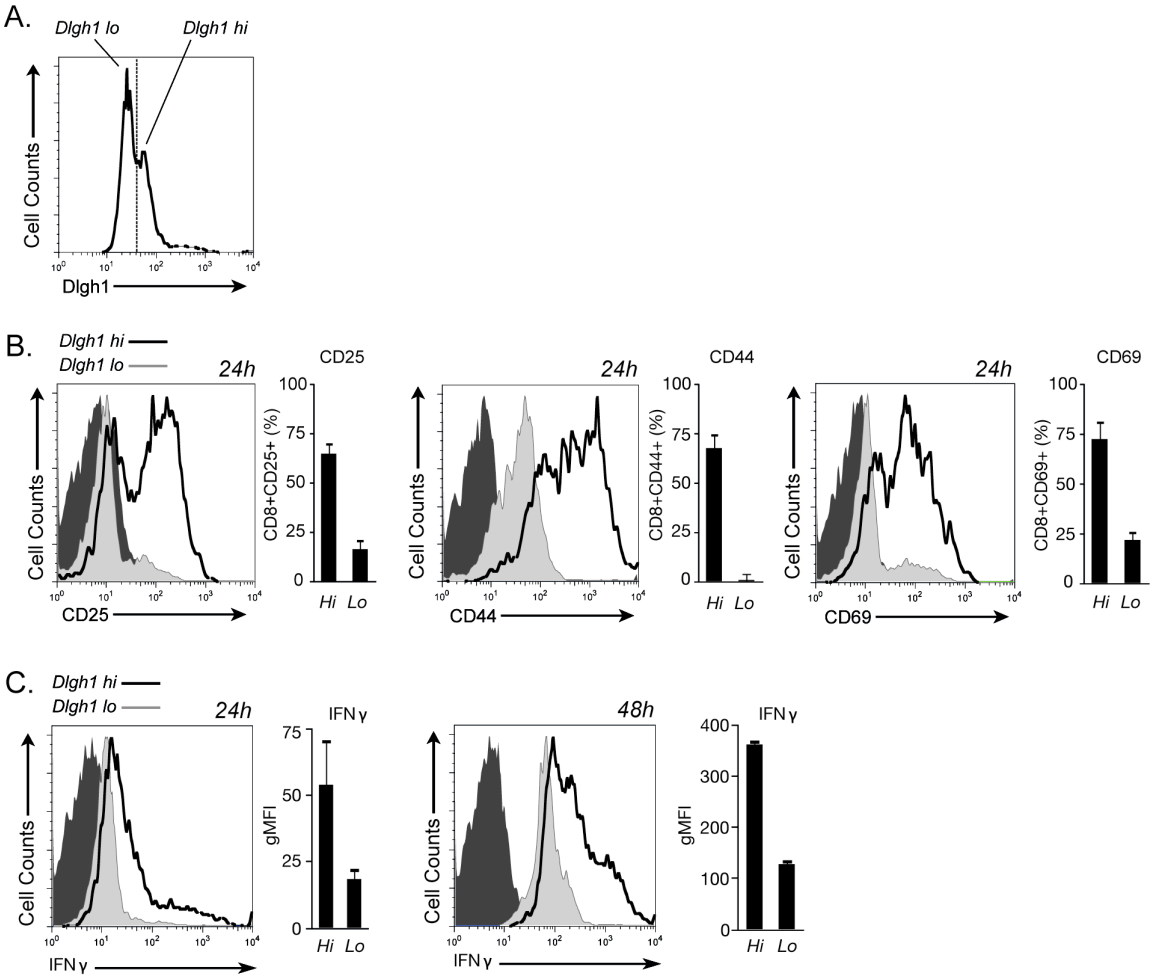
A.
Dlgh1 lo
Dlgh1 hi
Cell Counts
Dlgh1
B.
Dlgh1 hi
Dlgh1 lo
24h
CD25
CD8+CD25+ (%)
Hi Lo
CD44
CD8+CD44+ (%)
CD69
CD8+CD69+ (%)
C.
IFNγ
gMFI
48h

REFERENCES

1. Fooksman DR*, et al.* (2009) Functional Anatomy of T Cell Activation and Synapse Formation. *Annu Rev Immunol* 28:79-105.

2. Rincón M & Davis RJ (2007) Choreography of MAGUKs during T cell activation. *Nat Immunol* 8(2):126-127.

3. Thome M (2004) CARMA1, BCL-10 and MALT1 in lymphocyte development and activation. *Nat Rev Immunol* 4(5):348-359.

4. Jirmanova L, Giardino Torchia ML, Sarma ND, Mittelstadt PR, & Ashwell JD (2011) Lack of the T cell-specific alternative p38 activation pathway reduces autoimmunity and inflammation. *Blood* 118(12):3280-3289.

5. Jirmanova L, Sarma DN, Jankovic D, Mittelstadt PR, & Ashwell JD (2009) Genetic disruption of p38alpha Tyr323 phosphorylation prevents T-cell receptor-mediated p38alpha activation and impairs interferon-gamma production. *Blood* 113(10):2229-2237.

6. Hodge MR*, et al.* (1996) Hyperproliferation and dysregulation of IL-4 expression in NF-ATp-deficient mice. *Immunity* 4(4):397-405.

7. Guy CS*, et al.* (2013) Distinct TCR signaling pathways drive proliferation and cytokine production in T cells. *Nature Immunology* 14(3):262-270.

8. Round JL*, et al.* (2007) Scaffold protein Dlgh1 coordinates alternative p38 kinase activation, directing T cell receptor signals toward NFAT but not NF-kappaB transcription factors. *Nat Immunol* 8(2):154-161.

9. Round JL*, et al.* (2005) Dlgh1 coordinates actin polymerization, synaptic T cell receptor and lipid raft aggregation, and effector function in T cells. *J Exp Med* 201(3):419-430.

10. Lasserre R*, et al.* (2010) Ezrin tunes T-cell activation by controlling Dlg1 and microtubule positioning at the immunological synapse. *EMBO J* 29(14):2301-2314.

11. Adachi K & Davis MM (2011) T-cell receptor ligation induces distinct signaling pathways in naive vs. antigen-experienced T cells. *Proceedings of the National Academy of Sciences of the United States of America* 108(4):1549-1554.

12. Zanin-Zhorov A*, et al.* (2012) Scaffold protein Disc large homolog 1 is required for T-cell receptor-induced activation of regulatory T-cell function. *Proceedings of the National Academy of Sciences of the United States of America* 109(5):1625-1630.

13. Stephenson LM*, et al.* (2007) DLGH1 is a negative regulator of T-lymphocyte proliferation. *Mol Cell Biol* 27(21):7574-7581.

14. Humphries LA, *et al.* (2012) Characterization of in vivo dlg1 deletion on T cell development and function. *PLoS ONE* 7(9):e45276.

15. Zhou W, *et al.* (2008) GluR1 controls dendrite growth through its binding partner, SAP97. *J Neurosci* 28(41):10220-10233.

16. Park S-G, *et al.* (2009) The kinase PDK1 integrates T cell antigen receptor and CD28 coreceptor signaling to induce NF-κB and activate T cells. *Nat Immunol* 10(2):158-166.

17. Zhang J, *et al.* (1999) Antigen receptor-induced activation and cytoskeletal rearrangement are impaired in Wiskott-Aldrich syndrome protein-deficient lymphocytes. 190(9):1329-1342.

18. Schuh K, *et al.* (1998) The interleukin 2 receptor alpha chain/CD25 promoter is a target for nuclear factor of activated T cells. 188(7):1369-1373.

19. Kaech SM & Cui W (2012) Transcriptional control of effector and memory CD8(+) T cell differentiation. *Nature Reviews Immunology* 12(11):749-761.

20. Kalia V, *et al.* (2010) Prolonged interleukin-2Ralpha expression on virus-specific CD8+ T cells favors terminal-effector differentiation in vivo. *Immunity* 32(1):91-103.

21. Gmyrek GB, *et al.* (2013) Polarity gene discs large homolog 1 regulates the generation of memory T cells. *European Journal of Immunology* 43(5):1185-1194.

22. Chang JT, *et al.* (2011) Asymmetric Proteasome Segregation as a Mechanism for Unequal Partitioning of the Transcription Factor T-bet during T Lymphocyte Division. *Immunity* 34(4):492-504.

CHAPTER SIX

Conclusions:

Moving towards an understanding of Dlgh1 scaffolds

in T cell signaling, activation and function

Two decades after the discovery of the T cell receptor and the proximal non-receptor tyrosine kinases Lck and ZAP70, we are starting to learn how these proximal signals are specifically channeled to activate discrete signaling pathways and produce precise cellular behavior (1-4). Scaffolding proteins have emerged as critical molecular assemblies providing cellular infrastructure to numerous cytoskeletal and signaling proteins in T lymphocytes (5). In particular, the scaffold protein Discs large homolog 1 (Dlgh1) is a key molecular conduit coupling TCR engagement to signal transduction and cytoskeletal reorganization. Specifically, Dlgh1 channels Lck and ZAP70 kinase activity toward the activation of MAPK p38 and transcription factor NFAT (6-10). In addition, Dlgh1 controls F-actin polymerization, TCR and lipid raft clustering, and proper MTOC positioning during antigen recognition (6, 11, 12). Consequently, Dlgh1 promotes TCR-induced cytokine production and contact-dependent cytolysis in murine CD8+ CTLs, and suppressor activity in human CD4+CD25+ regulatory T cells (6, 10). Understanding the molecular mechanisms by which Dlgh1 *specifically* channels proximal TCR signals to trigger these and other distinct T cell functional outcomes in naïve, effector and memory T cells necessitates an understanding of how Dlgh1 is regulated, and an ability to delete Dlgh1 in vivo.

ALTERNATIVE SPLICING & PHOSHPORYLATION REGULATE DLGH1 IN T CELLS

Post-transcriptional and post-translational regulation of Dlgh1 drastically affects Dlgh1 composition, localization, stability, and function (13-17). In Chapter 2 alternative splicing was investigated as a mechanism to regulate Dlgh1-mediated CD8+ T cell effector functions. Murine CD8+ T cells expressed two unique Dlgh1 protein scaffolds due to alternative splicing: Dlgh1 AB and Dlgh1 B. These Dlgh1 protein variants differentially regulated the alternative p38 pathway, as Dlgh1 AB but not Dlgh1 B bound

Lck, promoted p38 phosphorylation and induced NFAT-dependent transcription. Furthermore, these Dlgh1 splice variants had different effects on lytic factor degranulation and proinflammatory cytokine production, owing to their ability to support alternative p38 activation. Namely, while both Dlgh1 AB and Dlgh1 B supported p38-independent degranulation, only Dlgh1 AB promoted the selective production of IFNγ and TNFα, but not IL-2 through the alternative p38 pathway (18). Lastly, Dlgh1-mediated p38-independent degranulation was found to require actin polymerization, the SH3-domain of Dlgh1 and the Dlgh1-SH3 ligand WASp (7). WASp, like Dlgh1, controls actin polymerization, CD8+ T cell cytotoxicity, NFAT activation, and cytokine production (19, 20). Interestingly, studies utilizing WASP proline-rich domain (PRD) mutants, mutants that lack the ability to bind SH3-ligands, have demonstrated a role for the PRD in actin polymerization but not NFAT activation (21). Indicating that the ability of WASp to drive actin polymerization can be uncoupled from its ability to induce NFAT-dependent transcription. Collectively, these results suggest that Dlgh1 splice variants may be able to nucleate two functionally discrete signaling complexes. A Dlgh1 AB/Lck/p38 complex that couples Lck and ZAP70 to a subset of NFAT-dependent genes (IFNγ and TNFα, but not IL-2), and a Dlgh1/WASp complex (note that Dlgh1 can be either Dlgh1 AB or Dlgh1 B), that couples TCR engagement to actin polymerization and lytic factor degranulation (Figure 6-1). This would allow CD8+ CTLs the ability to differentially control cytotoxicity and proinflammatory cytokine production, and similarly would afford researchers the opportunity to find therapeutics that selective inhibit a particular effector function and not the other. Such therapeutics would be particularly useful in biological situations where proinflammatory cytokine production may be detrimental, while cytotoxicity is required for an effective CD8+ T cell immune

response, as is the case in extremely virulent infections of influenza and adoptive T cell transfer therapy to combat cancer (22-25).

Evaluation of Dlgh1 alternative splicing in CD8+ effector T cells provided data to support a working model where Dlgh1 splice variants nucleate two functionally independent signaling complexes controlling p38-dependent proinflammatory cytokine production and p38-independent degranulation. Chapter 3 provides evidence to extend this working model and suggests that Dlgh1 AB tyrosine phosphorylation may be a possible mechanism to specifically regulate p38-dependent proinflammatory cytokine production. TCR stimulation of CD8+ effector T cells selectively phosphorylated Dlgh1 AB, but not Dlgh1 B. This phosphorylation event was found to require tyrosine kinase Lck, but not ZAP70. Furthermore, phosphorylation of tyrosine 222 (Y222) was found to be a major Lck-target as mutation of Y222 to phenylalanine (Y222F) reduced Dlgh1 AB tyrosine phosphorylation by approximately 40%. Lastly, Y222 phosphorylation was critical for controlling Dlgh1-mediated alternative p38 activation as the Y222F Dlgh1 mutant abrogated p38 phosphorylation, transcriptional activation of NFATc1 and production of proinflammatory cytokines IFNγ and TNFα, but not IL-2. These results indicate that tyrosine phosphorylation of Dlgh1 AB may be a critical post-translational modification regulating the Dlgh1 AB/Lck/p38 complex in CD8+ effector T cells. While the precise role of Y222 tyrosine phosphorylation is still unclear we speculate that it may be acting as a SH2-binding site for Lck or ZAP70, as the surrounding amino acid sequences generate a canonical SH2 domain (YEEI). Alternatively, phosphorylation at Y222 may be "opening" the Dlgh1 scaffold as it has been demonstrated to adopt a compact/closed confirmation that may prevent the proper assembly or positioning of the Dlgh1 AB/Lck/p38 complex (26). Future experiments will hopefully address these possibilities.

Although the combinatorial use of lytic factor degranulation and proinflammatory cytokine production is often required to efficiently clear intracellular pathogens, these CTL activities are not always coordinately invoked (22). Furthermore, there seems to be a hierarchy to CD8+ T cell effector functions based on the strength of antigenic stimulation. Notably, lower levels of antigenic stimulation are sufficient to trigger CTL cytotoxicity, however higher levels of antigenic stimulation are required to trigger both CTL cytotoxicity and proinflammatory cytokine production (27). Collectively, these data suggesting that signaling complexes, such as Dlgh1/WASp and Dlgh1 AB/p38, may be unique formed and differentially activated to produce these distinct CTL activities. As Dlgh1 tyrosine phosphorylation seems to specifically affect Dlgh1 AB, which mediates p38-dependent proinflammatory cytokine production it would be interesting to speculate that tyrosine phosphorylation may be a molecular switch allowing Dlgh1 AB to act as a rheostat controlling the induction of proinflammatory cytokines at high levels of antigenic stimulation. While we did not assess the state of Dlgh1 tyrosine phosphorylation under various TCR stimulatory conditions, it could be possible that a strong TCR stimulus is required to induce Dlgh1 AB tyrosine phosphorylation, while a feeble TCR stimulus cannot. Future experiments assessing the status of Dlgh1 AB tyrosine phosphorylation under various TCR/costimulatory situations will be very informative at assessing this working hypothesis.

ACUTE DLGH1 KNOCKOUT: THE METHOD OF CHOICE

Despite the discoveries that Dlgh1 regulation via alternative splicing and phosphorylation have significant effects on Dlgh1-mediated CD8+ T cell effector functions, there is a growing necessity to develop better tools to further explore the role of Dlgh1 in the adaptive immune system. Several studies have recently been published

describing the generation of Dlgh1 knockout (Dlgh1^{KO}) mice, however all of these studies (including the one presented in Chapter 4) have been largely unavailing. Specifically, while one group has observed conflicting results in T cell proliferation (28, 29), our analysis of one conditional and two germline Dlgh1^{KO} mouse models found no, or minor, observable defects in T cell development, morphology, migration, signaling, activation or proliferation (30). Because developmental compensatory mechanisms may have been responsible for the lack of functional effects observed an inducible Dlgh1^{KO} mouse was generated (Chapter 5). With much relief and excitement, acute knockout of Dlgh1 *in vitro* and *in vivo* prevented optimal T cell activation and effector function in CD8+ T cells. Dlgh1^{KO} T cells generated *in vitro* were defective in activating the alternative p38 dependent pathway, as Dlgh1^{KO} CD8+ T cells failed to optimally phosphorylate p38 in response to TCR stimulation. Furthermore, these Dlgh1^{KO} CD8+ T cells had a selective defect in TCR-induced upregulation of p38-dependent genes. This effect was specifically due to Dlgh1^{KO}, as re-expression of Dlgh1 AB was able to rescue p38-dependent gene expression. Finally, *in vivo* generated Dlgh1^{KO} T cells failed to upregulate early activation markers and demonstrated a selective impairment in the production of proinflammatory cytokines when stimulated *ex vivo*. These findings suggest that Dlgh1 is indeed a critical molecular scaffold coupling TCR engagement to T cell functional outcomes, and suggests that acute Dlgh1 knockout should be “the method of choice” for future *in vivo* studies assessing the role of Dlgh1 in T lymphocytes or other hematopoietic cells.

Figure 6-1. A Model By Which Dlgh1 Splice Variants Regulate CD8+ T cell Effector Functions.

Both Dlgh1 AB and Dlgh1 B are predicted to bind the cytoskeletal regulator WASp and promote actin-dependent lytic factor degranulation. However, only Dlgh1 AB can promote proinflammatory cytokine production by binds Lck, promoting alternative p38 phosphorylation and inducing NFAT-dependent transcription of IFNγ and TNFα.

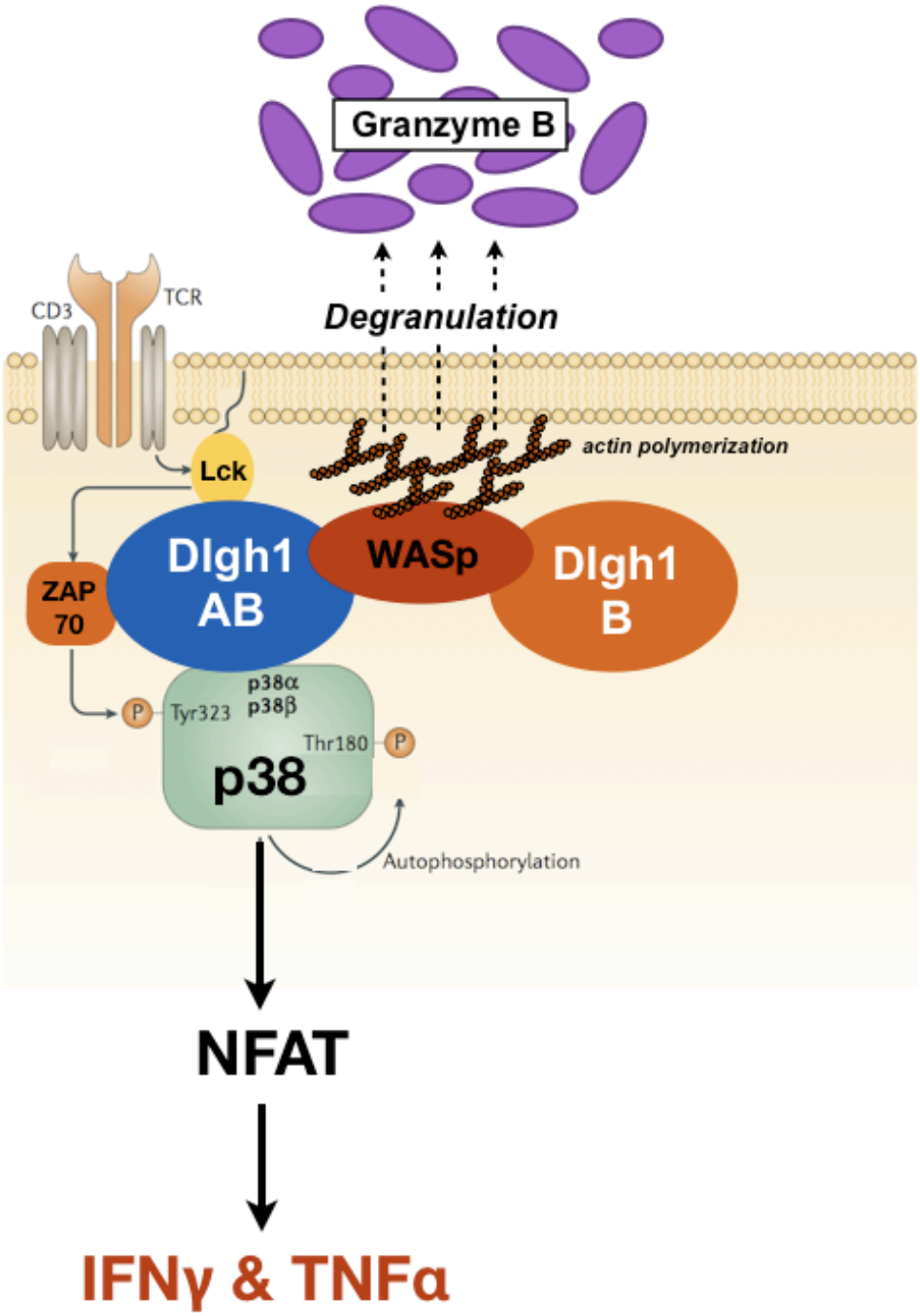
Granzyme B
Degranulation
CD3
TCR
Lck
actin polymerization
ZAP 70
Dlgh1 AB
WASp
Dlgh1 B
p38α
p38β
Tyr323
Thr180
p38
Autophosphorylation
NFAT
IFNγ & TNFα

REFERENCES

1. Haskins K, et al. (1983) The major histocompatibility complex-restricted antigen receptor on T cells. I. Isolation with a monoclonal antibody. The Journal of experimental medicine 157(4):1149-1169.

2. Straus DB & Weiss A (1992) Genetic evidence for the involvement of the lck tyrosine kinase in signal transduction through the T cell antigen receptor. Cell 70(4):585-593.

3. Chan AC, Iwashima M, Turck CW, & Weiss A (1992) ZAP-70: a 70 kd protein-tyrosine kinase that associates with the TCR zeta chain. Cell 71(4):649-662.

4. Guy CS, et al. (2013) Distinct TCR signaling pathways drive proliferation and cytokine production in T cells. Nature Immunology 14(3):262-270.

5. Shaw A & Filbert E (2009) Scaffold proteins and immune-cell signalling. Nature Rev Immunol 9(1):47-56.

6. Round JL, et al. (2005) Dlgh1 coordinates actin polymerization, synaptic T cell receptor and lipid raft aggregation, and effector function in T cells. J Exp Med 201(3):419-430.

7. Round JL, et al. (2007) Scaffold protein Dlgh1 coordinates alternative p38 kinase activation, directing T cell receptor signals toward NFAT but not NF-kappaB transcription factors. Nat Immunol 8(2):154-161.

8. Rebeaud F, Hailfinger S, & Thome M (2007) Dlgh1 and Carma1 MAGUK proteins contribute to signal specificity downstream of TCR activation. Trends Immunol 28(5):196-200.

9. Adachi K & Davis MM (2011) T-cell receptor ligation induces distinct signaling pathways in naive vs. antigen-experienced T cells. Proceedings of the National Academy of Sciences of the United States of America 108(4):1549-1554.

10. Zanin-Zhorov A, et al. (2012) Scaffold protein Disc large homolog 1 is required for T-cell receptor-induced activation of regulatory T-cell function. Proceedings of the National Academy of Sciences of the United States of America 109(5):1625-1630.

11. Lasserre R, et al. (2010) Ezrin tunes T-cell activation by controlling Dlg1 and microtubule positioning at the immunological synapse. EMBO J 29(14):2301-2314.

12. Lue RA, Brandin E, Chan EP, & Branton D (1996) Two independent domains of hDlg are sufficient for subcellular targeting: the PDZ1-2 conformational unit and an alternatively spliced domain. J Cell Biol 135(4):1125-1137.

13. Godreau D, Vranckx R, Maguy A, Goyenvalle C, & Hatem SN (2003) Different isoforms of synapse-associated protein, SAP97, are expressed in the heart and have distinct effects on the voltage-gated K+ channel Kv1.5. J Biol Chem 278(47):47046-47052.

14. Schlüter OM, Xu W, & Malenka RC (2006) Alternative N-terminal domains of PSD-95 and SAP97 govern activity-dependent regulation of synaptic AMPA receptor function. Neuron 51(1):99-111.

15. Massimi P, Narayan N, Cuenda A, & Banks L (2006) Phosphorylation of the discs large tumour suppressor protein controls its membrane localisation and enhances its susceptibility to HPV E6-induced degradation. Oncogene 25(31):4276-4285.

16. Narayan N, Massimi P, & Banks L (2008) CDK phosphorylation of the discs large tumour suppressor controls its localisation and stability. J Cell Sci 122(Pt 1):65-74.

17. Nikandrova YA, Jiao Y, Baucum AJ, Tavalin SJ, & Colbran RJ (2010) Ca2+/calmodulin-dependent protein kinase II binds to and phosphorylates a specific SAP97 splice variant to disrupt association with AKAP79/150 and modulate alpha-amino-3-hydroxy-5-methyl-4-isoxazolepropionic acid-type glutamate receptor (AMPAR) activity. J Biol Chem 285(2):923-934.

18. Jirmanova L, Sarma DN, Jankovic D, Mittelstadt PR, & Ashwell JD (2009) Genetic disruption of p38alpha Tyr323 phosphorylation prevents T-cell receptor-mediated p38alpha activation and impairs interferon-gamma production. Blood 113(10):2229-2237.

19. Thrasher AJ & Burns SO (2010) WASP: a key immunological multitasker. Nat Rev Immunol 10(3):182-192.

20. De Meester J, Calvez R, Valitutti S, & Dupré L (2010) The Wiskott-Aldrich syndrome protein regulates CTL cytotoxicity and is required for efficient killing of B cell lymphoma targets. Journal of Leukocyte Biology 88(5):1031-1040.

21. Silvin C, Belisle B, & Abo A (2001) A role for Wiskott-Aldrich syndrome protein in T-cell receptor-mediated transcriptional activation independent of actin polymerization. J Biol Chem 276(24):21450-21457.

22. Hufford MM, Kim TS, Sun J, & Braciale TJ (2010) Antiviral CD8+ T cell effector activities in situ are regulated by target cell type. The Journal of experimental medicine 208(1):167-180.

23. Braciale TJ, Sun J, & Kim TS (2012) Regulating the adaptive immune response to respiratory virus infection. Nature reviews Immunology 12(4):295-305.

24. Landsberg J, et al. (2012) Melanomas resist T-cell therapy through inflammation-induced reversible dedifferentiation. Nature 490(7420):412-416.

25. Schürch C, Riether C, Amrein MA, & Ochsenbein AF (2013) Cytotoxic T cells induce proliferation of chronic myeloid leukemia stem cells by secreting interferon-γ. The Journal of experimental medicine 210(3):605-621.

26. Wu H, et al. (2000) Intramolecular interactions regulate SAP97 binding to GKAP. EMBO J 19(21):5740-5751.

27. Valitutti S, Müller S, Dessing M, & Lanzavecchia A (1996) Different responses are elicited in cytotoxic T lymphocytes by different levels of T cell receptor occupancy. The Journal of experimental medicine 183(4):1917-1921.

28. Stephenson LM, et al. (2007) DLGH1 is a negative regulator of T-lymphocyte proliferation. Mol Cell Biol 27(21):7574-7581.

29. Gmyrek GB, et al. (2013) Polarity gene discs large homolog 1 regulates the generation of memory T cells. European journal of immunology 43(5):1185-1194.

30. Humphries LA, et al. (2012) Characterization of in vivo dlg1 deletion on T cell development and function. PLoS ONE 7(9):e45276.